CHEMICAL AND MECHANICAL CHARACTERIZATION OF FULLY DEGRADABLE DOUBLE-NETWORK HYDROGELS BASED ON PEG AND PAA

A Dissertation
Presented to
The Academic Faculty

by

Kevin Worrell

In Partial Fulfillment
of the Requirements for the Degree
Doctor of Philosophy in the
School of Materials Science & Engineering

Georgia Institute of Technology
August 2012

CHEMICAL AND MECHANICAL CHARACTERIZATION OF FULLY DEGRADABLE DOUBLE-NETWORK HYDROGELS BASED ON PEG AND PAA

Approved by:

Dr. Karl Jacob, Advisor
School of Materials Science and Engineering
Georgia Institute of Technology

Dr. Anselm Griffin
School of Materials Science and Engineering
Georgia Institute of Technology

Dr. Dongang Yao
School of Materials Science and Engineering
Georgia Institute of Technology

Dr. Youjiang Wang
School of Materials Science and Engineering
Georgia Institute of Technology

Dr. Rina Tannenbaum
School of Mechanical Engineering / Materials Science and Engineering
Georgia Institute of Technology

Date Approved: April 5, 2012

Dedicated to the memory of my grandparents:

Charles and Carmen Wood

And to my aunt:

Jacqueline Wood

ACKNOWLEDGEMENTS

I wish to thank God for the opportunity to complete this research, and I wish to thank my parents and relatives for their continuous and enduring support. I am grateful to my advisor, Dr. Karl Jacob, for his guidance and counsel not only in research but also in valuable life lessons. I would like to thank all of my committee members including Dr. Anselm Griffin for enlightening discussions, and Dr. Dongang Yao, Youjiang Wang and Rina Tannenbaum for invaluable suggestions and critique.

I would like to express gratitude to my research group (both past and present), especially Dr. Hongfeng Ren, Dr. Yi Liu, Zachary Kraus and Huaiping Rong, and fellow graduate students Ericka Johnson and Dr. Tolecia Clark for invaluable discussions.

I am very grateful to Dr. Anselm Griffin and Dr. Fred Cook for use of their research labs, Dr. Meisha Shofner and her research group, especially Dr. Jasmeet Kaur, Dr. Michelle Schlea and JiHoon Lee for use of and assistance with DMA and DSC equipment, Dr. Haskell Beckham and his group, especially Ipek Yucelen, for use of and assistance with FTIR, Dr. Leslie Gelbaum for assistance with NMR, Dr. Satish Kumar and his research group, especially Ericka Johnson for use of and assistance with FTIR, and Dr. Christopher Jones and his research group, including Steph Didas, for use of and assistance with DSC.

Finally, I would like to thank the School of Polymer, Textile and Fiber Engineering (now the School of Materials Science Engineering), the Southern Regional Education Board (SREB) and the GAANN Center for Drug Design, Delivery and Development for financial support.

TABLE OF CONTENTS

LIST OF TABLES

LIST OF FIGURES

LIST OF SYMBOLS

α	Linear expansion factors
χ_1	Flory polymer-solvent interaction parameter
$\chi_{1,2}$	Flory polymer-polymer interaction parameter between network 1 and 2
χ_i	Flory polymer-solvent interaction parameter of network *i*
C_n	Flory characteristic ratio
D	Sample thickness
$\overline{DP}_{PLA}$	Degree of polymerization of PLA
$\overline{DP}_{acry}$	Degree of polymerization of acrylate end-groups
E	Compressive storage modulus
$E^0_{R,i}$	Modulus of network *i* in the rubbery state
ΔG_{el}	Elastic free energy
$\Delta G_{hydrogel}$	Free energy of hydrogel network
ΔG_{mix}	Flory –Huggins free energy of mixing
l	Bond length along polymer backbone
λ	Number of links per unit
$\bar{M}_i$	Molecular weight of chains in network *i*
$\bar{M}_c$	Molecular weight between crosslinks
$\bar{M}_{Ci}$	Molecular weight between crosslinks of network *i*
$\bar{M}_n$	Number-average molecular weight
$\bar{M}_{ni}$	Number-average molecular weight of polymer *i*
M_r	Molecular weight of repeat unit
μ_1^0	Chemical potential of solvent outside gel
μ_1	Chemical potential of solvent inside gel

N	Number of bond vectors per chain
n_i	Moles of solvent (i =1) and polymer (i = 2)
$\emptyset_i^0$	Relaxed polymer volume fraction of network i
$\emptyset$	Swollen IPN volume fraction
$\emptyset_i$	Volume fraction of network i
q	Swelling ratio
Q	Volumetric Swelling ratio
R	Gas Constant
$\bar{r}_0^2$	Mean square end-to-end distance of network chains in unperturbed state
ρ	Crosslink density
ρ_i	Density of network i
ρ_p	Density of polymer
ρ_s	Density of solvent
ΔS_{el}	Entropic elasticity of the network
T	Temperature
T_g	Glass transition temperature
T_m	Melting temperature
$\bar{\nu}$	Specific volume
ν_1	Volume fraction of solvent
ν_2	Swollen polymer volume fraction
$\nu_{2,r}$	Relaxed polymer volume fraction
ν_e	# of effective network chains
ν_e^*	Effective network chain density
V_1	Molar volume of solvent
V_r	Volume of polymer in relaxed state

V_s	Volume of swollen polymer
w_i	Initial sample dry weight (as prepared)
w_d	Extracted sample dry weight
w_m	Final mass dry weight
w_s	Swollen sample weight
ξ	Mesh size
$\bar{x}_{PLA}$	Degree of polymerization of PLA per chain end
ζ_e	Moles of effective chains in network

LIST OF ABBREVIATIONS

AA	Acrylic acid
AAm	Acrylamide
DMA	Dynamic Mechanical Analysis
DN	Double Network
DSC	Differential Scanning Calorimetry
EO	Number of ethylene oxide units
FDA	Food and Drug Administration
FTIR	Foruier Transform Infrared Spectroscopy
GAGs	GlycosAminoGlycans
GPC	Gel Permeation Chromatography
IPC	Interpolymer Complx
IPN	Interpenetrating Polymer Network
K_2CO_3	Potassium Carbonate
LA	Number of lactic acid units
MW	Molecular weight
$NaNO_3$	Sodium Nitrate
N-BAAm	N,N-methylenebisacrylamide
NC	Nanocomposite Gels
NMR	Nuclear Magnetic Resonance Spectroscopy
PAA	Poly(Acrylic Acid)
PAAM	Polyacrylamide
PAMPS	Poly(2-Acrylomido-2-Methylpropane-Sulfonic acid)/
PBS	Phosphate buffer solution

PCL	Poly(ε-Caprolactone)
PCL-b-PEG-b-PCL	Poly(ε-Caprolactone)-*b*- Poly(Ethylene Glycol)-*b*- Poly(ε-Caprolactone)
PEG	Poly(Ethylene Glycol)
PEG-DA	Di-acrylated Poly(Ethylene Glycol)
PEG-DM	Di-methacrylated Poly(Ethylene Glycol)
PEO	Poly(Ethylene Oxide)
PHEMA	Poly(Hydroxyethyl Methacrylate)
PLA	Poly(Lactic Acid)
PLA-b-PEG-b-PLA	Poly(Lactic acid)-*b*- Poly(Ethylene Glycol)-*b*- Poly(Lactic acid)
PMMA	Poly(Methyl Methacrylate)
PNIPAAm	Poly(N-isopropylacrylamide)
PVA	Poly(Vinyl Alcohol)
Seq-IPN	Sequential Interpenetrating Polymer Network
sGAG	Sulfated Glycosaminoglycan
SR	Slide-Ring Gels
TE	Tissue Engineering
TEA	Triethylamine

SUMMARY

Biodegradable polymer hydrogels have become very promising materials for use in tissue engineering. Hydrogels are typically used as scaffolds within which cells can be seeded for regeneration of damaged tissue. Ideally, these hydrogels should be easily implanted in the body in a minimally invasive manner, should be relatively highly swollen in order to allow adequate transport of nutrients, and should degrade safely in the body while new tissue is regenerated. Additionally, for optimal success, an increasing number of studies indicate that matching the mechanical properties of the hydrogel with those of the tissue being replaced is a significant factor. While a wide variety of hydrogels with a number of these individual properties exist, few hydrogels have a combination of all these properties. For instance, it is rare for hydrogels to have good mechanical properties at high swelling degrees, and few hydrogels with persistently good mechanical properties are also biodegradable and/or easily implanted in a non-invasive manner. This study seeks to combine a number of the qualities that make a hydrogel ideal for tissue engineering by investigating the development of a fully injectable and biodegradable hydrogel with enhanced mechanical properties that persist at high degrees of swelling.

More specifically, the goal of this research is to develop and investigate the swelling, mechanical and degradation properties of biodegradable hydrogels with potentially enhanced stiffness mechanical properties, with the fundamental components consisting of a complex-forming polymer pair of poly(ethylene glycol) (PEG) and poly(acrylic acid) (PAA). The hydrogels are synthesized with a specific interpenetrating

polymer network (IPN) strategy, referred to as a double network (DN) strategy, that has been used to enhance the mechanical properties of a variety of non-degradable hydrogels but has only been applied to a few biodegradable hydrogels.

The biodegradable DNs were formed by adding degradable functionalities to the PEG and PAA network components. The biodegradable PEG component was prepared using an existing method, where ABA-type block copolymers were first synthesized in order to form poly(lactic acid)-*b*-ploy(ethylene glycol)-*b*-poly(lactic acid) (PLA-*b*-PEG-*b*-PLA) hydrogels with hydrolytically labile PLA units. Then, in order to make these copolymers photo-crosslinkable, the chain-ends of the copolymers were functionalized with acrylate groups to form di-acrylated PLA-*b*-PEG-*b*-PLA macromers. For experimental purposes, PEG molecular weights of 2000, 4000 and 8000 g/mol were used. The obtained macromers were then photo-polymerized in the presence of a photoinitiator to form biodegradable PLA-PEG-PLA hydrogels with molecular weight between crosslink ($\bar{M}_c$) values that depended on the PEG molecular weight. Additionally, during preparation of the hydrogels, two different macromer concentrations (25% and 50%) were used for each PEG molecular weight to yield hydrogels with additional variations in $\bar{M}_c$.

For the degradable PAA component, acrylic acid (AA) monomers were photopolymerized in the presence of a photoinitiator and a biodegradable crosslinker. The biodegradable crosslinker was made by synthesizing di-acrylated PLA-PEG-PLA macromers similar to the ones described above, but with a low PEG molecular weight of 600 g/mol. For photopolymerization of the PAA component with this crosslinker, a

constant AA volume fraction of 0.8 was used with two different crosslinker concentrations (1% and 8%).

The degradable DN hydrogels were prepared using a sequential polymerization process with PLA-PEG-PLA as the 1st network and the PAA component as the 2nd network. The PLA-PEG-PLA hydrogels were photopolymerized and then swollen to equilibrium in AA monomer solutions for subsequent photopolymerization of the degradable PAA component within the PLA-PEG-PLA hydrogel. Single-network PLA-PEG-PLA hydrogels and single-network PAA hydrogels (with biodegradable crosslinker) were also photopolymerized for comparison to the DNs. The chemical and structural characteristics of the obtained copolymers, macromers and networks were characterized by nuclear magnetic resonance (NMR), Fourier transform infrared (FTIR) spectroscopy, gel permeation chromatography (GPC) and swelling measurements. For all of the hydrogels, swelling and degradation were characterized over various time periods through gravimetric measurements, the storage modulus was characterized over appropriate degradation periods using dynamic mechanical analysis (DMA), and the thermal behavior was characterized using differential scanning calorimetry (DSC).

CHAPTER 1

INTRODUCTION

This research seeks to investigate the development of degradable DN hydrogels with mechanical properties that persist at high degrees of swelling, in an attempt to closely match the properties of natural tissues in the human body. Natural tissues such as cartilage are often made up of over 75% water by weight but still have surprisingly high strength and stiffness properties. DN hydrogels, which have received increasing attention since their development (over the last decade or so), seek to achieve similar mechanical properties by partially mimicking the structure of natural tissues. Yet, the development of *biodegradable* DN hydrogels with these properties has not received as much attention, despite the fact that degradation is a significant, regularly occurring process that takes place within the extracellular matrix of natural tissues. In the present study, fully degradable DN hydrogels were synthesized and their macroscopic properties were compared to those of the component single-network hydrogels. The thermal, swelling, degradation and mechanical properties of the single-network and DN hydrogels were characterized.

First (in Chapter II), background on the use of hydrogels in tissue engineering is presented, followed by a description of the properties and functions of natural tissues and the relative achievements of synthetic polymers. Next, the significance of the preparation techniques used in this study is related, and useful theories that have previously been developed for characterization of the properties of hydrogels are explained.

Chapter III describes the experimental methods used to prepare the single-network and DN hydrogels in this study. This begins with synthesis procedures for the copolymers and macromers of the PLA-PEG-PLA component and also includes methods used for photopolymerization of both the PLA-PEG-PLA and PAA networks. This chapter also describes the characterization techniques used to verify the chemical and physical structure of the copolymers, macromers and final networks. The actual characterization results are presented and discussed in the following chapter (Chapter IV) and are then used to understand and interpret the behavior (macroscopic properties) of the swollen single and DN hydrogels, which are presented in Chapter V.

Chapter VI presents concluding remarks and makes suggestions for future direction in which the work in the this study can be expanded. Appendix A contains the graphs obtained for GPC results, which were used to characterize $\bar{M}_n$ of the PAA networks for calculation of $\bar{M}_c$.

CHAPTER 2

BACKGROUND

In this chapter, a summary of the use of hydrogels in tissue engineering is given, with emphasis on systems where concurrent drug or growth factor transport is advantageous. The properties of hydrogels that are most significant for these applications are discussed. Additionally, the types of polymers and methods used in this study are described, and the definition and history of DN hydrogels is explained. Finally, theories relevant to the analysis and characterization of hydrogels are presented.

2.1 Hydrogels in Tissue Engineering

2.1.1 Hydrogels

Hydrogels are crosslinked polymer networks that can be swollen to several times their original weights without dissolving in aqueous environments. They have been studied at least since the 1960's when poly(hydroxyethyl methacrylate) (PHEMA) hydrogels were first synthesized by Wichterle and Lim [1, 2]. Since then, the biocompatibility of hydrogels has been widely recognized, and extensive research has been done on the characteristics of hydrogels that make them useful as biomedical materials [3-5]. Hydrogels have played a key role as implantable materials in biomedicine, particularly for applications such as tissue engineering [6-9] and controlled drug delivery [10-13]. In general, the effectiveness of hydrogels as a biomaterial comes from the similarities between the swollen network structure of hydrogels and the

hydrated, porous structure of many natural tissues. By one definition, at least 10% of the total weight (or volume) of a hydrogel is constituted by water, with superabsorbent hydrogels containing over 95% water [14].

Commonly used non-degradable biomedical hydrogels include those made from poly(methyl methacrylate) (PMMA), which has often been used in contact lenses, poly(acrylic acid) (PAA), which has often been used as a superabsorbent material in diapers, and poly(ethylene glycol) (PEG), which has been used in a wide range of drug delivery and tissue engineering applications. Biodegradable hydrogels are often made from natural polymers such as collagen, chitosan or agarose, as well as from synthetic polymers such as polyphosphazenes, polyphosphoesters, or block copolymers that incorporate biodegradable poly(α-esters) like poly(lactic acid) (PLA) and poly(ε-caprolactone) (PCL) [15-17]. When placed in the human body, degradation of these hydrogels occurs either enzymatically (in the presence of specific enzymes) or by hydrolysis in aqueous environments.

2.1.2 Tissue Engineering Strategies

Tissue engineering (TE) strategies typically involve the use of three main components: 1) a scaffold material that mimics the structural and chemical functions of the extracellular matrix, 2) cells that are seeded throughout the scaffold for the synthesis of new tissue, and 3) growth factors or other soluble drugs that are incorporated for the enhancement of tissue regeneration. For choice of a scaffold material, a wide variety of polymer hydrogels, sponges and fibrous meshes have been investigated. In particular, hydrogels are useful as scaffold materials because their precursor solutions can often be

injected into tissue defects of various sizes and shapes for subsequent formation. Using mild photopolymerization techniques, it is also possible to incorporate cells and soluble growth factors into the hydrogel precursor solution, resulting in a uniform distribution of these components after polymerization. Additionally the hydrophilic, swollen, porous nature of hydrogels makes them resistant to protein adsorption and helps to give them good transport properties, allowing for the diffusion of gases, nutrients and waste products during tissue regeneration. For the engineering of cartilage, the highly swollen nature of a three-dimensional hydrogel scaffold provides an environment similar to native cartilage that can allows the morphology and phenotype of the chondrocyte cartilage cells to be maintained for appropriate regeneration of new tissue [18].

From a biomimetic point of view, the equilibrium swelling properties of hydrogels can easily be made to match those of human tissues such as articular cartilage and bone (typically greater 75% water). However, until recently, hydrogels have generally been regarded as having far inferior mechanical properties compared to natural tissue, especially at high degrees of swelling. In fact, the poor mechanical properties of hydrogels has been one of the main limitations for the use of hydrogels in tissue engineering and drug delivery applications [7, 19].

Yet, a number of recent advances have succeeded in significantly improving the mechanical properties of these materials. For instance, the double network (DN) strategy, based on a specific kind of interpenetrating network formation, has led to the development of hydrogels with modulus and strength properties that approach those of natural cartilage. To date, the DN strategy has only been used for a few biodegradable

polymer hydrogels, with the majority of the research being carried out on non-degradable hydrogel combinations.

At the same time, recent studies show that the hydrogel mesh size, modulus and degradation capability all appear to have significant individual effects on the apoptosis, proliferation, differentiation and/or homeostasis of cells [20-24]. The effects of these factors on cellular activity vary depending on the type of cells and tissue being generated. As a result, one of the recurring suggestions made in these studies has been that matching not only the hydrogel modulus, but also the hydrogel mesh size (or permeability) and degradation rate to that of the native tissue may be advantageous for obtaining cellular behavior and regeneration of new tissue as desired. Since the extracellular matrices of natural tissues have a wide variety of permeability, degradation and modulus properties, developing hydrogels with unique combinations of these attributes may lead to new tissue regeneration possibilities.

2.1.3 Importance of Biodegradation

Ideally, hydrogels for tissue engineering applications should be biodegradable for a number of reasons. First, the use of biodegradable hydrogels helps to avoid the chronic inflammation responses associated with permanent implants or the need for invasive removal surgeries [25]. Secondly, biodegradability presents the opportunity for the degradation rate of the hydrogel to be matched with the rate of synthesis of new tissue, which has been found to be favorable for cellular viability [3, 26]. For instance, Bryant and Anseth investigated optimal hydrogel degradation rates and characteristics for tissue regeneration and found that degradation uniquely allows hydrogels to initially support

high physiologically relevant compressive loads while allowing changes in mesh size over time that can facilitate regeneration [20, 27, 28]. In one study, they found that degradable hydrogels of PLA-PEG-PLA copolymerized with di-acrylated PEG (PEG-DA) had several favorable outcomes when a higher percentage of degradable crosslinks were incorporated [28]. They found that DNA content in the hydrogels doubled, the total collagen content increased significantly, and type II collagen was distributed more uniformly when the hydrogels had higher percentages of degradable crosslinks. In a related follow-up study, it was found that chondrocytes in biodegradable hydrogels of high initial modulus yielded cartilage that was rich in glycosaminoglycans (GAGs) and collagen [27]. Furthermore, in a more extensive study, Benoit et al. found similar results for di-methacrylated PEG (PEG-DM) hydrogels copolymerized with PLA-PEG-PLA. They found that metabolic activity, alkaline phosphatase production, osteopontin and collagen type I gene expression, and mineralization all increased as the content of degradable PLA-PEG-PLA in the hydrogels was increased [29].

Lastly, when growth factors or other drugs are incorporated into the hydrogel for release, degradation can be used to complement diffusion-controlled release, providing an additional method of control over the drug-release profile [30-32]. A wide variety of biodegradable hydrogels have been identified with the ability to undergo tunable enzymatic and hydrolytic degradation under physiological conditions [15].

2.1.4 Significance of Mechanical Properties

As an increasing amount of attention has been paid to the role of biomechanics in the success of tissue engineering approaches, the need for biodegradable scaffolds with

mechanical properties that approach those of the native tissue has also become more evident [26, 33]. A growing number of studies has revealed that mechanical properties on both the microscopic and the macroscopic level play significant roles in cell-signaling and hence on the synthesis of extracellular matrix tissues, which can be mimicked in the regeneration of tissues from cell-seeded scaffolds [6, 34]. On the micromechanical scale, the stiffness modulus of the scaffold is responsible for the transmission of physical cues to cells, which affects the differentiation, proliferation and migration of these cells [21, 33, 35, 36]. Several studies have found that a relatively high initial hydrogel compressive modulus (~ 0.1 – 0.5 MPa) can lead to increased type II collagen and sulfated glycosaminoglycan (sGAG) synthesis as well as homogenous GAG distribution [20, 23, 27]. This research suggests that ultimately the modulus can help to determine the type, quality, amount and spatial arrangement of tissue that is synthesized [37]. Therefore the stiffness modulus should ideally be tailored to mimic the mechanical environment of the tissue being synthesized [38]. As more information is learned about the effects of stiffness on various types of cells, tuning the modulus of hydrogel substrates could have great implications in regenerative applications including cardiomyoplasty, muscular dystrophy and neuroplasty [37, 39, 40].

Additionally, the stiffness of the hydrogel is important because a number of tissue engineering strategies have shown that applying mechanical stimulation to cell-seeded hydrogels can lead to enhanced tissue regeneration. However the results are highly dependent on the type of hydrogel in a manner that appears to depend at least partly on the hydrogel modulus. For instance, compared to PED hydrogels, it was found that the application of dynamic loads to cell-seeded agarose hydrogels resulted in more functional

tissue-engineered cartilage, with the obtained constructs having enhanced mechanical properties compared to those of free-swelling constructs. The outcome of the study suggested that the local biomechanical cues sensed by hydrogel-seeded cells are as dependent on the existing mechanical properties of the hydrogels as on the external loads and frequencies applied to the hydrogels [18].

2.1.5 Significance of Hydrogel Mesh Size

The hydrogel mesh size (ξ), and its effect on the equilibrium swelling of a hydrogel, are very important parameters for tissue engineering. The mesh size and the equilibrium swelling of hydrogels have been found to affect the synthesis of regenerated tissue directly through effects on cellular behavior and also less directly through effects on nutrient, oxygen and metabolite transport and the amount of space in the cellular microenvironment [21]. In one study on photopolymerized poly(ethylene glycol) (PEG) hydrogels, high swelling ratios of $q = 9.3$ (water content ~ 90%) lead to homogenous diffusion of glycosaminoglycan (GAG) diffusion throughout the hydrogel-tissue construct, whereas lower swelling ratios of $q < 5.2$ (water content $<$ 80%) lead to localization of GAGs in the pericellular region [20]. Several other studies have found that cell proliferation increased with the swelling ratios of the hydrogels investigated [21, 41, 42]. On the other hand, some studies have also shown that increasing the mesh size can have undesired effects for some types of cells and tissues as measured through rate of cell dispersion, collagen content or collagen expression [22, 24]. At the same time, it was suggested that these results may be related to the small fineness (diameter) of the investigated cartilage fibrils relative to the hydrogel mesh size, which may have lead to

collagen being lost. Compared to the nascent tissues investigated in the study (fibrils 10 to 20 nm in diameter), cartilage fibrils range widely in diameter from 10 to 150 nm depending on the zone and maturity of cartilage [22]. Thus, it was suggested that conflicting results for the effects of mesh size on tissue regeneration may be settled by future investigations into the regeneration of various types of tissues. The development of new systems and techniques allowing mesh size effects to be independently investigated in 3D hydrogels (which is already underway) will likely aid in this endeavor.

2.1.6 Properties of Cartilage and Bone

For the engineering of high load-bearing tissues such as cartilage and bone, the compression and shear modes are the primary modes of loading in vivo [43]. Cartilage in particular is subjected mostly to compressive strains [44]. The average water-content of human articular cartilage has been reported to have a minimum value around 72% [45, 46]. Yet due to the nature and structure of the extracellular matrix components, compressive modulus values for human native articular cartilage have been reported in the ranges of 0.5 – 1.0 MPa [20, 44] and 1.9 – 14.4 MPa [45, 46].

It is known that a pres-stress condition arises in cartilage between the confining collagen structure and proteoglycans that expand in the presence of water, resulting in resistance to applied mechanical loads [47]. At the same time, many of the extracellular matrix components are capable of being degraded by enzymes in the body for the appropriate remodeling of the matrix in coordination with both the transport needs and the actions of cells for the maintenance of the tissue. Finally, the high water-content of

cartilage aids in the transport of growth factors and other nutrients and helps to increase cell-affinity.

2.1.7 Photopolymerization of Hydrogels for TE

Photopolymerization has been used to form crosslinked hydrogel networks for a wide variety of biomedical applications, including hydrogels used as scaffolds for tissue regeneration and for drug delivery [8, 48, 49]. Photopolymerizable monomers or macromers usually contain two reactive groups. Such monomers and macromers include PEG di-acrylate or di-methacrylate based molecules, dextran methacrylate, modified poly(vinyl alcohol) (PVA), PLA-*b*-PEG-*b*-PLA, collagen and polysaccharides. Typically, bulk photopolymerization is used where a monomer or macromer is dissolved in solution with a photoinitiator and exposed to a light source that initiates free radical polymerization (through cleavage or hydrogen abstraction of the photoinitiator). For tissue engineering applications, photoinitiators are usually incorporated at low concentrations in the range of 0.0125 – 2 % w/w [48]. At the same time, crosslinkers, drugs and/or cells can be incorporated into the solution to form (for instance) a crosslinked network with cells seeded in the network scaffold (Figure 2.1). For photopolymerization with cells or tissues, this can safely be done if requirements such as low light intensity, short UV exposure time and an appropriate physiological temperature range are met. For subcutaneous tissue regeneration and drug delivery, the photopolymerization solution can be injected into the body and the light source can be applied transdermally for formation of the hydrogel [8]. UV light sources with wavelengths in the range of 330 - 450 nm and incident light intensities in the range of 2 -

100 mW/cm^2 have often been used for tissue engineering, drug delivery and cell encapsulation [48].

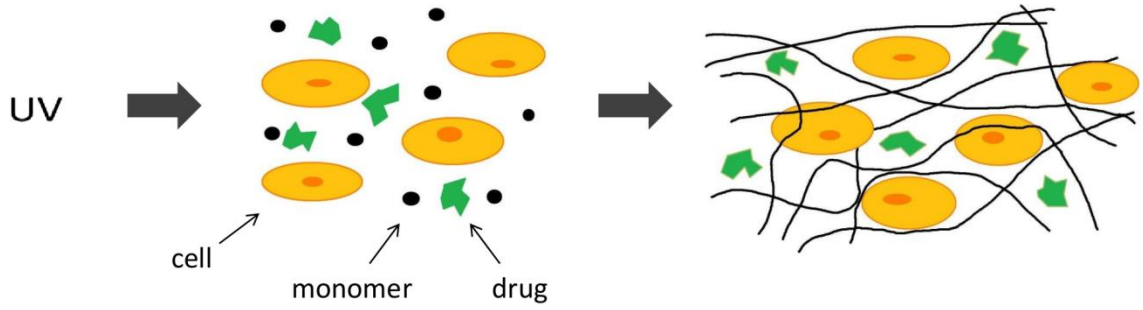

Figure 2.1. Idealized photopolymerization of polymer network with cells and drug incorporated

One of the advantages of photopolymerization includes the ability to have spatial and temporal control over the formation of the hydrogel, which can be performed *in vivo* non-invasively under the right conditions [48]. Additionally, complex shapes can be filled using photopolymerization, and macromers can be incorporated with a wide range of degradation and other characteristics [27]. Compared to other polymerization schemes, photopolymerization usually occurs rapidly (in a few minutes) which is advantageous for the incorporation of proteins and cells since minimal prolonged exposure to thermal energy can be avoided [50].

2.2 Types of Hydrogels

Hydrogel scaffolds commonly used for tissue regeneration of tissues such as cartilage have included natural polymers such as collagen, alginate and chitosan, as well as synthetic scaffolds such as polyl(lactic acid) (PLA) and poly(lactic-co-glycolic acid) (PLGA). Synthetic polymers are generally regarded as being easier to tailor for a wide range of mechanical and chemical properties, particularly through manipulation of factors such as molecular weight and crosslink density or through chemical modifications [51]. In particular, the use of block copolymers or end-linked hydrogels with well-defined structures and predictable, reproducible properties are advantageous.

2.2.1 PLA-*b*-PEG-*b*-PLA Hydrogels

Photopolymerized poly(lactic acid)-*b*-ploy(ethylene glycol)-*b*-poly(lactic acid) (PLA-*b*-PEG-*b*-PLA) hydrogels were most notably synthesized by Sawhney et al. in 1993 for use in biomedical applications [52]. Since then a number of groups have investigated the use of these hydrogels as degradable tissue engineering scaffolds and drug delivery matrices [28, 53-59]. The hydrogels are formed by first making ABA block copolymers of PLA and PEG [60, 61] and then adding either acrylate or methcrylate functionalities to the chain-ends to make them photopolymerizable. A schematic of the macromers obtained for photopolymerization of these hydrogels is shown in Figure 2.2.

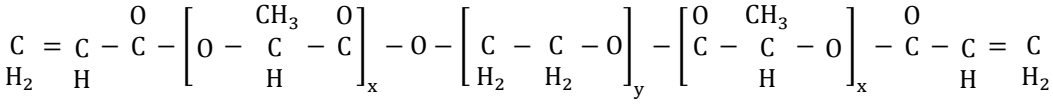

Figure 2.2. Photopolymerizable and biodegradable PLA-b-PEG-b-PLA hydrogels

The PEG component is hydrophilic and is responsible for the high-swelling of the hydrogels crosslinked from these macromers. At the same time, PLA provides points for degradation and the acrylate groups provide double bonds for network formation through processes such as photopolymerization. PEG is a biocompatible polymer that is resistant to protein adsorption, has good permeability, and has widely been used in biomedical applications [18, 22, 62, 63]. PLA is a United States FDA approved biodegradable polymer that is hydrophobic in nature and as has also been used extensively in biomedical applications [64].

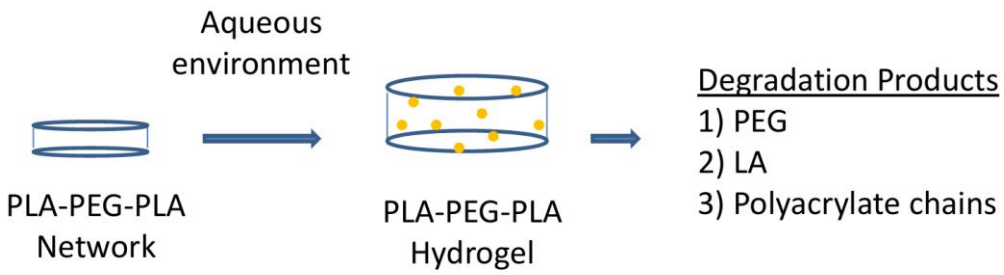

Figure 2.3. Degradation products of PLA-b-PEG-b-PLA hydrogels

The degradation scheme of the PLA-PEG-PLA hydrogels is shown in Figure 2.3 [54]. In aqueous environments the PLA ester linkages are hydrolyzed, and once enough PLA bonds are broken then fragments of the network begin to be released. The final degradation products are PEG chains, oligo(acrylic acid) chains (or polyacrylate chains) and monomeric or oligomeric lactic acid (LA) residues [52, 54]. The PEG blocks can be eliminated by the kidneys when the PEG MW is less than about 10,000 g/mol [65]. The degree of polymerization of the oligo(acrylic acid) chains is expected to be small enough to be soluble and relatively non-toxic, while the degradation products of lactic acid are natural metabolites that are naturally cleared by the body [52].

2.2.2 Degradable PAA Hydrogels

Poly(acrylic acid) PAA hydrogels have been used widely in tissue engineering and drug delivery applications due to their hydrophilic and pH-sensitive nature, permeability and biocompatibility [12, 46, 66]. While PAA is not degradable, it has previously been used as a crosslinked, copolymerized, grafted or semi-interpenetrated component in enzymatically and hydrolytically biodegradable hydrogels for a number of colon-specific drug delivery and cardiovascular tissue engineering investigations [12, 67-72]. Additionally, similar polyelectrolyte hydrogels such as meth(acrylic acid) (PMAA), have been crosslinked using biodegradable di-methacrylated poly(*ε*-caprolactone)-*b*-poly(ethylene glycol)-*b*-poly(*ε*-caprolactone) (PCL-*b*-PEG-*b*-PCL) crosslinkers for use as smart, pH-sensitive drug delivery systems [73]. Similarly, N-isopropylacrylamide (PNIPAAm) and acrylamide (AAm) copolymer hydrogels have been synthesized with biodegradable PLA-*b*-PEG-*b*-PLA crosslinkers, with potential use in drug delivery [74].

2.2.3 PEG/PAA IPNs

IPNs of PEG and PAA have previously been investigated by several authors, where the existence and effects of hydrogen bonding between the components has been one of the main interests [75-78]. PEG/PAA IPN hydrogels have also been investigated for a number of biomedical uses, including PEG/PAA DNs which have been developed and tested for use as artificial cornea implants and tissue engineering scaffolds [46, 79-86].

Additionally, in the dry state, the miscibility of PEO/PAA IPNs has previously been characterized [76]. For equimolar concentrations of PEO and PAA in an IPN, the

miscibility has been found to depend on two main characteristics: (1) the molecular weight of the PEO chains (which directly affects $\bar{M}_c$) in the first network and, (2) the crosslinking degree (or the $\bar{M}_c$) of the PAA second network. Intermediate PEO MWs (ranging from 600-2,000 g/mol) resulted in three transitions attributed to relaxations of the PEO-rich phase, the PEO-PAA complex and the PAA-rich phase. At the lowest PEO MW of 300 g/mol, only two transitions representative of the PEO- and PAA- rich phases were observed, suggesting that no complex-phase was formed at all. In contrast, at the highest PEO MW of 6,000 g/mol, a single loss modulus transition (or T_g) was observed, attributed to the existence of a single complex phase. However, for the 6,000 g/mol PEO network, only the lowest mol % crosslinker concentrations (0.5 to 2 mol %) for the PAA component yielded IPNs with a single T_g. When the PAA crosslinker mol % was increased above 2%, three loss moduli transitions appeared again. As mentioned above, this behavior is typical for IPNs consisting of polymer pairs that exhibit miscibility, although it is opposite to the behavior of regular IPNs, in which miscibility is usually enhanced by higher crosslinking of either component. Interestingly, the study also found that varying the MW of the PEO component (the first network) had a greater effect on the miscibility of the IPN than the crosslinking degree of the (second) PAA network did. This behavior was consistent with a determination by Sperling that the effect of the crosslink density of the first network on the domain sizes of phases in a seq-IPN should be about 10 times greater than the effect of the crosslink density of the second network [76, 87].

2.2.4 Summary of Hydrogels with Unique Mechanical Properties

A number of recent strategies have been successful in obtaining hydrogels with unique mechanical properties. For instance, nanocomposite (NC) and slide-ring (SR) hydrogels have been developed with extremely high extensibilities (up to 1000% for NC gels) [88, 89]. The key feature leading to the extensibilities of these gels are their mobile cross-link junction points, with the use of figure-eight shaped crosslinks for the SR gels and homogenously dispersed clay crosslinkers for the NC gels. In addition, scaffolds with geometrically fabricated (electrospun or micropatterned) structures have been developed with a range of mechanical properties. However, these scaffolds must be formed outside of the body and therefore require surgery for implantation.

For the development of robust, injectable hydrogel scaffolds that can be photopolymerized or otherwise formed in vivo, double network (DN) hydrogels are a very promising approach. Double network (DN) hydrogels are a class of interpenetrating polymer network (IPN) hydrogels that are formed through sequential polymerization using combinations of polymers with favorable interactions. The DN network strategy has been used successfully to obtain hydrogels with significantly enhanced strength and/or modulus properties. The choice of polymers used in the system is significant as the existence of favorable enthalpic interactions is believed to play a role in the enhancement of the hydrogel strength, through the formation of additional secondary-bond cross-links that help to stabilize main cross-link junctions. The enhancement of the young's modulus of the DN hydrogels is believed to be due to the existence of a "pre-stress" condition that arises due to differences in the equilibrium swelling of the two

interpenetrated networks used to form the DN hydrogel. DN hydrogels, as first introduced, generally tend to have the following characteristics in common:

1) The first network is made with a low molecular weight between cross-links ($\bar{M}_c$) and is usually brittle

2) The second network is made with a high $\bar{M}_c$ and is usually ductile (the strategy has also been successful when the second "network" or component has been un-crosslinked (leading to a semi-IPN) as long as the linear chains had a molecular weight above a critical value, $\bar{M}_{cr}$

3) The second component usually constitutes the majority of the overall network (is usually present in a higher molar ratio)

4) One of the networks is a neutral, flexible polymer and the other network is a polyelectrolyte

5) Favorable interactions usually exist between the two components, due for instance to the formation of inter-polymer complexes (IPCs)

6) The DNs are usually sequentially polymerized

DN hydrogel combinations that have been made with enhanced mechanical properties include poly(2-acrylomido-2-methylpropane-sulfonic acid)/polyacrylamide (PAMPS/PAAM) DN hydrogels [90] and poly(ethylene glycol)/poly(acrylic acid) (PEG/PAA) DN hydrogels [46]. The DN strategy has been used to obtain hydrogels at around 90% water-content with compression fracture strength on the order of up to 40 MPa despite the individual network components having strengths on the order of 0.2 MPa

[91]. At the same time, PEG/PAA DN hydrogels have successfully been made with a water-content around 65% and a modulus around 12 MPa, which is comparable to the properties of the human cornea and human cartilage [46]. While the properties of a number of the non-degradable DN hydrogels are similar to those of cartilage, there remain very few biodegradable hydrogels with mechanical properties similar to cartilage.

The toughening of the DN hydrogels has been connected to the favorable attractive enthalpic interactions between the polymer components of the DN hydrogels [92]. For instance, it was recognized that the toughness is greater for DN hydrogels composed of polymers with favorable intermolecular interactions than for DN hydrogels with no favorable intermolecular interactions. Hence, DN hydrogels of PAMPS/PAAM and PAA/PAAM were found to yield significantly better mechanical properties than DN hydrogels of PAMPS/PAMPS, PAA/PAA or PAAM/PAAM. Particularly, when strong cooperative interactions exist between polymers, (such as those that arise during interpolymer complex formation) it has been found that the regular repeating structure can lead to more uniformly distributed energy-dissipating mechanisms that help to prevent run-away fracture, potentially leading to enhanced fracture strength [92].

The enhances in initial modulus, on the other hand, are believed to be due to a pre-stress condition that is imparted as a result of the difference in swelling of the two networks [46]. This pre-stress condition arises due to the neutral nature of the first network and the high swelling of the second network, which is maximized particularly under ionizing conditions (typically at pH 7.4). As observed through the variation of parameters such as the molecular weights of each component, it is believed that the pre-stress condition tends to result in a higher initial modulus and an increase in the rate of

strain hardening over the stress-strain profile. A similar pre-stress condition exists in cartilage, in which proteoglycans expand against the main confining structure of cartilage resulting in an osmotically pre-stressed matrix system that resists mechanical loads [47].

2.3 Theory of Hydrogel Networks

A number of theories have been developed to characterize the swelling and mechanical properties of hydrogels. These theories can be used to calculate structural characteristics of the hydrogels such as the molecular weight between crosslinks ($\bar{M}_C$), the mesh size (ξ), and the crosslink density (ρ), and the effective number of cross-linked subunits, ν_e.

2.3.1 Equilibrium Swelling Theory

For the characterization of these parameters, equilibrium swelling theory and is very useful. The theoretical model developed by Flory and Rehner is one of the most established theories for determining the structural characteristics of hydrogels. Characterization of hydrogel swelling with this theory is based on the Flory-Huggins free energy of mixing between the polymer and solvent (ΔG_{mix}), balanced by the elastic free energy associated with expansion of the polymer network chains (ΔG_{el}) [5, 93]:

$$\Delta G_{hydrogel} = \Delta G_{mix} + \Delta G_{el} \quad (1)$$

The Flory-Huggins equation derived for ΔG_{mix} is [94]

$$\Delta G_{mix} = RT\left(n_1 \ln \nu_1 + n_2 \ln \nu_2 + \chi_1 n_1 \nu_2\right) \quad (2)$$

where n_1 and n_2 are the number of moles of solvent and polymer, and ν_1 and ν_2 are the volume fractions of solvent and polymer. χ_1 is the Flory polymer-solvent interaction parameter. The first two terms in the parentheses account for increases in entropy due to an increased number of distinguishable spatial arrangements that arise when polymer segments are mixed with solvent molecules, compared to the number of spatial arrangements possible for pure polymer or solvent molecules. Mixing is favored when

$\Delta G_{mix} < 0$, so these two entropic terms favor mixing ($\ln \nu_1$ and $\ln \nu_2$ are always negative). The last term in the equation incorporates the effects of polymer-polymer, solvent-solvent and polymer-solvent interaction energies, accounted for by χ_1. χ_1 depends on temperature and has been found to vary with ν_2.

For crosslinked polymer networks, the second term in parentheses becomes negligible since fully crosslinked networks are essentially made up of one molecule, which means that n_2 approaches zero. Therefore, for crosslinked polymer networks ΔG_{mix} simplifies to

$$\Delta G_{mix} = RT\left(n_1 \ln \nu_1 + \chi_1 n_1 \nu_2\right) \quad (3)$$

For the elastic energy contribution, ΔG_{el}, to the free energy ($\Delta G_{hydrogel}$) of the crosslinked polymer network, rubber elasticity theory is useful. The crosslinked networks are assumed to behave like an ideal rubber, responding to externally applied stresses only by uncoiling rather than by bond bending or stretching, thereby deforming without significant change in internal energy $(\partial E/\partial L = 0)$ [93]. For amorphous crosslinked materials above their glass transition temperature ($T > T_g$), this is a valid assumption since experimentally $\partial E/\partial L$ has been found to be very small. Therefore, the elasticity of the network is defined by its entropic elasticity [93]:

$$\Delta G_{el} = -T\,\Delta S_{el} \quad (4)$$

The entropic elasticity of the network, ΔS_{el}, is characterized by a decrease in the ability of the polymer network chains to assume as wide a variety of spatial conformations as the chains are extended during deformation (in response to applied force or to swelling of the network). Both Gaussian and non-Gaussian distributions have been used in the

derivation of ΔS_{el} to account for changes in the probabilities of accessible chain conformations during deformation. For instance, assuming a Gaussian distribution, derivation of the ΔS_{el} term leads to

$$\Delta S_{el} = -\frac{R\,\zeta_e}{2}\left(\alpha_x^2 + \alpha_y^2 + \alpha_z^2 - 3\right) \tag{5}$$

where α_x, α_y and α_z are linear expansion factors in the x, y and z directions accounting for positional changes in the ends of polymer segments during deformation. ζ_e is the moles of effective chains in the network. For isotropic swelling of a rubber-like polymer network in a solvent $(\alpha_x = \alpha_y = \alpha_z = \alpha)$, this equation simplifies to

$$\Delta S_{el} = -\frac{3\,R\,\zeta_e}{2}\left(\alpha^2 - 1\right) \tag{6}$$

which leads to

$$\Delta G_{el} = -T\,\Delta S_{el} = \frac{3RT\,\zeta_e}{2}\left(\nu_2^{-2/3} - 1\right) \tag{7}$$

since

$$\alpha = \nu_2^{-1/3} \tag{8}$$

The sum of ΔG_{mix} (Equation 3) and ΔG_{el} (Equation 4) gives the free energy of a swollen polymer network hydrogel:

$$\Delta G_{hydrogel} = RT\left(n_1 \ln \nu_1 + \chi_1 n_1 \nu_2\right) + \frac{3RT\,\zeta_e}{2}\left(\nu_2^{-2/3} - 1\right) \tag{9}$$

During swelling and expansion of the polymer networks, the force due to mixing decreases and the elastic force restricting swelling of the network increases until a balance is achieved leading to equilibrium swelling. At equilibrium, the chemical potentials μ_1 and μ_1^0 of the solvent inside the gel and of the pure solvent outside of the gel are equal. Since $\mu_1 - \mu_1^0$ is equal to the derivative of $\Delta G_{hydrogel}$ with respect to n_1 at

constant temperature (T), pressure (P) and n_2, the derivative can be set equal to zero at equilibrium swelling. By rearranging and substituting the derivative, the following equation for $\bar{M}_c$ can be obtained for networks with tetra-functional crosslinks, as was derived by Flory and Rehner [5, 95, 96]:

$$\bar{M}_c = -\rho_p V_1 \left(1 - \frac{2\bar{M}_c}{\bar{M}_n}\right)\left(\nu_2^{1/3} - \frac{\nu_2}{2}\right) [(\ln(1-\nu_2) + \nu_2 + \chi_1 \nu_2^2]^{-1} \quad (10)$$

where ρ_p is the density of the polymer, V_1 is the molar volume of the solvent, and $\bar{M}_n$ is the number-average molecular weight of the polymer before crosslinking (of the un-crosslinked polymer) [5]. The factor $(1 - 2\bar{M}_c/\bar{M}_n)$ arises as a correction for network imperfections accounting for loose dangling chain ends only connected to the network by one end. For perfect networks or for situations where $\bar{M}_n \gg \bar{M}_c$, the correction becomes negligible and approaches a value of one [5, 97].

In cases where the value of $\bar{M}_n$ is needed but is not immediately available, as in the preparation of a hydrogel by copolymerization or crosslinking with a crosslinker, $\bar{M}_n$ can be determined from polymerizing the main monomer under the same experimental conditions without the crosslinker [5]. $\bar{M}_n$ can also be calculated by using equations developed for free radical polymerization initiated by thermal homolysis of an initiator [98] or for a photopolymerized network [99] if values of the required parameters are available.

The value of ν_2, the polymer volume fraction, can be calculated from the dry weight (w_d) and the swollen weight (w_s) of the hydrogel using [100, 101]:

$$\nu_2 = \left[1 + \left(\frac{\rho_p}{\rho_s}\right)\left(\frac{w_s}{w_d} - 1\right)\right]^{-1} \quad (11)$$

which arises from the relationship $\nu_2 = 1/Q$ where Q is the volumetric swelling ratio ($Q =$ [volume polymer + volume solvent] / volume polymer) [22], and ρ_p and ρ_s are the densities of the polymer and solvent. For this calculation, volume additivity of the polymer and solvent adsorbed in swelling is assumed [101].

Equation 10, developed by Flory and Rehner, is for the swelling of networks that were crosslinked in the solid state. A similar equation was later derived by Peppas and Merrill for the equilibrium swelling of networks that were crosslinked from a solution [5]:

$$\bar{M}_c = -\rho_p V_1 \left(1 - \frac{2\bar{M}_c}{\bar{M}_n}\right)\left[\left(\frac{\nu_2}{\nu_{2,r}}\right)^{1/3} - \frac{1}{2}\left(\frac{\nu_2}{\nu_{2,r}}\right)\right](\nu_{2,r})[(\ln(1-\nu_2) + \nu_2 + \chi_1\nu_2^2]^{-1} \quad (12)$$

Here, $\nu_{2,r}$ is the polymer volume fraction immediately after crosslinking but before swelling, known as the relaxed polymer volume fraction. For a hydrogel crosslinked in the solid state $\nu_{2,r} = 1$ and Equation 12 simplifies back to Equation 10.

In addition to Equation 10 and Equation 12, which are based on a Gaussian model, non-Gaussian models have also been used to characterize the equilibrium swelling of highly crosslinked hydrogel networks. Highly crosslinked networks are better characterized using non-Gaussian models because Gaussian distributions assume that the end-to-end distance between network chain ends is much smaller than the contour length of the actual network chains. Peppas et al. [102] and Kovac [103] have made similar derivations of non-Gaussian models for highly crosslinked hydrogels. A useful model, developed by Kovac [103] provides the non-Gaussian calculation of $\bar{M}_c$ using a statistical treatment tailored for short chains and large deformations:

$$\bar{M}_c = -\rho_p V_1 \left(\nu_2^{1/3} + \frac{\nu_2^{-1/3}}{N} \right) [(\ln (1-\nu_2) + \nu_2 + \chi_1 \nu_2^2]^{-1} \quad (13)$$

where N is the number of bond vectors per chain and can be calculated from the relationship [5]

$$N = \frac{\lambda \bar{M}_c}{M_r} \quad (14)$$

λ is the number of links per repeating unit, which has a value of λ = 2 for all vinyl polymers. M_r is the molecular weight of the repeating unit.

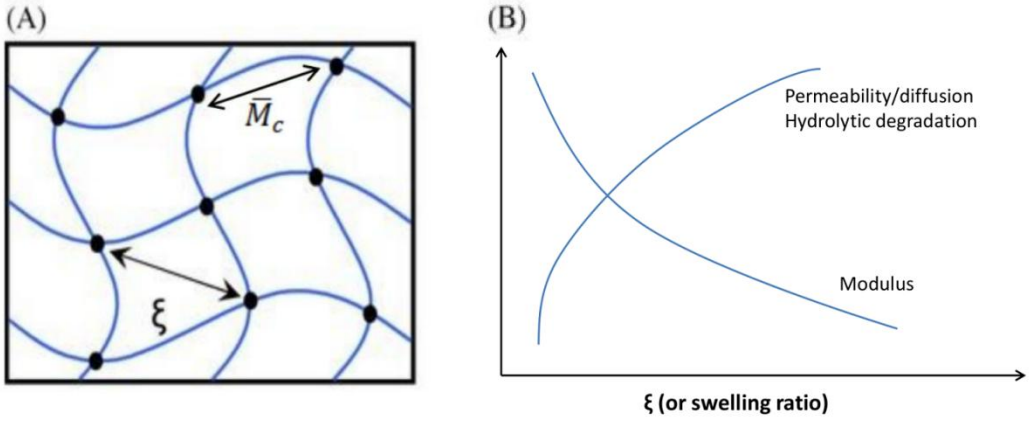

Figure 2.4. A) Hydrogel $\bar{M}_c$ and ξ, B) Effect of crosslink density on hydrogel properties (adapted from [50]

The crosslinking density of the polymer network, ρ, as defined by Flory [95] and Peppas and Merrill [104], is the average number of effective chains in the swollen volume of the polymer network. ρ can be calculated from the specific volume ($\bar{\nu}$) of the polymer and $\bar{M}_c$ as follows:

$$\rho = 1/(\bar{\nu}\, \bar{M}_c) \quad (15)$$

A theoretical crosslink density can also be calculated when a crosslinking agent is used, assuming both vinyl groups become effective with formation of an ideal network

without any free chain-ends [102]. In this case, the theoretical number of effective chains is

$$\nu = 2c \tag{16}$$

where c is the concentration of the crosslinking agent.

The polymer mesh size, ξ, is another significant parameter for swollen hydrogel networks that measures the actual space available for solute transport within the hydrogel. Since ξ is measured in angstroms (Å), it can be compared directly to the sizes of peptide and protein drugs that can be incorporated into the hydrogel for subsequent drug release. For tissue engineering purposes, the mesh size could be correlated to the potential transport of nutrients and growth factors when implanted in the body. The mesh size of the hydrogel network is calculated from $\bar{r}_0^2$, the mean-square end-to-end distance of the polymer network chains in the unperturbed state (without the effects of interactions between far-apart chain elements along the chains) [105]:

$$\bar{r}_0^2 = C_n N l^2 \tag{17}$$

C_n (obtained at large values of N) is the Flory characteristic ratio (or rigidity factor) of the polymer which arises from considering short-range chain interactions [98]. N is the number of bond vectors per chain (or number of links between crosslink junctions) as defined above in Equation 14, ($N = 2\,\bar{M}_c/M_r$). Additionally, l is the bond length along the polymer backbone chain. For C-C bonds, $l_{C-C} = 1.53$ Å, and for C-O bonds $l_{C-O} = 1.43$ Å [105, 106].

Then the mesh size, ξ, in the swollen state is calculated as [5]

$$\xi = \alpha\,(\bar{r}_0^2)^{1/2} = \nu_2^{-1/3}\,(\bar{r}_0^2)^{1/2} \tag{18}$$

which leads to

$$\xi = \nu_2^{-1/3} C_n^{1/2} \left(\frac{2\bar{M}_c}{M_r}\right)^{1/2} l \tag{19}$$

2.3.2 Rubber Elasticity Theory

For hydrogels crosslinked from solutions, expressions for the stress, τ, in terms of the deformation or extension ratio, α, have been developed and modified by several authors, including Silliman, and Peppas and Merrill [5, 107]. The following equation, developed by Peppas and Merrill, is applicable to a swollen outstretched sample crosslinked from solution [5]:

$$\tau = RT\, Q^{2/3} \left(\frac{\nu_e}{V_s}\right) \left(\frac{\bar{r}_i^2}{\bar{r}_0^2}\right) \left(\alpha - \frac{1}{\alpha^2}\right) \tag{20}$$

where ν_e is the number of effective chains in the network. The front factor $\left(\frac{\bar{r}_i^2}{\bar{r}_0^2}\right)$, which is the ratio of the mean square end-to-end distance of chains in a real network compared to that of isolated chains, is often assumed to be 1 [5, 108].

A similar equation has been developed for the compressibility modulus of a swollen hydrogel crosslinked from solution [109, 110]:

$$\tau = RT \left(\frac{\nu_{2,r}}{\nu_2}\right)^{2/3} \nu_2\, \nu_e^* \left(\alpha - \frac{1}{\alpha^2}\right) \tag{21}$$

where ν_e^* is the effective crosslink density (mol/cm^3 of effective network chains). Then, using constitutive relationships, the compressive modulus is

$$E = RT \left(\frac{\nu_{2,r}}{\nu_2}\right)^{2/3} \nu_2\, \nu_e^* \tag{22}$$

which leads to [101, 111]

$$E = RT\,\nu_{2,r}^{2/3}\nu_2^{1/3}\,\nu_e^* \tag{23}$$

2.3.3 IPN Hydrogel Theory

A general equation for the equilibrium-swelling characterization of seq-IPNs with a single T_g has been developed by Li et al. [112]. The equation has been proposed as a means of quantitatively characterizing the extent of physical crosslinks in IPNs that exhibit miscibility. It is based on an initial derivation by Thiele and Cohen that was developed to characterize the equilibrium swelling of homo-IPNs (specifically polystyrene/polystyrene IPNs) [113]. Thiele and Cohen's derivation was later modified by Siegfried, Thomas and Sperling to account for internal energy changes on swelling [114]. These equations have been found to fit the equilibrium swelling of IPNs better than the Flory-Rehner equation, which was developed for single-network hydrogels. The derivation by Li et al. is based on these developments, taking into consideration the theory of ternary systems consisting of two polymers in a solvent, leading to [112, 115]:

$$\begin{aligned}\ln(1-\emptyset) + \emptyset + \emptyset(\chi_1\emptyset_1 + \chi_2\emptyset_2) - \chi_{1,2}\emptyset_1\emptyset_2 = \\ -\frac{\rho_1 V_1}{\bar{M}_{C1}}\left(1-\frac{2\bar{M}_{C1}}{\bar{M}_1}\right)\left(\frac{1}{\emptyset_1^0}\right)^{2/3}\left(\emptyset_1^{1/3}-\frac{\emptyset_1}{2}\right) \\ -\frac{\rho_2 V_1}{\bar{M}_{C2}}\left(1-\frac{2\bar{M}_{C2}}{\bar{M}_2}\right)\left([\emptyset_2^0]^{2/3}\,\emptyset_2-\frac{\emptyset_2}{2}\right)\end{aligned} \tag{24}$$

where $\emptyset$ is the overall IPN volume fraction and $\emptyset_1$ and $\emptyset_2$ are the volume fractions of the two polymers in the IPN in the equilibrium-swollen state (so that

$\emptyset = \emptyset_1 + \emptyset_2$). $\emptyset_1^0$ and $\emptyset_2^0$ are the volume fractions of each polymer network component in the dry state of the IPN. χ_1, χ_2, and $\chi_{1,2}$ are the polymer-solvent and polymer-polymer interaction parameters, ρ_1 and ρ_2 are the densities of the two polymers, and V_1 is the molar volume of the solvent. $\bar{M}_{C1}$ and $\bar{M}_{C2}$ are the molecular weight between crosslinks of the individual polymer networks (as calculated through Flory-Rehner swelling measurements), and $\bar{M}_1$ and $\bar{M}_2$ represent the molecular weights of the two polymer networks (assumed to be ideal, so that $\bar{M}_1$ and $\bar{M}_2 \rightarrow \infty$). This assumption leads to slightly high values of $\emptyset$, especially at lower crosslink densities.

Siegfried, Thomas and Sperling developed an equation for the rubbery modulus of compatible seq-IPNs assuming good continuity and minimal chain conformation perturbation of the second polymer in the IPN. For additivity of the modulus contributions of the two network components, mutual network dilution and co-continuity of the two networks are assumed and any additional internetwork physical crosslinks are neglected. This leads to an equation for the modulus, $E_{R,IPN}$, of seq-IPNs composed of two polymers above their respective glass transition temperatures [114-116]:

$$E_{R,IPN} = 3RT\left(\emptyset_1^{1/3} N_1 + \emptyset_2 N_2\right) \tag{25}$$

$$E_{R,IPN} = \emptyset_1^{1/3} E_{R,1}^0 + \emptyset_2 E_{R,2}^0 \tag{26}$$

Here, $\emptyset_1$ and $\emptyset_2$ are the volume fractions of the two polymers components, N_1 and N_2 are the number of moles of network chains per cm^3 for each of the polymer components, R is the gas constant and T is the absolute temperature. N_1 and N_2 are determined from the rubbery modulus of the unperturbed single networks using the relationship $E = 3N_iRT$ (assuming a front factor of unity). Alternatively, $E^o_{R,1}$ and $E^o_{R,2}$, the modulus of the single networks in the rubbery state, can be used as in Equation 26. Since the single

networks are used to determine N_1 and N_2 (or $E^o_{R,1}$ and $E^o_{R,2}$), effects such as physical crosslinking, branching, and incomplete crosslinking in the seq-IPN are expected to be highlighted by experimental differences from the theoretically calculated modulus. Additionally, since both Equation 25 and Equation 26 ignore contributions due to mutual entanglements or added crosslinks, the experimental values of the IPN volume fraction and rubbery modulus are expected to be larger than those calculated from the theories [115].

CHAPTER 3

EXPERIMENTS

3.1 Synthesis and Preparation of Hydrogels

3.1.1 Synthesis of di-acrylated PLA-PEG-PLA Macromers

The di-acrylated PLA-b-PEG-b-PLA macromers, illustrated in Figure 3.1, were made in a two-step method by adapting procedures described in the literature [52, 53, 59, 117]. The PLA-PEG-PLA macromers were primarily made for the preparation of PLA-PEG-PLA hydrogels with varied chain lengths (using PEG MWs of 2000, 4000 and 8000 g/mol). Additionally, a fourth PLA-PEG-PLA macromer was made for use as a biodegradable crosslinker in the preparation of the PAA hydrogels (using a PEG MW of 600 g/mol).

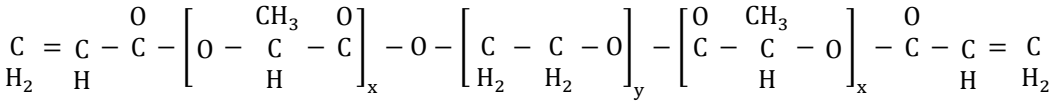

Figure 3.1. Di-acrylated PLA-b-PEG-b-PLA macromer

In the first step of the synthesis of the di-acrylated PLA-b-PEG-b-PLA macromers, tri-block PLA-b-PEG-b-PLA copolymers were formed through ring-opening polymerization. PEG was reacted with given amounts of d,L-lactide (3,6-dimethyl-1,4-dioxane-2,5-dione, Mw = 144.1 g/mol) at 120 °C , using stannous octoate as a catalyst. Prior to this reaction PEG was dried by azeotropic distillation in benzene and d,L-lactide was double-recrystallized in ethyl acetate. All glassware was dried at 100 °C for 24 hrs prior to the reaction. In a typical reaction, PEG (1 equiv) and d,L-lactide (5.5 equiv) were placed in a round-bottom flask, dissolved in anhydrous toluene (PEG concentration ≈ 50mM) and heated under stirring and argon flow until they were fully dissolved and

mixed well (around 90 °C). The reaction mixture was then cooled to room temperature, stannous octoate (tin-II-ethyhexanoate, 0.5 equiv) was added, and the reaction mixture was heated to 120 °C under stirring for 24hrs in an argon-flow atmosphere. At the end of 24 hrs, the copolymer was precipitated in heptane (250-500 mL) and then dried in a vacuum oven for 24 hrs at 40 °C.

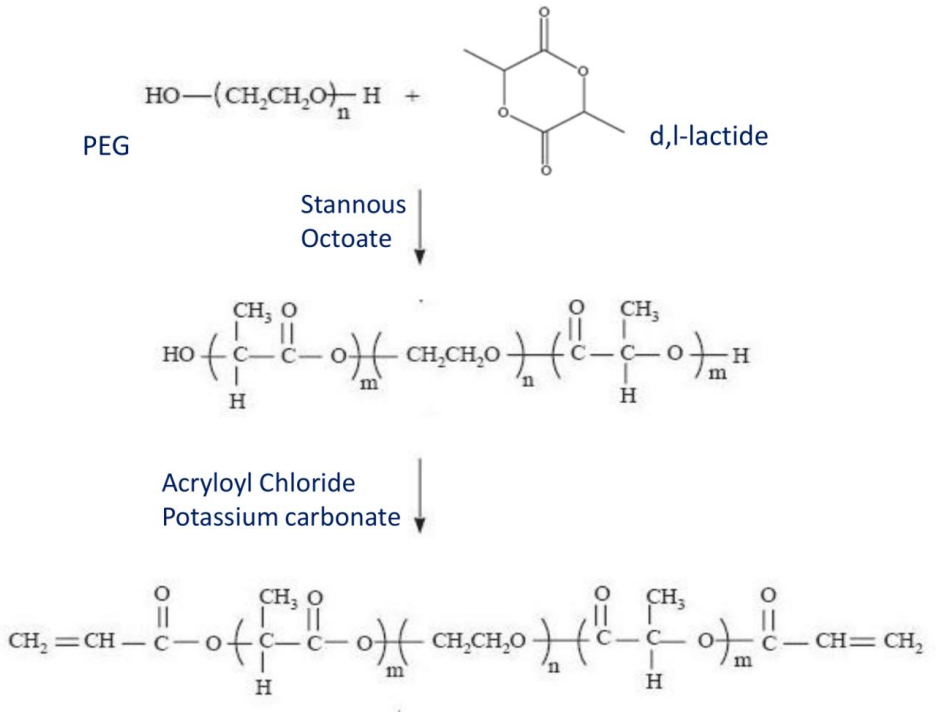

Figure 3.2. Synthesis steps for di-acrylated PLA-b-PEG-b-PLA macromer (adapted from [8])

In the second step, the obtained PLA-b-PEG-b-PLA copolymers were reacted with acryloyl chloride to functionalize the hydroxyl chain-ends with photo-crosslinkable acrylate chain-ends. In the literature, triethylamine (TEA) has been widely used as a proton scavenger for these kinds of reactions. However, potassium carbonate (K_2CO_3) was substituted for TEA in this study as has been done in a few recent studies due to concerns about the color-inducing effect and cytotoxicity of TEA [117, 118]. Prior to the reaction, K_2CO_3 was dried overnight at 110 °C and then cooled in a vacuum oven immediately before use. In a typical reaction, a PLA-b-PEG-b-PLA copolymer (1 equiv) was dissolved in dichloromethane (PLA-b-PEG-b-PLA concentration ≈ 15mM) in a

round-bottom flask with a magnetic stirrer and cooled to 0 °C in an ice bath. K_2CO_3 (30 equiv) was added to the solution under stirring and then acryloyl chloride (30 equiv) dissolved in ~ 2-10 mL dichloromethane was added drop by drop under argon flow. After all acryloyl chloride was added, the reaction was left for 24 hrs at room temperature under argon with vigorous stirring. At the end of the reaction, the mixture was filtered in order to remove solid side-products and unreacted K_2CO_3. The filtrate was then precipitated in heptane (250-600 mL), redissovled in dichloromethane and precipitated in heptane a second time. At that point, solid powders or waxy solids were obtained and were dried in a vacuum oven at 40 °C for 24 hrs.

3.1.2 Photopolymerization of PLA-PEG-PLA Hydrogels

A series of PLA-PEG-PLA hydrogels was made for single-network characterization and another series was made for use in the formation of PLA-PEG-PLA/PAA DN hydrogels. For preparation of each series, the di-acrylated PLA-PEG-PLA macromers described above (PEG Mw = 2000, 4000 and 8000 g/mol) were dissolved in distilled water to macromer concentrations of either 25 or 50 wt%. A photoinitiator, 2-hydroxy 2-methylpropiophenone (Darocur 1173), was added to the solution at a concentration of 1 % w/w photoinitiator with respect to the PLA-b-PEG-b-PLA macromer. This solution was then stirred well, sonicated in some instances to remove air bubbles, and pipetted into a square-shaped mold approximately 1.5 cm wide and 1mm deep. Next, argon gas was bubbled through the solution for 5 minutes in order to remove any dissolved oxygen, and the solution was placed into a UVX photo-crosslinker oven for a total of 4 hrs of UV exposure at a wavelength of 365 nm and an intensity of 4.5 mW/cm^2. Mid-way through the 4 hour period the crosslinked polymer

was flipped to allow even exposure to both sides. Thus, crosslinked PLA-PEG-PLA networks were obtained and disk-shaped samples were cut from the square films. The samples were then dried in a vacuum oven for 24 hrs at 50 °C and weighed to obtain an initial dry weight (w_i). Next, they were extracted though swelling in chloroform for 24 hrs, and dried and weighed again to obtain an extracted dry weight (w_d). The first series of PLA-PEG-PLA networks (diameter = 2.5 mm) was then used for the swelling, mechanical and degradation testing of single-network PLA-PEG-PLA hydrogels. The second series of PLA-PEG-PLA networks (diameter = 2 mm) was used for the formation of PLA-PEG-PLA/PAA DN hydrogels, as described further below.

3.1.3 Photopolymerization of PAA Hydrogels with Biodegradable Crosslinker

Degradable single-network poly(acrylic acid) (PAA) hydrogels were made by adapting procedures used in the literature for the preparation of (non-degradable) PAA hydrogels [46], degradable poly(N-isopropylacrylamide-co-acrylamide) (poly(NIPAAm-co-AAm) hydrogels [74], and degradable poly(methacrylic acid) (PMMA) hydrogels [73]. A photo-crosslinkable solution was made consisting of acrylic acid (AA) monomer, distilled water, Darocur 1173 photo-initiator (1 % v/v with respect to AA monomer), and a biodegradable PLA-PEG-PLA crosslinker. Prior to the solution preparation, the AA monomer was distilled by vacuum distillation for the removal of inhibitor. The biodegradable PLA-PEG-PLA crosslinker was synthesized using the method described above for synthesis of the di-acrylated PLA-PEG-PLA macromers, using a PEG MW of 600 g/mol. The solutions were made with a constant AA volume fraction of 0.8 and crosslinker concentrations of either 1 % or 8% v/v (with respect to the AA monomer).

The solutions were pipetted between 1 mm-thick glass slides using 0.2 mm-thick Teflon spacers and then placed in the UVX photo-crosslinker oven for a total of 4 hrs of UV exposure at a wavelength of 302 nm and an intensity of 4.5 mW/cm^2. After the first 10 min of UV exposure, the top glass slide was removed for direct UV exposure, and mid-way through the 4-hour period the crosslinked films were flipped. At the end of 4 hrs, the fully crosslinked PAA films were removed and cut into disk-shaped samples (diameter = 2.5 mm) which were then dried in a vacuum oven for 24 hrs at 50 °C and weighed (w_i). Next, the samples were extracted through swelling in absolute ethanol for 24 hrs, and dried and weighed again (w_d). At this point, these samples were used for the swelling, mechanical and degradation testing of the single-network degradable PAA hydrogels.

3.1.4 Photopolymerization of DN PLA-PEG-PLA/PAA Hydrogels

The DN PLA-PEG-PLA–PAA hydrogels were made through a sequential polymerization process. First, disk-shaped PLA-PEG-PLA networks (diameter = 2 mm, thickness ≈ 0.6 - 0.8 mm) were prepared as described above with PEG MWs of 2000, 4000 and 8000 g/mol. Then a photo-crosslinkable AA monomer solution was made in a manner similar to that described above for preparation of the degradable PAA hydrogels. The AA monomer solutions were made with a constant AA volume fraction of 0.8, a constant Darocur 1173 photoinitiator concentration of 1% v/v, and a biodegradable PLA-PEG-PLA crosslinker concentration of either 1 % or 8% v/v (with respect to the AA monomer). The disk-shaped PLA-PEG-PLA networks were swollen to equilibrium in these AA monomer solutions. After an hour of swelling, the swollen networks were

removed, carefully blotted dry with tissue paper, and irradiated in the UVX- photo-crosslinker oven for 4 hrs (flipping them after the first 2 hrs) in order to crosslink a PAA network interpenetrated within the PLA-PEG-PLA network. A UV wavelength of 365 nm was used. When crosslinking was complete, the interpenetrated DNs were removed, dried in vacuum at 50 °C for 24 hrs and weighed (w_i). They were then extracted through swelling in absolute ethanol for 24 hrs, dried again for 24 hrs and re-weighed (w_d).

3.2 Characterization of Macromers and Hydrogels

3.2.1 NMR Characterization of PLA-PEG-PLA macromers

The synthesized PLA-PEG-PLA macromers were characterized through use of proton nuclear magnetic resonance (^{1}H NMR). The macromers were dissolved in deuterated chloroform and the spectra were run on a Varian Mercury Vx 300 machine. PLA-b-PEG-b-PLA block copolymer formation was confirmed using the presence of a NMR spectrum peak at 4.3 ppm that represents the CH_2 protons of PEG at the linkages between PEG and PLA [119]. The average degree of polymerization of PLA ($\overline{DP}_{PLA}$) was calculated from the NMR peaks at 3.6 and 5.2 ppm, which correspond to the main-chain CH_2 protons of PEG and the CH protons of PLA respectively [119]. It was calculated using the equation

$$\overline{DP}_{PLA} = (M_{nPEG}/44) \times (LA/EO) \tag{27}$$

where M_{nPEG} is the molecular weight of the PEG center block (2k, 4k or 8k), 44 g/mol is the molecular weight of the ethylene oxide (EO) repeat units, and LA/EO is the ratio of lactic acid (LA) to EO repeat units. LA/EO was calculated as

$$\left(\frac{LA}{EO}\right) = Intensity\ of\ 5.2\ ppm\ peak/(Intensity\ of\ 3.6\ ppm\ peak/4) \tag{28}$$

Assuming that the PLA block lengths at each PLA-PEG-PLA chain-end are approximately equal, the average number of lactic acid units per PLA-PEG-PLA chain-end was calculated as

$$\bar{x}_{PLA} = \overline{DP}_{PLA}/2 \tag{29}$$

The di-acrylation of the PLA-PEG-PLA macromers was also characterized by ^{1}H NMR. Chain-end functionalization of the PLA-PEG-PLA copolymers with acrylate groups was quantified by calculating an average degree of polymerization for the acrylate groups ($\overline{DP}_{acry}$). Since the goal is to functionalize each chain-end with an acrylate group, ideally $\overline{DP}_{\text{acry}} = 2$. The $\overline{DP}_{acry}$ was calculated by comparing the intensity of acrylate vinyl group (CH_2=CH) peaks in the 5.79 - 6.43 ppm range with a peak at 4.3 ppm that represents the PEG CH_2 groups directly next to PLA block segments [59]. Since there are 2 such linkages per macromer chain, $\overline{DP}_{acry}$ was calculated as

$$\overline{DP}_{acry} = 2 \times \left(\frac{Intensity\ of\ 6\ ppm\ peaks/3}{Intensity\ of\ 4.3\ ppm\ peaks/2} \right) \tag{30}$$

From the calculations of $\overline{DP}_{PLA}$ and $\overline{DP}_{\text{acry}}$, $\bar{M}_n$ of the di-acrylated PLA-PEG-PLA macromers was calculated using the equation

$$\bar{M}_n = \bar{M}_{nPEG} + (\overline{DP}_{PLA} \times 72) + \left(\overline{DP}_{acry} \times 27\right) \tag{31}$$

where 72 g/mol is the molecular weight of the PLA repeating unit and 27 g/mol is the molecular weight of the acrylate end groups.

3.2.2 FTIR Characterization of Network Photopolymerization

The photo-crosslinked PLA-PEG-PLA, PAA and PLA-PEG-PLA/PAA samples were analyzed using an FTIR microscope. Thin films (< 1mm thick) were cut into circular disks (0.5 cm in diameter) and placed into a sample holder for FTIR analysis. Transmission Mode was used with 32 scans per sample in a wavenumber range of 4000 to 600 cm^{-1}. A background channel was run prior to the scans, and a baseline correction

was applied when the FTIR spectra were obtained. Crosslinking of the macromers was confirmed by the absence of FTIR spectra peaks in the 1650 – 1620 cm^{-1} range (representing stretching of C=C bonds). Peak assignments of other chemical groups were made, including assignment of a 1750 cm^{-1} peak representing C=O stretching due to copolymer formation with the PLA component [52, 60, 119, 120]. For the PAA and PLA-PEG-PLA/PAA networks, peak assignments at 1700 and 1730 cm^{-1}

3.2.3 Thermal/DSC Characterization of Hydrogel Networks

The thermal properties of the single and double networks were investigated by differential scanning calorimetry (DSC) (TA DSC Q200 V24.2 Build 107). DSC scans were run in the temperature range of -80 °C to 150 °C. Initially, the samples were cooled to -80 °C and held there for 2 min. For the first run, the temperature was ramped at a heating rate of 5 °C/min to 150 °C, where it was held for 2 min. Next (second run) the temperature was cooled to -80 °C at a rate of 5 °C/min and held for 2 min. Finally (third run), it was ramped once more to 150 °C at 5 °C /min. Melting temperatures (T_m) were taken from the first run using onset values, and glass transition temperatures (T_g) were taken from the third run using mid-point values.

3.2.4 Swelling and Degradation of Hydrogels

The swelling and degradation of the PAA and PLA-PEG-PLA single-networks and of the PLA-PEG-PLA/PAA DNs were characterized over various time periods. The samples were typically placed in about 20ml of phosphate buffered solution (PBS) (BDH

buffer solution, pH 7.4) in capped vials and placed in an oven at 37 °C over the swelling/degradation time periods. These time periods ranged from 2 hrs to 4 weeks. Prior to swelling in PBS, the samples were extracted by swelling them in given solvents (described above) for 24 hrs and were then removed, dried for 24 hrs, and weighed to obtain an initial extracted dry weight (w_d) with soluble content (sol content) removed. After swelling in PBS, the samples were removed at given time points, patted with tissue paper to remove excess PBS, and weighed to obtain a swollen weight (w_s). The swelling of the networks was then characterized by calculating the PBS content of the samples, using the equation [46]:

$$PBS\ content\ (\%) = \frac{w_s - w_d}{w_s} \times 100\% \tag{32}$$

Alternately, the swelling of the networks could also be reported in terms of the equilibrium swelling ratio, $q = \frac{w_s}{w_d} = \frac{1}{1-PBS\ content}$ (where PBS content is expressed as a fraction) [46, 120], or in terms of the volumetric swelling ratio, $Q = 1 + \left(\frac{\rho_p}{\rho_s}\right)\left(\frac{w_s}{w_d} - 1\right)$ [22, 121].

For characterization of the degradation of the networks, the swollen hydrogels were removed from PBS solution at various time points and dumped into Buchner funnels equipped with a vacuum pump. The various hydrogels were then treated as follows to obtain measurements of the final dry polymer weight (w_m): The single-network PLA-PEG-PLA samples were air dried for two hours and then dried in a vacuum oven for 24 hrs at 50 °C in order to obtain w_m. The swollen PAA and DN PLA-PEG-PLA/PAA samples were treated according to a method previously used for degradable poly(methacrylic acid) (PMAA) hydrogels [73]. First, they were washed extensively by

extracting them in an excess of distilled water for 24 hrs, changing the distilled water every 6 to 8 hours. In order to change the distilled water, the samples were dumped out into Buchner funnels equipped with a vacuum pump. At the end of the 24 hr period, the PAA and PLA-PEG-PLA/PAA samples were removed a final time, allowed to air-dry for a few hours, and then dried in a vacuum oven for 24 hrs at 70 °C in order to obtain w_m.

Then, the degradation of all of the networks was characterized though calculation of the mass loss using the equation [73, 120]:

$$mass\ loss\ (\%) = \frac{w_d - w_m}{w_d} \times 100\% \tag{33}$$

For the swelling and degradation calculations, an average of three samples was used for each hydrogel type and formulation at each removal time point.

3.2.5 PBS-Content Change of Hydrogels During Experiments

Swelling measurements were carried out in order to determine how much the PBS contents of the single and DN hydrogels typically change during the course of a DMA experiment. Single and DN 8k-2 PLA-PEG-PLA hydrogels were swollen to equilibrium in PBS over a 2hr period at 37 °C, at which point they were removed from the PBS, patted dry and weighed. The hydrogels were then placed uncovered in an oven at 37 °C for 15 minutes, with samples being removed and weighed in 5-minute intervals. These conditions were used to mimic the environment of the hydrogels during DMA testing, which typically requires about 5 minutes per sample.

3.2.6 Modulus/DMA Measurements of Hydrogels

The compressive storage modulus (*E*) of the hydrogels was measured using a Mettler Toledo (SDTA861e) DMA machine at a frequency of 1 Hz. The linear region in the strain plot was used for measurements of *E*. The measurements were performed at 37 °C with displacements between 0.4 and 11 μm. The *E* of the PAA and PLA-PEG-PLA single-networks and of the PLA-PEG-PLA--PAA DNs was tested over a degradation period of two weeks. The hydrogel samples were swollen in PBS solution (pH 7.4) at 37 °C for given lengths of time (2hrs, 24hrs, 3 days, 1 week, and 2 weeks) prior to the measurements of *E*. The samples were then removed, patted with tissue paper for removal of excess PBS solution, weighed, measured for their dimensions (thickness and diameter), and then placed in the DMA sample holder for testing. A maximum period of 2-3 min was allowed for measurement of each sample. For each hydrogel type and formulation at each removal time point, an average of three samples was used for the measurements of *E*.

3.2.7 GPC Determination of linear PAA MW

Gel Permeation Chromatography (GPC) was used to determine the MW of PAA in the absence of crosslinks under the same synthesis conditions used for preparation of the PAA hydrogels. First, un-crosslinked PAA samples were prepared by mixing a solution of AA monomer, distilled water and Darocur 1173 photoinitiator without any crosslinker. As in preparation of the PAA hydrogels, a volume fraction of 0.8 was used for AA monomer with 1% v/v photoinitiator with respect to the monomer. The same photopolymerization conditions were used as described above, using 20 min of UV

exposure. The PAA samples were then dissolved (10-20 mg/mL) in a 0.05 M $NaNO_3$ distilled water solution which was used as the eluent. GPC measurements were carried out with a Waters 1525 binary pump coupled to a Waters 2414 refractive index detector. Three PAA standards of known MW (50000, 100000 and 250000 g/mol) were used.

3.2.8 Structural Characteristics of Hydrogels

The structural characteristics of the hydrogels were calculated using Flory-Rehner equations, after swelling the networks for 2hrs in phosphate buffer solution (PBS) at 37 °C. 2hrs was chosen as an initial point of equilibrium swelling before degradation appeared to have a significant influence on swelling. This was based on the swelling and degradation profiles (shown below) of all the single and double network hydrogels. Beyond 2 hrs, further increases in swelling were seen but could be matched up with the degradation profile of the hydrogels (especially for the 8k hydrogel series).

Equation 12, the Peppas-Merrill equation, was used to calculate $\bar{M}_c$ of all of the hydrogels. For convenience, Equation 12 is restated here (solved for $1/\bar{M}_c$):

$$\frac{1}{\bar{M}_c} = \frac{2}{\bar{M}_n} - \frac{\left(\frac{1}{\rho_p V_1}\right)\left[\ln(1-\nu_2) + \nu_2 + \chi_1 \nu_2^2\right]}{\nu_{2,r}\left[\left(\frac{\nu_2}{\nu_{2,r}}\right)^{1/3} - \frac{1}{2}\left(\frac{\nu_2}{\nu_{2,r}}\right)\right]} \tag{34}$$

As described above, $\bar{M}_n$ is the number-average molecular weight of the polymer before crosslinking (in the absence of crosslinking), ρ_p is the density of the polymer, V_1 is the molar volume of the solvent (18.1 cm^3/mol for water/PBS), and χ_1 is the Flory polymer-solvent interaction parameter. $\nu_{2,r}$ and ν_2 are the polymer volume fraction in the relaxed state (immediately after crosslinking but before swelling) and in the swollen

state, respectively. The assumption $\nu_{2,r}$ = 1 was made here since the photopolymerized hydrogels in this study were dry at the end of polymerization (there was no weight loss after further drying) [122, 123]. A similar assumption has also been made in previous studies for photopolymerized PLA-b-PEG-b-PLA hydrogels [55, 58] and for acrylate-based hydrogels [100, 121, 124], where $\bar{M}_c$ was determined for the characterization of solute-release properties.

ν_2 was calculated from Equation 11, restated here for convenience [100, 101]

$$\nu_2 = \left[1 + \left(\frac{\rho_p}{\rho_s}\right)\left(\frac{w_s}{w_d} - 1\right)\right]^{-1} \quad (35)$$

where ρ_s is the density of the solvent (0.994 g/cm^3). The dry weight (w_d) and the swollen weight (w_s) of the networks were obtained from an average of three samples. For this equation, volume additivity of the polymer and solvent adsorbed during swelling was assumed [101].

For the single-network PLA-PEG-PLA hydrogels, $\bar{M}_n$ values of the di-acrylated PLA-b-PEG-b-PLA macromers (as calculated through NMR, Table 4.1) were used since the networks were formed by end-linking the macromers [58]. ρ_p was taken as the density of PEG = 1.1 g/cm^3 [98]. A value of χ_1= 0.426 was used for the Flory-Huggins interaction parameter for the PEG-water (or PEG-PBS) system [20, 125]. In a previous study, this value of χ_1 for PEG-water was found to be nearly independent of ν_2, at least in the investigated range of $0.04 \geq \nu_2 \leq 0.2$ [125]. In the present study, ν_2 fell within this range for all of the PLA-b-PEG-b-PLA hydrogels throughout their degradation, except for the 2k-50 hydrogels which had ν_2 values in the range of 0.196 – 0.29. Therefore, it is possible that χ_1 may not accurately represent the interaction parameter for

the 2k-50 hydrogels, because χ_1 generally shows a dependence on v_2. A second consideration is that using the χ_1 parameter of PEG neglects the PLA end-blocks of the polymer chains as well as the acrylate end-groups, which would also make a contribution to the value of χ_1 (for instance, PLA makes the chains more hydrophobic which could make the actual value of χ_1 higher, while the acrylate groups could have an opposite effect) [11, 58]. However, due to the small size of these end-groups, their contribution to χ_1 is expected to be relatively small, particularly at high PEG MWs.

For the single-network PAA hydrogels, the values $\rho_p = 1.22$ g/cm^3 and $\chi_1 = 0.45$ were used for PAA and the PAA-water system [126, 127]. $\bar{M}_n$ (the molecular weight in the absence of crosslinks) was estimated as $\bar{M}_n = 50{,}000$ g/mol based on the GPC results. This is expected to be a lower bound for the $\bar{M}_n$ of PAA.

For the DN PLA-PEG-PLA/PAA hydrogels, Equation 12 (same as Equation 34) was also used to characterize $\bar{M}_c$, in a manner similar to that previously used to estimate the $\bar{M}_c$ of IPNs [124, 126, 128]. Weighted averages were used to calculate values of ρ_p and χ_1 (based on mole fractions of ethylene oxide (EO) and acrylic acid (AA) repeat units in the DNs). In a similar fashion, mole fractions of PEG and PAA were used to obtain average values of $\bar{M}_n$ for the DNs. Since the AA uptake during sequential polymerization of the DNs (during swelling of the PLA-PEG-PLA networks with AA solution) was different for each PLA-PEG-PLA network type (2k-25 through 8k-50), the calculated mole fractions varied with each DN type.

Finally, the mesh size, ξ, of all of the networks was calculated using Equation 19, restated here:

$$\xi = \nu_2^{-1/3} C_n^{1/2} \left(\frac{2\bar{M}_c}{M_r}\right)^{1/2} l \quad (36)$$

For the PLA-b-PEG-b-PLA hydrogels, the $C_n = 4.1$ of PEG was used and an average length of C-C bonds ($l_{C-C} = 1.53$ Å) and C-O bonds ($l_{C-O} = 1.43$ Å) was taken, leading to $l = 1.463$ Å [105, 106]. For the PAA networks, the C_n = 6.7 of PAA was used with $l = 1.53$ Å [100, 126]. $M_r = 44$ g/mol was used for PLA-PEG-PLA repeat units and $M_r = 72$ g/mol for the PAA repeat units.

CHAPTER 4

SYNTHESIS AND PHOTOPOLYMERIZATION OF SINGLE AND DOUBLE NETWORK HYDROGELS

For formation of the double network hydrogels, PLA-PEG-PLA networks were used as the first component and novel degradable PAA hydrogels were used as the second component. Single networks of each component were also prepared for comparison to the double networks. First, using a combination of previous methods [52, 59], PLA-PEG-PLA copolymers were made and their chain-ends were terminated with acrylate groups to yield di-acrylated PLA-PEG-PLA macromers. Then, these macromers were photo-crosslinked into PLA-PEG-PLA networks by adapting a procedure previously used to form PEG networks [46]. Next, the degradable PAA network components were prepared based on a method found in the literature for the crosslinking of similar vinyl monomers [73, 74]. To ensure that the polymers in the present study were synthesized as desired, the PLA-PEG-PLA and PAA copolymers, macromers, single networks and double networks were characterized using NMR, FTIR, GPC and structural characteristic measurements.

In addition, for preparation of all of the hydrogels, several experimental parameters were varied leading to structural differences in the hydrogels. The structural characteristics of the hydrogels were analyzed using swelling and modulus measurements as well as NMR spectroscopy (to determine properties of the copolymers). For instance, for preparation of the PLA-PEG-PLA hydrogels, the MW of the center PEG block was varied using MWs of 2k, 4k and 8k during the copolymer formation step. NMR was then

used to calculate $\bar{M}_n$ of the copolymer chains, which could later be correlated to to the resulting Mc of the PLA-PEG-PLA hydrogels. In addition, two macromer concentrations of 25% and 50% were used in the preparation of the PLA-PEG-PLA hydrogels leading to different crosslinking degrees. Similarly, for the PAA component, biodegradable crosslinker concentrations of 1% and 8% v/v (with respect to the AA monomer) were used to vary the degree of crosslinking. For all of these hydrogels, Peppa-Merrill equations based on swelling and modulus measurements were used to determine structural characteristics.

4.1 PLA-PEG-PLA Single-Network

4.1.1 NMR Characterization of PLA-PEG-PLA Copolymer

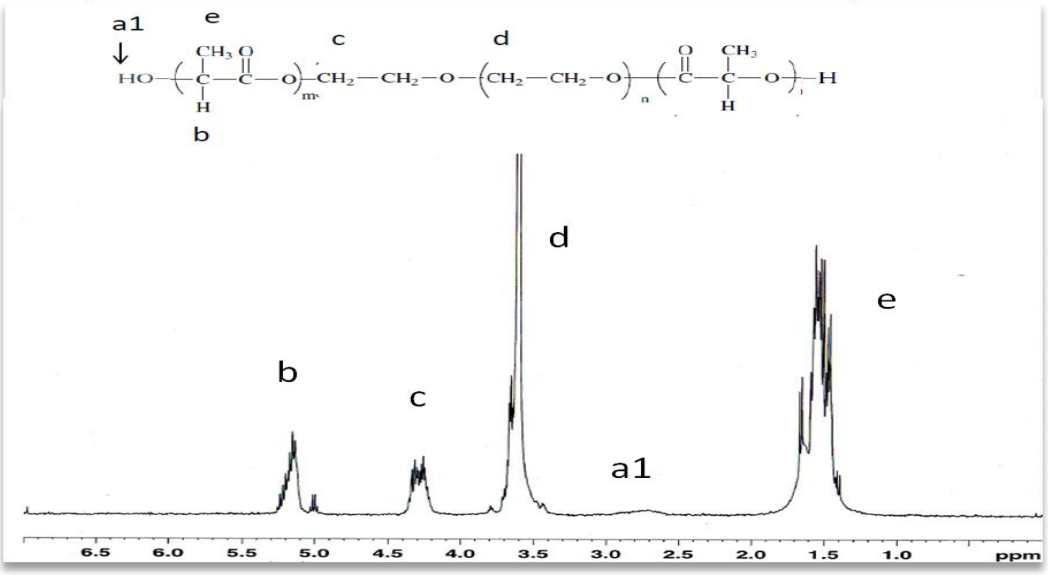

Figure 4.1. ^{1}H NMR spectrum of PLA-PEG-PLA copolymer (PEG MW = 600 g/mol)

A representative ^{1}H NMR spectrum (PEG MW 600) of the PLA-PEG-PLA block copolymers synthesized in this study is shown in Figure 4.1. Assignment of the NMR peaks matched those found in the literature for PLA-PEG-PLA block copolymers [61,

119, 129, 130]. NMR spectra bands at 4.3 ppm (**c**), which represent the CH_2 protons of PEG directly next to PLA blocks (–CH_2–O–CO–), confirmed formation of the block copolymers. The peak at 3.6 ppm (**d**) represents the PEG CH_2 groups within the main PEG block. Peaks at 5.2 ppm (**b**) and 1.5 ppm (**e**) were representative of the CH and CH_3 groups of the PLA blocks, respectively. Additionally, peaks at 5.0 and 1.69 ppm appeared on some spectra due to the CH and CH_3 protons of free (un-polymerized) lactide, as has also been found in previous studies [130]. For the copolymers before di-acrylation of the chain-ends, a peak around 2.8 – 2.9 ppm (**a1**) could be made out on some spectra due to the hydroxyl (OH) end groups of the copolymers.

Further, the degree of polymerization of the PLA blocks ($\overline{DP}_{PLA}$) was calculated from integration of the NMR peaks using the known molecular weight of the PEG center blocks. As described above, a lactic acid (LA) to ethylene oxide (EO) ratio was calculated from the NMR peaks at 5.2 and 3.6 ppm (representing the CH protons of PLA and the main-chain CH_2 protons of PEG) using Equation 28. $\overline{DP}_{PLA}$ was then found using Equation 27, and the average number of lactic acid units per PLA-PEG-PLA chain-end was approximated as $\bar{x}_{PLA} = \overline{DP}_{PLA}/2$ (Equation 29).

As shown in Table 4.1, for the 600, 2k, 4k and 8k block copolymers, $\bar{x}_{PLA}$ ranged from 3 to 8 LA groups per chain end. This led to low $\overline{DP}_{PLA}/\overline{DP}_{PEG}$ ratios for the 2k, 4k and 8k copolymers of around 10 to 20%. However, the ratio for the 600 copolymer was higher, around 44%. Nonetheless, all of the copolymers were soluble in distilled water. This is in keeping with previous reports in the literature that water solubility is imparted below a $\overline{DP}_{PLA}/\overline{DP}_{PEG}$ ratio of around 45% for these copolymers [52], and that lower PEG MWs favor solubility [119].

Table 4.1. ^{1}H NMR Characterization of the di-acrylated PLA-PEG-PLA Macromers

Macromer (PEG MW)	Copolymer: Molar feed ratio lactide/PEG	Copolymer: $\left(\overline{DP}_{PLA}\ \textbf{per chain end}\right)$	Copolymer: Ratio of $\overline{DP}_{PLA}/\overline{DP}_{PEG}$	$\left(\overline{DP}_{acry}\ \textbf{per chain end}\right)$	$\bar{M}_n$ of macromer (g/mol)
600 *	4	3	0.44	0.87	1079
2k	5.5	4.5	0.20	1.05	2705
4k	5.7	4.5	0.10	1.11	4708
8k	10	8	0.09	1.09	9211

4.1.2 ^{1}H NMR Characterization of Di-acrylated PLA-PEG-PLA Macromer

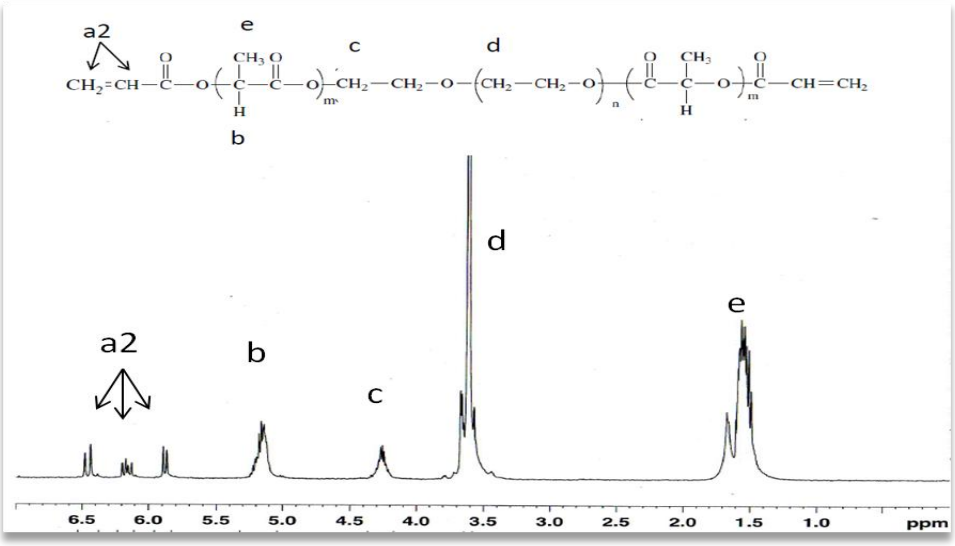

Figure 4.2. ^{1}H NMR spectrum of di-acrylated PLA-PEG-PLA macromer (PEG MW = 600 g/mol)

Figure 4.2 shows a representative NMR spectrum (PEG MW 600) obtained after di-acrylation of the PLA-PEG-PLA copolymers. Three sets of peaks around 6 ppm (**a2**) are representative of the protons of the vinyl (CH2=CH) groups, confirming acrylation of the end-groups of the copolymers. The peaks occur more specifically in the ranges of

6.46–6.50 ppm, 6.14–6.21 ppm and 5.88–5.91 ppm. As described above, integration of these peaks was compared to integration of the NMR peak at 4.3 ppm (**c**, representing the PEG CH_2 groups directly next to PLA block segments) in order to calculate $\overline{DP}_{acry}$ of the macromers (Equation 30).

As shown in Table 4.1, the $\overline{DP}_{acry}$ per chain end **(**$\bar{x}_{acry}$**)** was found to be approximately 1 for the 2k, 4k and 8k macromers, as calculated from NMR. This suggests that each chain-end of these macromers was functionalized with a photo-crosslinkable acrylate group as desired. For the 600 macromer (which was used for crosslinking of the PAA hydrogel), $\bar{x}_{acry}$ was found to have a slightly lower value of 0.87, which suggests that most, though not quite all, of the chain-ends were functionalized. These values of $\bar{x}_{acry}$ are consistent with those found in the literature for di-acrylation of PLA-PEG-PLA macromers [55, 57, 59].

In addition, the number average molecular weight ($\bar{M}_n$) of the di-acrylated PLA-PEG-PLA macromers was calculated using the known molecular weight of the PEG center blocks and the $\overline{DP}_{PLA}$ and $\overline{DP}_{acry}$ values calculated from NMR. These $\bar{M}_n$ values, obtained using Equation 31, are shown in Table 4.1.

4.1.3 FTIR Characterization of PLA-PEG-PLA Network Photopolymerization

The dry PLA-PEG-PLA networks were characterized through FTIR spectroscopy analysis. Figure 4.3 shows a representative FTIR spectrum obtained for the networks in this study. The FTIR spectrum matches up well with previous findings for PLA-PEO-PLA copolymers [52, 60, 119], PLA-PEO-PLA di-acrylated macromers [52, 120] and crosslinked networks. The absence of vinyl group (C=C stretching) peaks around 1650,

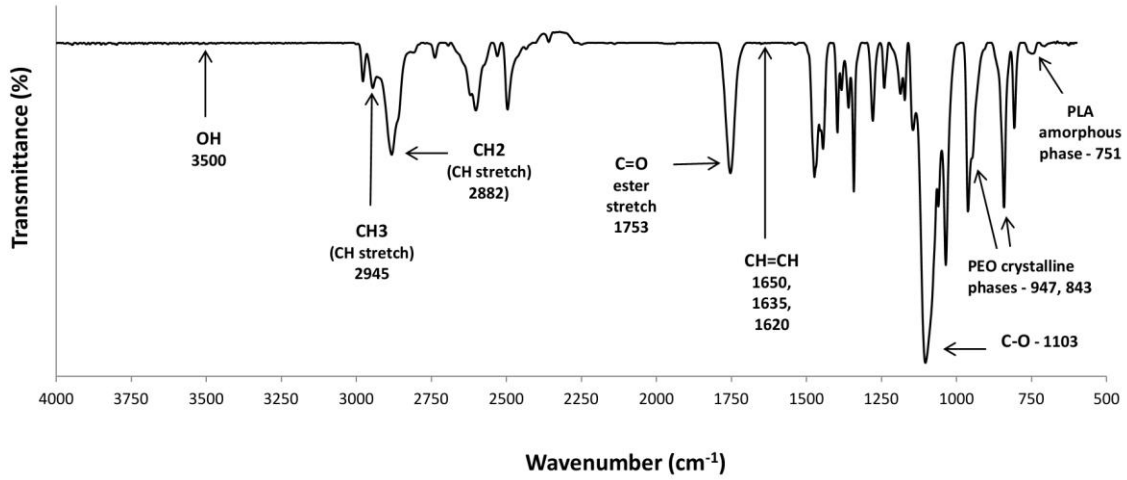

Figure 4.3. FTIR spectrum of photo-crosslinked PLA-PEG-PLA network (PEG MW = 8,000 g/mol)

1635 and 1620 cm^{-1} confirmed that crosslinking of the di-acrylated PLA-PEG-PLA macromers into networks occurred [73, 117, 131]. As is also expected, no hydroxyl (OH) end-group peaks are seen in the region of 3500 cm^{-1}. FTIR spectrum peaks at 1753 cm^{-1} and 1103 cm^{-1} were assigned to the carbonyl (C=O) and ether (C-O) groups, respectively. Other features of PEG and PLA were also present, such as a CH stretch peak from PEG CH_2 groups at 2882 cm^{-1}, and a CH stretch peak due to PLA CH_3 groups at 2945 cm^{-1}. Finally, the FTIR peaks at 947 cm^{-1} and 843 cm^{-1} suggested that PEG existed at least partially in the crystalline phase, while a peak at 751 cm^{-1} suggested that PLA was present in the amorphous phase.

4.1.4 Structural Characteristics of PLA-PEG-PLA Hydrogels

The initial $\bar{M}_c$ and ξ of the single network PLA-PEG-PLA hydrogels are shown in Table 4.2 (based on 2hrs of swelling in pH 7.4 PBS at 37 °C).

Table 4.2. Mc and mesh size of the PLA-PEG-PLA and PAA single-networks

Single-Network Hydrogel	$\bar{M}_n$ of macromer (g/mol)	$\bar{M}_c$ (Initial, g/mol)	Mesh size (ξ) (Å)
2k-25	2705	847	33
2k-50		427	20
4k-25	4708	1756	56
4k-50		1539	49
8k-25	9211	3705	97
8k-50		3160	80
PAA-1	50,000	24,569	364
PAA-8		22,342	274

$\bar{M}_c$ of the networks varied with both PEG MW (or $\bar{M}_n$ of the PLA-PEG-PLA macromer) and the macromer concentration used during photopolymerization. As expected, $\bar{M}_c$ values were highest for the 8k hydrogels and lowest for the 2k hydrogels, corresponding with differences in Mn of the macromers used for each network. At the same time, for a given PEG MW (2k, 4k or 8k), $\bar{M}_c$ was higher for the networks made with an initial macromer concentration of 25% than for those made with 50%. This occurs because decreasing the macromer concentration (or increasing the solvent concentration) in non-linear free radical polymerization reactions leads to an increase in the formation of primary cycles, a lower degree of crosslinking, and a higher $\bar{M}_c$ [53, 132]. Since the crosslinking of the PLA-PEG-PLA hydrogels in this study appeared to follow this scheme, the 25% macromer hydrogels are expected to have more chain loops that don't contribute to the elastic or structural integrity of the network (Figure 4.5).

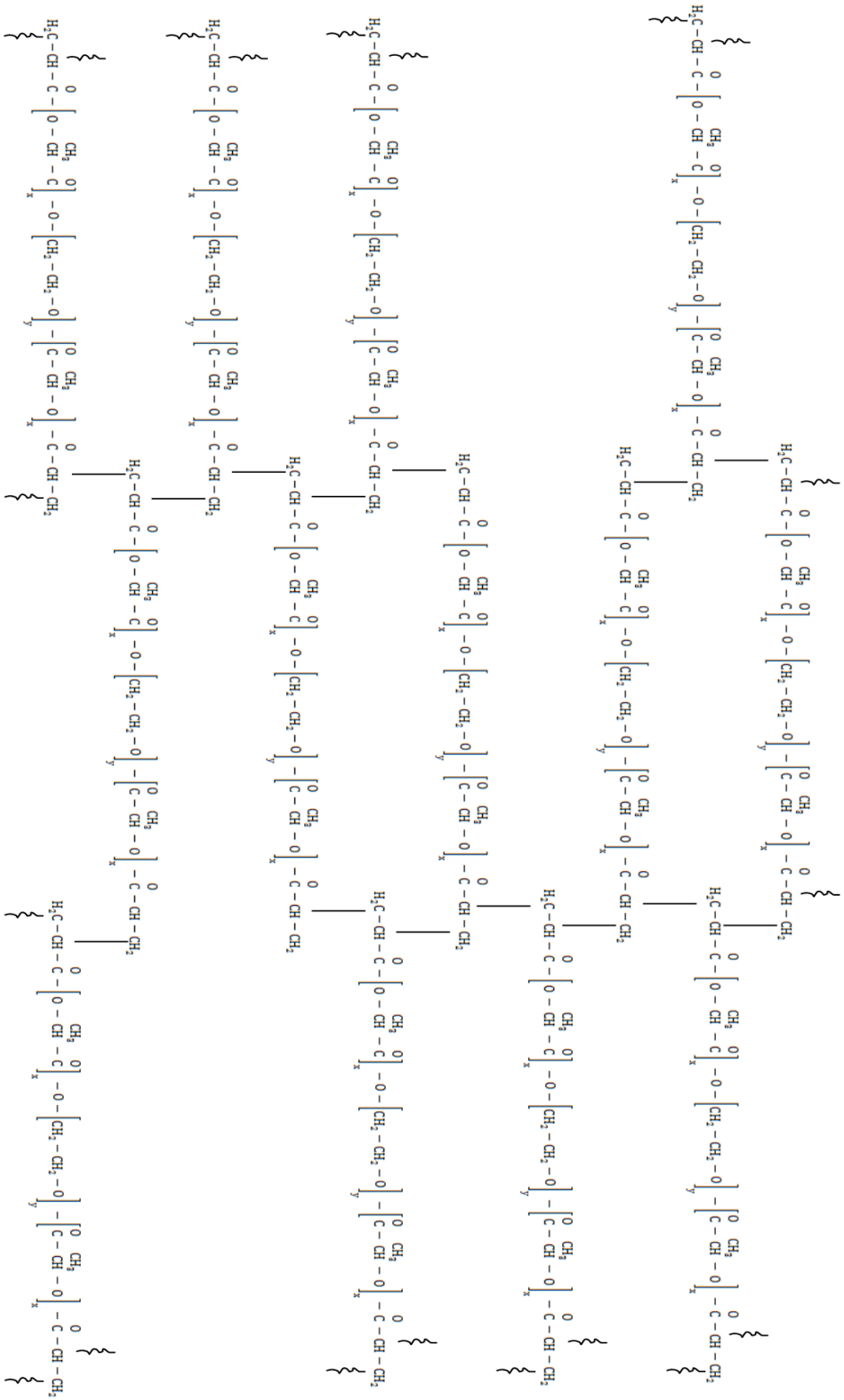

Figure 4.4. Idealized photo-crosslinked PLA-PEG-PLA network with formation of polyacrylate backbone chains (straight and squiggly lines) and network imperfections (chain loops not shown) [55, 133]. $\overline{DP}_{PEG} \geq 45$.

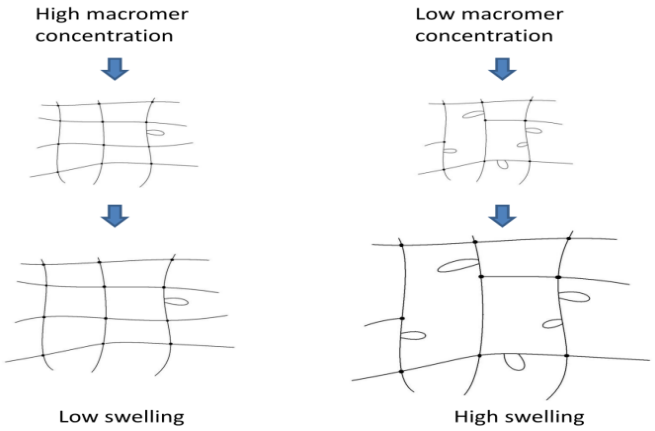

Figure 4.5. Effect of macromer concentration on cyclization and swelling

Table 4.2 also shows the mesh size, ξ, of the PLA-PEG-PLA hydrogels, which is an estimation of the actual physical dimensions of the distance between crosslinks, based on $\bar{M}_c$. For the 2k and 4k PLA-PEG-PLA hydrogels, the mesh size was around 56 Å or lower. The mesh size of the 8k hydrogels fell in a higher range of 80-100 Å. These mesh sizes are similar to those found previously for PEG-DA hydrogels made with $\bar{M}_n$ values in a similar range [22].

4.2 Degradable PAA Single-Network

4.2.1 NMR Characterization of Biodegradable PLA-PEG-PLA Crosslinker

The results for the biodegradable PLA-PEG-PLA crosslinker that was used for crosslinking of the PAA networks are shown in Table 4.1, along with the PLA-PEG-PLA macromers used for formation of PLA-PEG-PLA hydrogels. The total $\bar{M}_n$ of the macromer was found to be 1079 g/mol, due to a PEG center block of 600 g/mol, an average of 3 LA units per chain-end, and end-capped acrylate groups.

4.2.2 FTIR Characterization of Degradable PAA Network Photopolymerization

The FTIR spectrum of a PAA-1 single-network is shown in Figure 4.6 (along with a 4k-25/PAA-1 DN for comparison). The main carbonyl peak at 1700 cm^{-1} can be seen for the PAA-1 single-network. The appearance of this peak at 1700 cm^{-1} rather than at 1750 cm^{-1} suggests that intra-chain hydrogen bonding occurs between the carboxylic acid groups of PAA, and that PAA may have a dimer structure [76]. At the same time, the absence of peaks at 1635 cm^{-1} and 1650 cm^{-1} suggests that crosslinking of the PAA single-networks occurred.

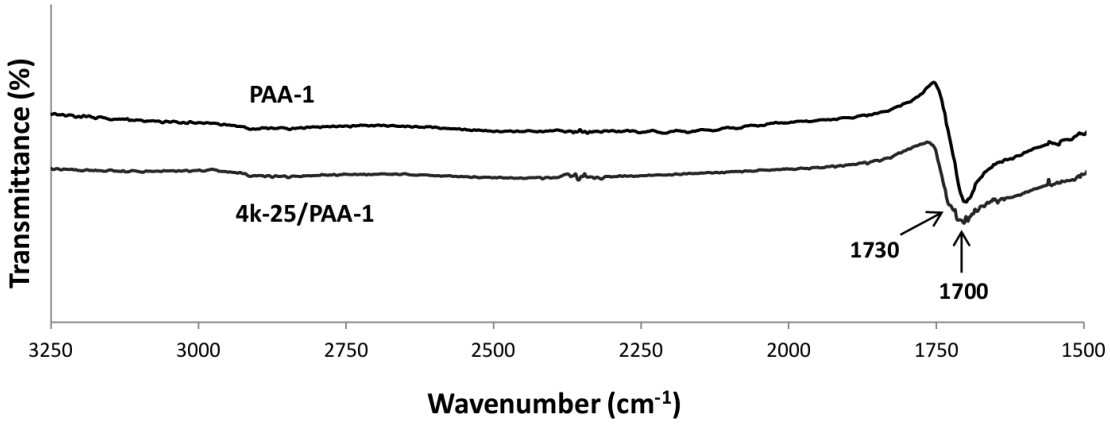

Figure 4.6. Representative FTIR spectrum of PAA single-network and PLA-PEG-PLA/PAA DN

4.2.3 GPC determination of un-crosslinked PAA MW

Gel permeation chromatography (GPC) was used to estimate a value of $\bar{M}_n$ for PAA in the un-crosslinked state for subsequent calculation of $\bar{M}_c$ of the PAA networks. The GPC curves obtained for the un-crosslinked PAA sample was compared to two PAA standards of known MWs (50k and 100k g/mol). The curves are shown in Appendix A. The GPC sample curve revealed that the un-crosslinked PAA had a broad MW distribution. The onset of the sample curve occurred at 55.6 min, which was earlier than that of both the 50k and 100k standards (56.4 min and 57.4 min respectively). This indicated that at least a portion of the sample MW is larger than 100k g/mol. At the same time, elution times corresponding to the peak and the tail-end of the GPC sample curve were only slightly quicker than those of the 50k PAA standard (Peak values: 100k – 59.8 min, sample – 60.1 min, 50k – 60.2 min; Tail-end values: 100k – 70.6 min, sample – 71.1 min, 50k – 71.2 min). As a result, it was concluded from the GPC curves that $\bar{M}_n >$ 50,000 g/mol could safely be used as a lower-bound estimate for PAA in the absence of crosslinks.

4.2.4 Structural Characteristics of the Degradable PAA Hydrogel

The initial $\bar{M}_c$ and ξ of the degradable PAA hydrogels are shown in Table 4.2, along with the results for the PLA-PEG-PLA hydrogels for comparison. The $\bar{M}_c$'s of the PAA hydrogels are much larger than those of the PLA-PEG-PLA hydrogels. This is due both to the much larger $\bar{M}_n$ of the PAA hydrogels and the higher swelling that occurs due to ionization of the PAA hydrogels under the swelling conditions of pH 7.4. As a result,

the initial ξ values of the PAA hydrogels are in the range of 274 -364 Å, which are over 3 times larger than those of the PLA-PEG-PLA hydrogels.

The effect of crosslinker concentration on $\bar{M}_c$ of the PAA hydrogels can also be seen in Table 4.2. As expected, $\bar{M}_c$ of the PAA-1 hydrogel is larger than that of the PAA-8 hydrogel. However, the two values are still relatively close despite the 8-fold increase in crosslinker concentration for PAA-8. This suggests that either some of the crosslinker was not incorporated into the PAA hydrogels or that a high degree of cyclization occurred in the PAA-8 hydrogels leading to more chain loops that don't contribute to the elasticity of the networks. The latter situation has been found previously for the crosslinking of PAA where only 2-6% of the feed crosslinker (N,N-methylenebisacrylamide – N-BAAm) lead to effective crosslinks in the network due to high cyclization [127]. This situation is expected to be alleviated to some degree by the larger crosslinking molecule used in the present study (compared to N-BAAm or TEGDMA) and by the relatively high AA monomer concentration, which favor reduced cyclization and hence lowering of Mc [132]. Nonetheless, the overall degree of cyclization for the PAA hydrogels in this study still appears to be very high, leading to high $\bar{M}_c$ values for both PAA hydrogels.

4.3 PLA-PEG-PLA/PAA Double Networks (DNs)

4.3.1 FTIR Characterization of PLA-PEG-PLA/PAA DNs

A representative FTIR spectrum of the PLA-PEG-PLA/PAA DNs (4k-25/PAA-1) is shown in Figure 4.6 (along with the PAA-1 FTIR spectrum). As for the PAA-1 single network, the main carbonyl peak of PAA is also seen at 1700 cm^{-1} for the 4k-25/PAA-1 DN. However, an additional peak also appears at 1730 cm^{-1}, which is an indication that inter-chain hydrogen bonding occurs between the carboxylic acid hydrogens of PAA and the ether oxygens of PEG in the DNs. These results are similar to those previously found for PEG/PAA IPNs and are similar to well-documented results for hydrogen-bonding between PEG and PMAA [76, 134]. The DSC results (discussed below) provide further evidence that hydrogen bonding occurs between PLA-PEG-PLA and PAA of the DNs in the present study, despite the incorporation of PLA. This is likely made possible by the short length of the PLA blocks and the fact that the blocks are restricted to the chain-ends of the crosslinked PLA-PEG-PLA component.

4.3.2 Structural Characteristics of PLA-PEG-PLA/PAA DN Hydrogels

The initial $\bar{M}_c$ and ξ of the DN PLA-PEG-PLA/PAA hydrogels are shown in Table 4.3, compared to $\bar{M}_c$ of the single-network PLA-PEG-PLA hydrogels. For DNs made from a given PLA-PEG-PLA 1st network, incorporation of either PAA-1 or PAA-8 as the 2nd component lead to significant increases in both initial $\bar{M}_c$ and ξ. While the single-network PLA-PEG-PLA hydrogels all have initial mesh sizes less than 100 Å, the initial DN hydrogel mesh sizes range from 34 to 275 Å. In many cases, ξ of the DN

hydrogels was over three times more than those of the corresponding PLA-PEG-PLA single-networks. These increases corresponded to three to five-fold increases in $\bar{M}_c$.

Table 4.3. Mc and mesh size of DN hydrogels (compared to PLA-PEG-PLA single-networks)

DNs		$\bar{M}_c$	Mesh size (ξ)
1st network (PLA-PEG-PLA)	2nd network (PAA)	(Initial, g/mol)	(Å)
	-	847	33
2k-25	PAA-1	5236	110
	PAA-8	3673	79
	-	427	20
2k-50	PAA-1	1410	41
	PAA-8	1083	34
	-	1756	56
4k-25	PAA-1	12,501	214
	PAA-8	11,772	191
	-	1539	49
4k-50	PAA-1	9440	156
	PAA-8	9641	161
	-	3705	97
8k-25	PAA-1	19,186	296
	PAA-8	14,857	198
	-	3160	80
8k-50	PAA-1	17,864	275
	PAA-8	15,275	212

At the same time, for DNs comprised of a given PLA-PEG-PLA 1st network, those with PAA-1 as the 2nd network had higher $\bar{M}_c$'s and ξ's than those with PAA-8. This matched up with the lower crosslinker concentration of the PAA-1 components which allowed DNs with PAA-1 to swell to a higher degree than those with PAA-8. It is also worth noting that the ξ's of the 8k-25 and 8k-50 DN hydrogels approach those of the PAA single-network hydrogels (Table 4.2).

4.4 Water-Content Change of Hydrogels During Experiments

In order to determine appropriate testing conditions for measurement of macroscopic properties of the hydrogels, preliminary water-content change experiments were carried out on single and DN hydrogels similar to the ones eventually used in this study (not shown). The dehydration of the hydrogel samples, tested at 37 °C, depended greatly on the type of hydrogel. For instance, the single-network hydrogels were found to become de-hydrated at a much faster rate than the DN hydrogel samples. The water-content of the single network hydrogels dropped from 76% to 62% after the first 5 min, dropping to essentially 0% after 15 min in the oven. The dehydration of the DN hydrogels occurred at a much slower rate, with the highest-swelling samples having the slowest rates. For instance, the highest-swelling 8k DN hydrogels only dropped from 92% to 90% after 15 min, whereas the water content of the lowest-swelling DN hydrogels dropped from 75% to 62% after 15 min.

These findings showed that great care had to be taken in testing the mechanical properties of the hydrogels as quickly and efficiently as possible in order for reliable results to be obtained. In particular, for the single network hydrogels, obtaining storage modulus within the first two minutes of testing was critical. For DMA testing, efforts were made to reweigh samples after the experiment and to discard results where the PBS content change was significant.

CHAPTER 5

MACROSCOPIC PROPERTIES OF SINGLE AND DOUBLE NETWORK HYDROGELS

5.1 Thermal Properties

5.1.1 PLA-PEG-PLA Single-Networks

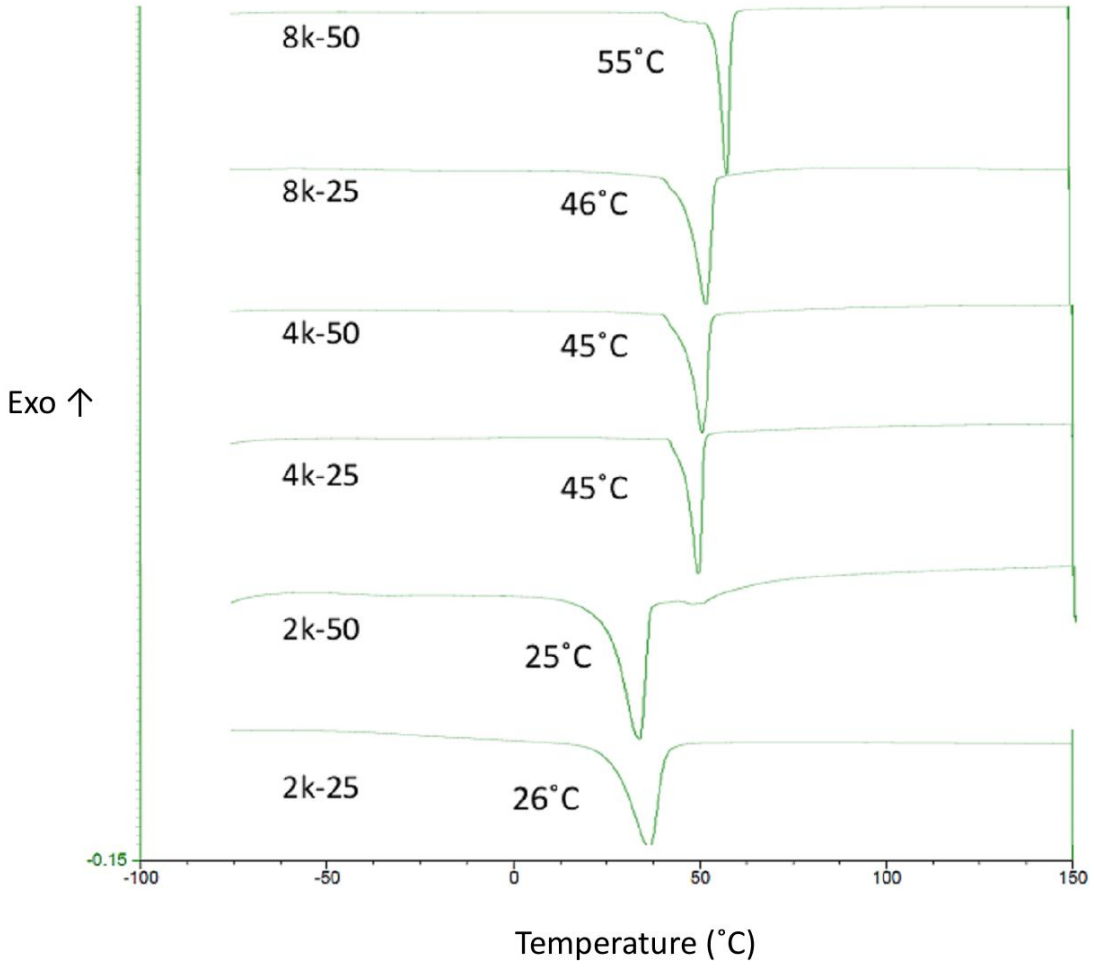

Figure 5.1. DSC thermograms of PLA-PEG-PLA single-networks

Figure 5.1 shows DSC thermograms for the single-network PLA-PEG-PLA hydrogels in the dry state over a temperature range of -70 to 150 °C. The melting temperature (T_m) of these networks was seen, due to melting of the crystalline regions formed between the PEG blocks in the networks. T_m increased as the molecular weight of PEG was increased from 2k to 4k to 8k, corresponding to increases in $\overline{M}_c$ of the networks. This is similar to previous reports for PLA-PEG-PLA copolymers [60, 119] and is expected since longer PEG chains favor crystallization (since higher crosslink densities tends to hinder chain flexibility and potentially decrease crystallinity). The presence of PLA end groups along the network chains is also expected to affect PEG crystallization. The crystallization of PEG segments in PLA-PEG-PLA copolymers has previously been shown to be decreased by the presence of short PLA blocks, and this effect was more significant for lower $\overline{DP}_{PEG}$ [60]. For the 2k networks in the present study, the low Tm is probably also due in part to the fact that the 2k macromers have a higher $\overline{DP}_{PLA}/\overline{DP}_{PEG}$ ratio of 0.2 compared to lower ratios of 0.10 and 0.09 for the 4k and 8k networks, respectively. Macromer concentration (25 or 50 wt%) had little effect on T_m, except for the 8k networks, where there was a significant jump in Tm for the 8k-50 network compared to that of 8k-25.

No T_g values were observed for the single PLA-PEG-PLA networks in the temperature range studied. Previous reports for PLA-PEG-PLA copolymers detected a T_g for PEG (MW = 600-2000 g/mol) when the $\overline{DP}_{PLA}/\overline{DP}_{PEG}$ was about 0.08 or higher but not when it was 0.04 or lower (using a temperature range of about -60 °C to 70 °C with a scan rate of 10 °C/min) [60]. When the PEG T_g was detected, it appeared to increase from -60 °C to -37 °C as the $\overline{DP}_{PLA}/\overline{DP}_{PEG}$ was increased. In the present study,

it is possible that the T_g of PEG did not appear because the PEG molecular weights were generally above those mentioned in the previous study, which lead to increased significance of the crystalline regions within the PEG block segments. This result is also consistent with previous reports where no T_g was observed for PEG due to the low content of amorphous phase in PEG (MW = 1000 g/mol; temperature range of -70 °C to 150 °C) [135].

Similarly, no T_g corresponding to PLA was observed. This is likely due to the fact that the $\overline{DP}_{PLA}$ is low, and could further be obscured by the fact that T_g for PLA and T_m for PEG tend to be close, which sometimes makes extracting a T_g for PLA in PEG-PLA copolymers difficult [60].

5.1.2 PAA Single-Networks

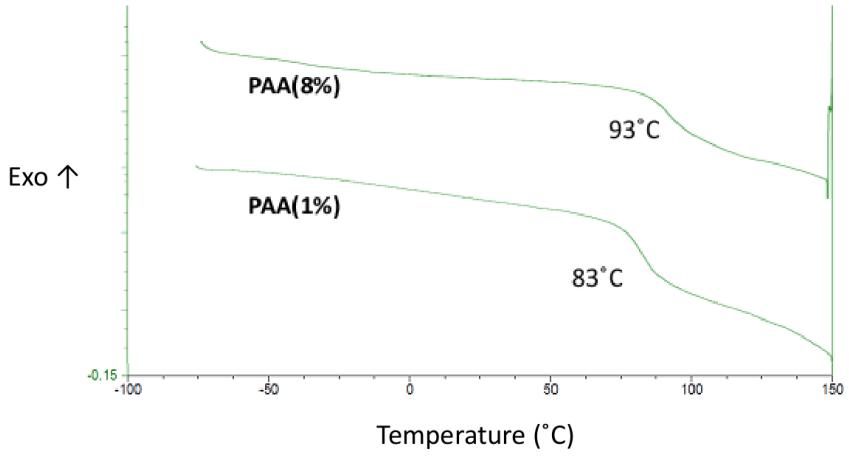

Figure 5.2. DSC thermograms of PAA single-networks

DSC thermograms of the degradable single-network PAA hydrogels (in the dry state) are shown in Figure 5.2. The PAA-8 network was found to have a higher T_g than

the PAA-1 network. This is expected and is due to the higher crosslinking degree of the PAA-8 network which results in increased restriction of polymer chain motion [135]. Because the crosslink junctions are permanently frozen in, it takes a higher temperature for the transition to occur.

5.1.3 PLA-PEG-PLA/PAA Double Networks (DNs)

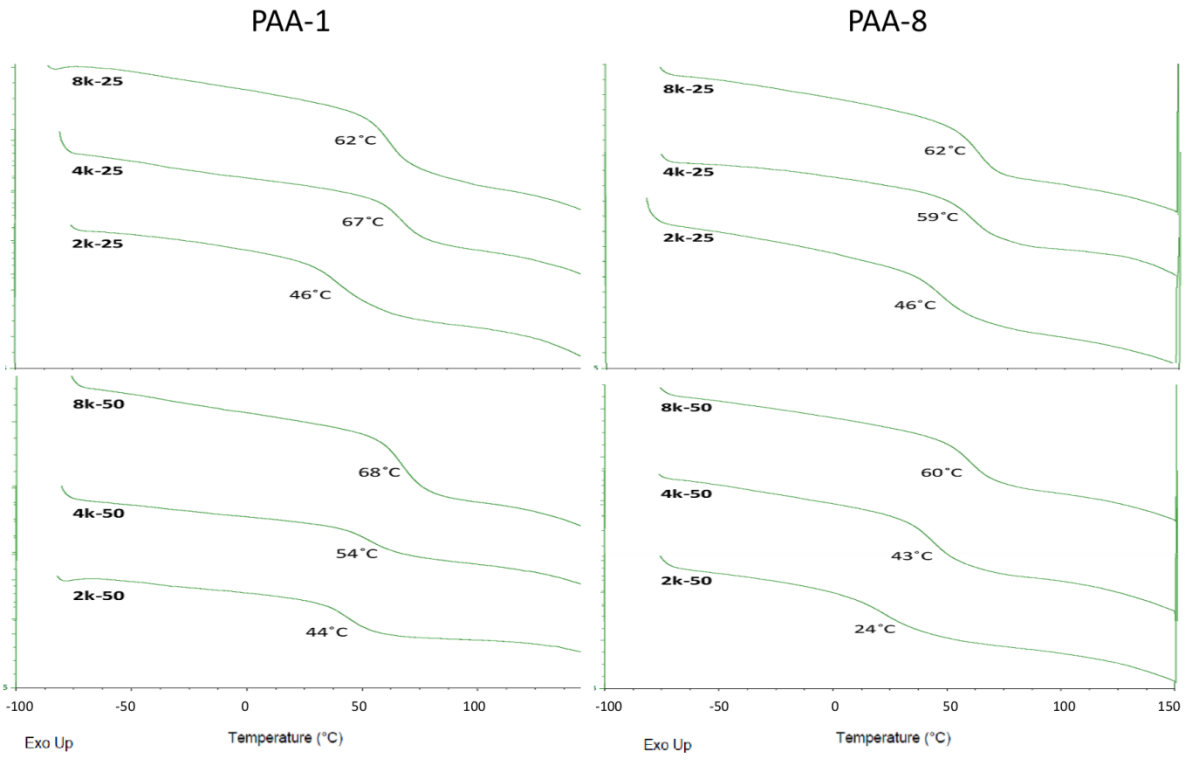

Figure 5.3. DSC thermograms of PLA-PEG-PLA/PAA DNs

Figure 5.3 show DSC thermograms for all of the DN PLA-PEG-PLA/PAA hydrogels in the dry state. A single T_g, dependent on composition, was observed for all of the DNs over the temperature range of -70 to 150 °C. This implies that the components are fully miscible on a dimensional scale between 20 and 40 nm [135, 136]. For a given PLA-PEG-PLA macromer concentration (25 or 50%) and amount of PAA

crosslinker (1% or 8%), the value of T_g tended to increase as the MW of PEG in the PLA-PEG-PLA component increased from 2k to 8k. This occurred in all cases except for the 8k-25/ PAA-1 DN, which had a lower T_g than that of the 4k-25/PAA-1 DN. Apart from that, T_g increased with PEG MW, which implies that miscibility of the two networks increased as $\bar{M}_c$ of the PLA-PEG-PLA network increased. This is contrary to the behavior observed for regular IPNS, where miscibility is usually enhanced as the crosslink density increases and tends to decrease as the MW of the components increases [112, 137]. Instead, the observed thermal behavior matches trends previously found for IPNs in which hydrogen bonding occurs between the networks [135, 136].

Similar results have previously reported for PEO/PAA seq-IPNs of equimolar PEO:PAA composition, formulated with PEO MWs of 300, 600, 1000, 2000 and 6000 g/mol [76]. In that study, a single T_g was observed for IPNs with the highest PEO MW of 6000 g/mol, while two or three temperature transitions were found for IPNs with lower PEO MWs. At the same time, the maximum loss modulus temperature (which showed behavior analogous to T_g) of the PEO:PAA complex phase in the IPNs increased by about 10-15 °C not only as the PEO MW increased but also as the crosslink density of the PAA component was decreased. After an FTIR analysis, hydrogen bonding was found to occur between the ether groups of PEG and the carboxyl groups of PAA. Furthermore, hydrogen bonding between these groups has previously been implicated in other studies of PEG and PAA IPNs and blends [138, 139].

In the current study, the DN DSC results suggest that a significant degree of hydrogen bonding also occurs within the PLA-PEG-PLA/PAA DNs. This is supported by a second feature of the DSC thermograms. For a given PEG molecular weight and

macromer concentration (comparing straight across horizontally in Figure 5.3), the DNs made with PAA-1 tended to have higher T_g values than those made with PAA-8. This is also contrary to the behavior of regular IPNs, since the single-network PAA-8 has higher crosslinking (as determined below) and a higher T_g than the single-network PAA-1. Therefore, higher T_g values for the PAA-1 DNs suggest that miscibility is also enhanced when the PAA network is less crosslinked (when Mc of PAA is higher). This effect was more pronounced for the DNs with tightly crosslinked PLA-PEG-PLA components (2k-50, 4k-50 and 8k-50). For these DNs, T_g's of the DNs containing PAA-1 were up to 20 °C higher than those containing PAA-8.

A third feature of the DN DSC results is that for a given PEG MW and PAA crosslinking degree, the PLA-PEG-PLA-25 DNs have a higher T_g than the corresponding PLA-PEG-PLA-50 DNs. For instance, comparing only the DNs made with PAA-1, the 2k-25 DN has a higher T_g than the 2k-50 DN. (Again the one exception is the 8k-25/PAA-1 DN). Nonetheless, the general trend further supports the likelihood that hydrogen bonding is responsible for the observed thermal behavior.

Compared to the previously mentioned study on PEG/PAA IPNs, the current PLA-PEG-PLA/PAA DN systems may favor hydrogen bonding because it has higher molar compositions of PAA (0.52 – 0.87). Another previous study on PEO/PAA IPNs (PEO MW ≈ 8000 g/mol) found that a single T_g was observed for IPNs with PAA contents of 31 mol% or higher (at least up to 65 mol%), whereas both a T_m and T_g were found for lower PAA mol percentages [75]. At the same time, T_g increased significantly at the highest PAA contents. Previous studies on complexes between PEO and PAA also

found two phases to be present below PAA contents of 50% (by weight), with single T_g's occurring above that and a maximum T_g at 90% PAA [140].

Secondly, the end-groups of the PLA-PEG-PLA networks in this study are relatively "neutral" in the sense that they do not encourage intra-chain hydrogen bonding. In the case of the equimolar PEO/PAA IPN study described above, the PEO chains were crosslinked in a manner that resulted in urethane groups at the chain-ends (by the crosslink junctions). As a result, hydrogen bonding between the urethane groups was possible and became increasingly significant as the PEO MW decreased (due to the decreasing ratio of ether groups to chain-end groups: 22/1 for PEO = 2000 g/mol). No such competitive hydrogen bonding is expected to occur between the PLA end groups of the PLA-PEG-PLA networks, which means miscibility is more probable.

Lastly, the MW of the PAA network is probably also significant for hydrogen bonding. As is discussed above (GPC results), the chains in the PAA networks have a wide distribution of MWs with a minimum around 50,000 g/mol and a significant portion above 100,000 g/mol. The high MW of the PAA network chains likely favors hydrogen bonding.

5.2 Swelling

5.2.1 PLA-PEG-PLA Single-Network Hydrogels

Figure 5.4 shows the swelling (measured as PBS % content) of the PLA-PEG-PLA single-networks over a 14-day period. As the PEG molecular weight was increased from 2k to 4k to 8k, the initial PBS content of the hydrogels increased. At each PEG MW, the initial PBS content was higher for the hydrogels made from a 25% macromer concentration than from the 50% macromer concentration. The initial PBS content of the PLA-PEG-PLA hydrogels was as low as 70% for the 2k-50 hydrogels and as high as 93% for the 8k-25 hydrogels. The trends seen for the swelling of these hydrogels are a result $\bar{M}_c$ increasing with PEG MW and decreasing with initial macromer concentration, as is expected for non-linear free radical polymerization reactions [53, 132]. It is also similar to trends in previous studies of PLA-PEG-PLA hydrogels [53, 58].

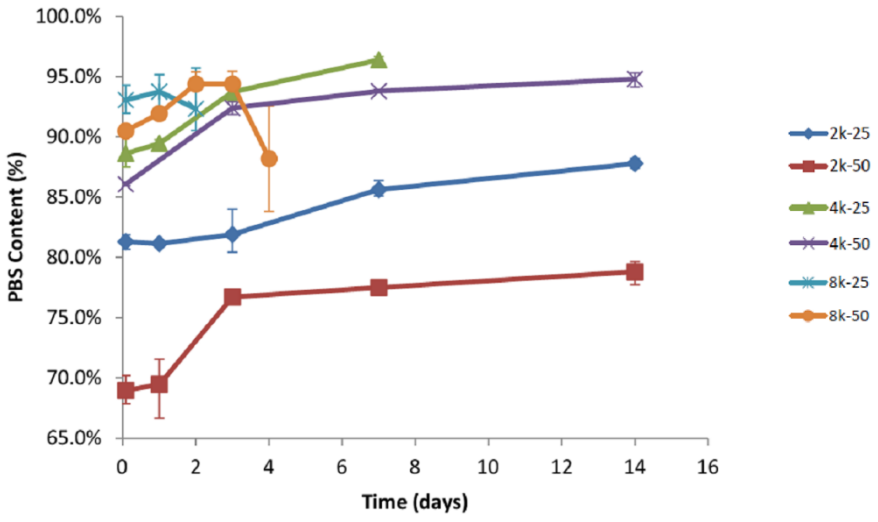

Figure 5.4. PBS Content Swelling of the single-network PLA-PEG-PLA hydrogels

The swelling of the PLA-PEG-PLA hydrogels also increases with time over the 14-day swelling period. These changes in swelling occur in coordination with degradation of the hydrogels (discussed below) due to the hydrolysis of the PLA blocks in the crosslinked PLA-PEG-PLA chains. For the 8k-25 and 8k-50 hydrogels, the PBS-content swelling profiles show an initial increase followed by a drop off by the 2nd and 4th days of swelling, respectively. When matched up with the degradation results, the drop off in swelling appears to be due to the quick degradation of these 8k hydrogels, which both have a mass loss of greater than 60% by their respective drop off points. The drop off in PBS content at those points is due partly to inaccuracy inherent in the calculation of the PBS content at high degrees of mass loss (Equation 32).

5.2.2 Degradable PAA Single-Network Hydrogels

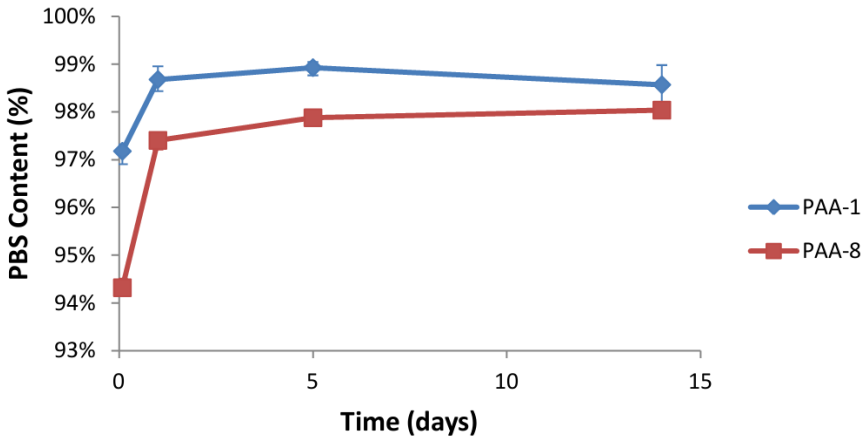

Figure 5.5. PBS Content Swelling of the single-network PAA hydrogels

The swelling of the degradable PAA single-network hydrogels is shown in Figure 5.5. These hydrogels appeared to reach equilibrium swelling after about 24 hrs, after which swelling tended to increase very slowly. The gradual increase in swelling after 24

hrs is due to the very slow degradation of both networks (shown below) that occurred over time. The swelling of the PAA-1 network was always higher than that of the PAA-8 network due to the higher crosslinker concentration used for polymerization of the PAA-8 network. As discussed above, the higher crosslinker concentration lead to a lower $\bar{M}_c$ for the PAA-8 hydrogels. These results for the PAA single-networks are similar to previous studies where vinyl monomers were crosslinked using di-acrylated PEG crosslinkers of 600 g/mol (similar to the PLA-PEG-PLA crosslinker used in the present study). In that study, a similar dependence of both Mc and swelling on crosslinker concentration was seen [132].

The swelling of these degradable PAA hydrogels is also higher than the swelling of the PLA-PEG-PLA hydrogels at all time points. Since at pH 7.4, PAA is more than 99% ionized, the high swelling of the PAA hydrogels is due largely to the ionization of the COOH groups, which occurs above PAA's pK_a of 4.7 [46]. At the same time, the high degree of swelling and the relatively small influence of crosslinker concentration on swelling for these PAA hydrogels suggests that a high degree of cyclization probably occurred, as has been found previously for the crosslinking of PAA and polyacrylamide networks where only small percentages of crosslinker in the feed formed effective crosslinks [127]. This finding is supported by the high $\bar{M}_c$ values of both PAA hydrogels despite an 8-fold increase in amount of crosslinker for PAA-8 compared to PAA-1.

5.2.3 PLA-PEG-PLA/PAA DN Hydrogels

The swelling of the PLA-PEG-PLA/PAA DNs over periods of up to weeks is shown in Figure 5.6, where single-network PLA-PEG-PLA hydrogel swelling is also

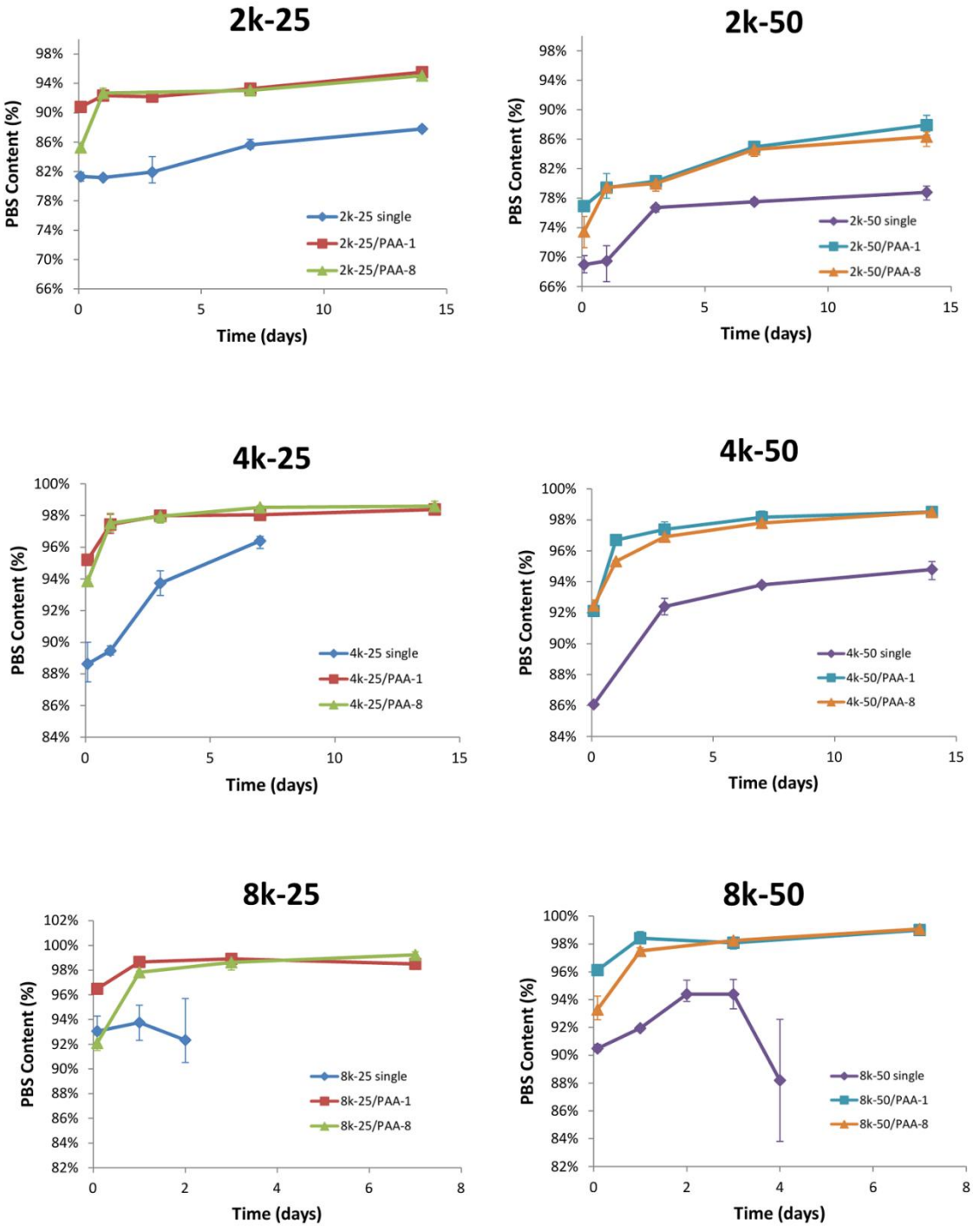

Figure 5.6. PBS content swelling of the PLA-PEG-PLA/PAA DN hydrogels. Swelling of the single-network PLA-PEG-PLA hydrogels is included for comparision.

shown for comparison. Over time, swelling increases for all of the DNs due to the degradation and increasing $\bar{M}_c$ of the DN components (discussed below). For each PLA-PEG-PLA hydrogel type (2k-25 through 8k-50), the swelling of the corresponding DNs (with 2nd networks PAA-1 and PAA-8) is higher than the single-network PLA-PEG-PLA hydrogels. At the same time, DNs made from a particular PLA-PEG-PLA 1st network tend to have similar swelling profiles over much of the investigated time range whether the 2nd network was PAA-1 or PAA-8. This is similar to what was found for the single-network PAA-1 and PAA-8 hydrogels, where a high degree of cyclization seemed to limit attempts to obtain significantly higher crosslinking (and lower swelling) of PAA-8 despite an 8-fold increase in crosslinker concentration. This likely carried over to the DNs, where the swelling of both PAA 2nd network components is also restricted by the lower-swelling PLA-PEG-PLA component.

The restriction of the swelling of the DNs by the PLA-PEG-PLA hydrogel component can further be seen through the effects of changing the PLA-PEG-PLA hydrogel parameters. Figure 5.6 shows that as the PEG MW is increased from 2k to 8k (for either the 25% or 50% macromer concentration), the overall swelling of the DNs tends to increase. Additionally, for a given PEG MW, the swelling is generally lower for the DNs made from 50% PLA-PEG-PLA macromer concentrations (single networks of which have a lower $\bar{M}_c$) compared to 25%. The effects are most exaggerated for DNs consisting of 2k PLA-PEG-PLA components (single-networks of which swell the least) and are least exaggerated for DNs made from 8k PLA-PEG-PLA component (single-networks of which swell the most).

The results for the dependence of DN swelling on PEG MW are very similar to what was found for PEG/PAA DNs [46]. Therefore, the incorporation of degradable LA units into the 1st network (PLA-PEG-PLA in this study) and the use of a biodegradable crosslinker for the PAA component do not affect the ability of the DN swelling to be tuned by changing the Mw of the 1st network. Additionally, the present study shows that the macromer concentration of the 1st network can also have a significant effect on the swelling of the DNs. These patterns are hold and are consistent up to a swelling/degradation period of two weeks.

5.3 Degradation

5.3.1 PLA-PEG-PLA Single-Network Hydrogels

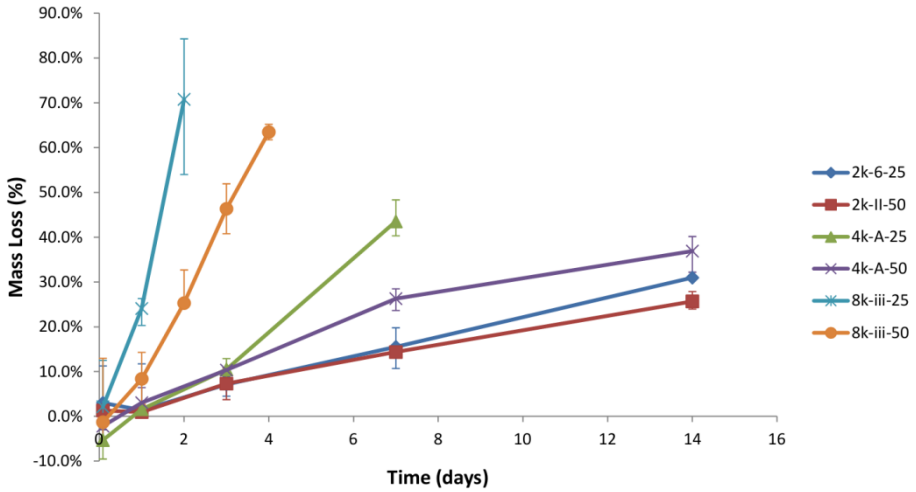

Figure 5.7. Mass loss (%) of the single-network PLA-PEG-PLA hydrogels

The mass loss behavior of the PLA-PEG-PLA single-network hydrogels over a period of up to 14 days is shown in Figure 5.7. The behavior was consistent with the $\bar{M}_c$ and swelling measurement results in this study, and also matched previous studies [52, 53, 58]. The degradation of these hydrogels was fastest for the PLA-PEG-PLA hydrogels with the highest PEG MW (8k), and was slowest for the hydrogels with lowest PEG MW (2k). For hydrogels of a given PEG MW, higher initial macromer concentrations also appeared to lead to slower degradation. The fast degradation of the 8k hydrogels is due to the higher initial swelling of those hydrogels, which allowed more water into the hydrogel networks, allowing increased access for hydrolytic degradation of the PLA blocks and quicker release of polymer (or oligomer) segments that were separated from the networks [52]. For the hydrogels made from higher macromer

concentrations, the lower $\bar{M}_c$ values lead to lower swelling and therefore also slower degradation.

For PLA-PEG-PLA hydrogels, the length of the PLA blocks is also known to have an effect on degradation. In a previous study, the presence of PLA slightly decreased initial swelling of the hydrogels due to PLA's hydrophobic nature, but thereafter longer PLA blocks lead to faster degradation rates and a faster increase in swelling with time [58]. For the PLA-PEG-PLA hydrogels in the current study, the 8k hydrogels have longer PLA blocks ($\overline{DP}_{PLA-end} = 8$) than the 2k and 4k hydrogels ($\overline{DP}_{PLA-end} = 4.5$). This condition also likely facilitated the quicker rate at which the 8k hydrogels degraded. As a result, while the 2k hydrogels sustained a mass loss of less than 30% over a 14-day period, the 8k hydrogels sustained a mass loss of over 60% after only 4 days.

5.3.2 PAA Single-Network Hydrogels

The degradation of the single-network PAA hydrogels is shown in Figure 5.8. The PAA-1 and PAA-8 hydrogels degraded very slowly over the first week, after which a significantly greater amount of degradation can be seen to occur for the PAA-1 hydrogels by two weeks. This is likely due to the higher swelling of the PAA-1 network, which allows greater access of imbibed water to the hydrolysable PLA blocks of the crosslinker and also allowed faster diffusion of degraded segments out of the PAA-1 hydrogels. At the same time, a large deviation between the swelling of the PAA-1 and PAA-8 networks is not seen at 2 weeks, which could be related to the PAA-1 network having a different structure from the PAA-8 hydrogels. For instance, while the PAA-8 hydrogels have a.

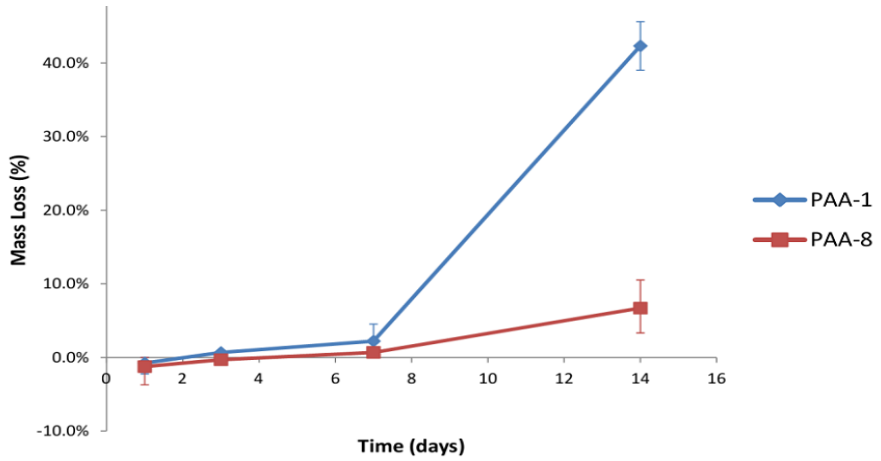

Figure 5.8. Mass loss (%) of the single-network PAA hydogels

higher crosslink density (or a lower $\bar{M}_c$) than the PAA-1 hydrogels, the relative closeness in swelling between the two suggests that the PAA-8 hydrogels may also have a higher degree of cyclization (where a high percentage of feed crosslinker formed ineffective crosslinks) which prevented them from having an even higher crosslink density. In a previous study on PAA hydrogels, a similar situation was found where increases in crosslinker concentration were believed to have lead to an increased compactness of intramolecularly crosslinked microgel particles without leading to reductions in $\bar{M}_c$ [127]. The possible difference in structure between PAA-1 and PAA-8, coupled with the likely release of degraded segments from PAA-1 at the two-week degradation point, could explain the closeness in the calculated swelling of the two hydrogels despite the disparity in degradation

5.3.3 PLA-PEG-PLA/PAA DN Hydrogels

The degradation of the PLA-PEG-PLA DNs is shown in Figure 5.9. The degradation profiles of the DNs were largely dependent on the PEG MW of the PLA-

PEG-PLA component. Whether the hydrogels were made with a 2nd network of PAA-1 or PAA-8, DNs with a 1st network of 2k-50 and 2k-25 had the slowest degradation rates, followed by 4k-50, 4k-25 and then the 8k DNs. The pattern was clearest for the PAA-8 DNs, whereas for the DN-1 the 8k-25 and 8k-50 hydrogels were very similar, probably due to the highest overall swelling and fastest degradation of these DNs. The dependence of DN degradation on PEG MW is similar to the dependence found for DN swelling on PEG MW. The combination of these results suggests that faster degradation of the DNs is closely tied to higher swelling. This is further evidenced by the fact that for a given 1st network of PLA-PEG-PLA, DNs with a 2nd network of PAA-1 tended to degrade faster than those with PAA-8.

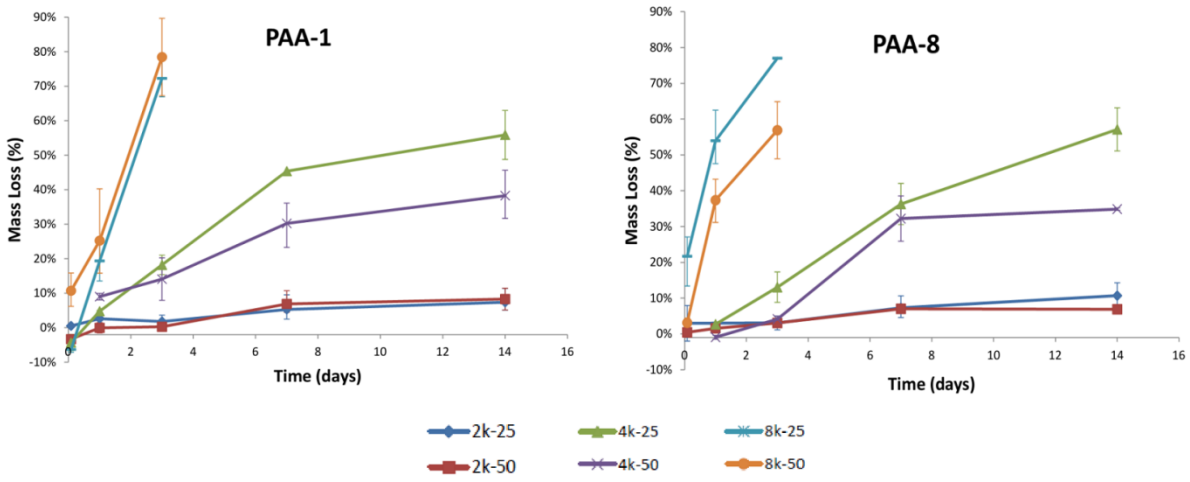

Figure 5.9. Mass loss (%) of the PLA-PEG-PLA/PAA DN Hydrogels

In comparing the degradation of the DN hydrogels to that of corresponding single-network PLA-PEG-PLA hydrogels (Figure 5.7), the degradation of the DNs is faster in most cases. The main exception is the 2k DN hydrogels, which have mass losses of slightly less than 10% at two weeks compared to losses of around 20% for the single-

network PLA-PEG-PLA hydrogels. This occurs despite higher swelling of the 2k DN hydrogels compared to the 2k PLA-PEG-PLA hydrogels. In this case, it is possible that the degradation of the PAA component, which starts out very slowly even in the high-swelling single-network PAA environment (PBS content > 97% at 24hrs), could be stifled in the lower-swelling 2k DN hydrogel environments (PBS contents ~ 93% and 80% at 24 hrs). Therefore, while the 2k PLA-PEG-PLA components are likely to undergo faster degradation within the DN structure (since they are in a higher-swelling environment compared to their single networks), the PAA component may remain intact for a longer time within the 2k DNs, leading to an overall slower degradation of the DNs compared to the 2k PLA-PEG-PLA single-networks. Since the 2k DN hydrogels consist of up to a 0.7 mole fraction of AA units compared to EO units (fewer but significantly longer PAA chains) the effect could be quite significant. The degradation of the PAA component also plays a role for DNs made with 4k and 8k PLA-PEG-PLA 1st networks, but is likely not as restricted since the swelling of these DN hydrogels is almost on par with that of the single-network PAA hydrogels.

5.4 Storage Modulus

5.4.1 PLA-PEG-PLA Single-Network Hydrogels

The compressive storage modulus of the single-network PLA-PEG-PLA hydrogels is shown over various degradation periods in Figure 5.10. The storage modulus showed a similar dependence on PEG MW and macromer concentration as the swelling (Figure 5.4) and degradation (Figure 5.7) did. The modulus of the 2k-50 hydrogels was significantly higher than that of the other PLA-PEG-PLA hydrogels over the entire degradation range, which matched up with their significantly lower swelling. The highest-swelling hydrogels, the 8k-25, 8k-50 and 4k-25 hydrogels, had the lowest storage modulus over the entire range.

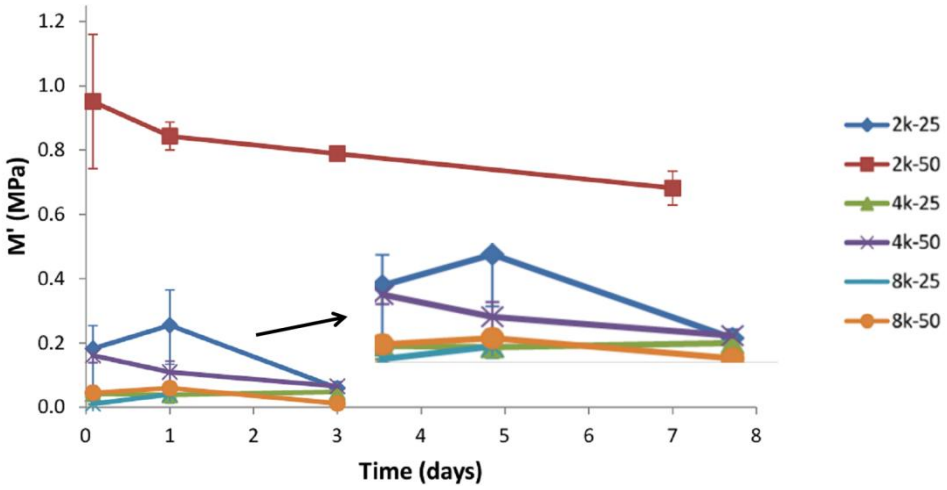

Figure 5.10. Compressive storage modulus of the single-network PLA-PEG-PLA hydrogels

After one week of degradation, the modulus of the 2k-50 hydrogel dropped to about 7/10 of its initial value. Similar decreases can be seen in Figure 5.10 for the curves of the other PLA-PEG-PLA hydrogels over a shorter time of 3 days. Again, the

quick decrease in modulus matched up with the higher swelling and faster degradation of the 4k and 8k hydrogels. The decreases in modulus corresponded with increases in $\overline{M}_c$ and hence a decrease in structural integrity during degradation of the hydrogels (not shown).

5.4.2 PAA Single-Network Hydrogels

The compressive storage modulus of the single-network PAA hydrogels is shown over time in Figure 5.11. The storage modulus of the PAA-8 hydrogels was higher than that of the PAA-1 hydrogels over the entire degradation period investigated. This is expected since the PAA-8 hydrogels had a lower initial $\overline{M}_c$ and consistently lower swelling than the PAA-1 hydrogels over time (Figure 5.5). Additionally, the initially high modulus of the PAA-8 hydrogels at 2 hrs is due to the initially slower swelling of these hydrogels and appears to have occurred before equilibrium swelling was fully reached.

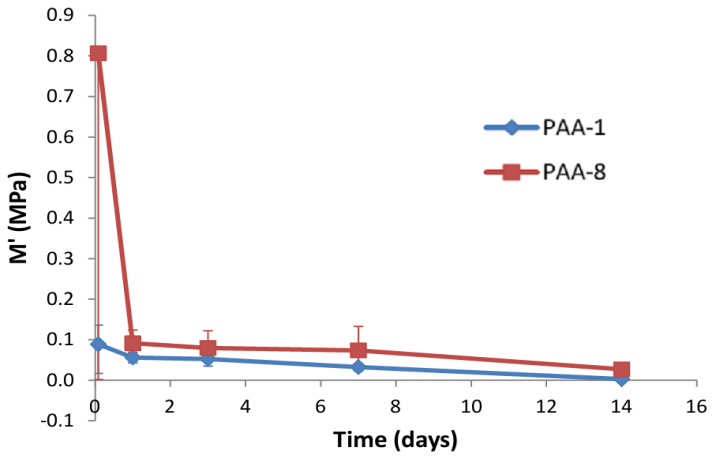

Figure 5.11. Compressive storage modulus of the single-network PAA hydrogels

Beyond 2 hrs, the storage modulus of both single-network PAA hydrogels was comparable to that of the 4k-25 and 8k PLA-PEG-PLA single-network hydrogels and was therefore relatively low. The similarity in modulus is probably related to the fact that swelling of the 4k-25 and 8k PLA-PEG-PLA hydrogels approaches that of the PAA hydrogels. Specifically, the low PAA modulus was due to the very high swelling of the PAA hydrogels, which are almost fully ionized at the physiological pH of 7.4 used in this study. In addition, at this high degree of swelling and ionization, the inter-chain hydrogen bonding observed for the dry PAA networks (during FTIR analysis) is more than likely eliminated in the swollen state.

At the same time, the PAA modulus values appeared to be sustained over a longer period (1 week) before dropping to the values reached by the 4k-25 and 8k PLA-PEG-PLA hydrogels at 3 days. The slower decay of the PAA hydrogel modulus is due to the slower degradation of the PAA hydrogels over the first week (Figure 5.8) relative to the degradation of the PLA-PEG-PLA hydrogels (Figure 5.7) over the same period.

5.4.3 DN PLA-PEG-PLA/PAA DN Hydrogels

The compressive storage modulus of the PLA-PEG-PLA/PAA DN hydrogels is shown in Figure 5.12 (where results for the single-network PLA-PEG-PLA hydrogels are also shown for comparison). The modulus of the DN hydrogels was very dependent on the PEG MW and macromer concentration of the PLA-PEG-PLA 1st network component. The modulus values were highest for DNs composed of PLA-PEG-PLA 1st networks with low PEG MWs and high macromer concentrations. Hence, the DNs

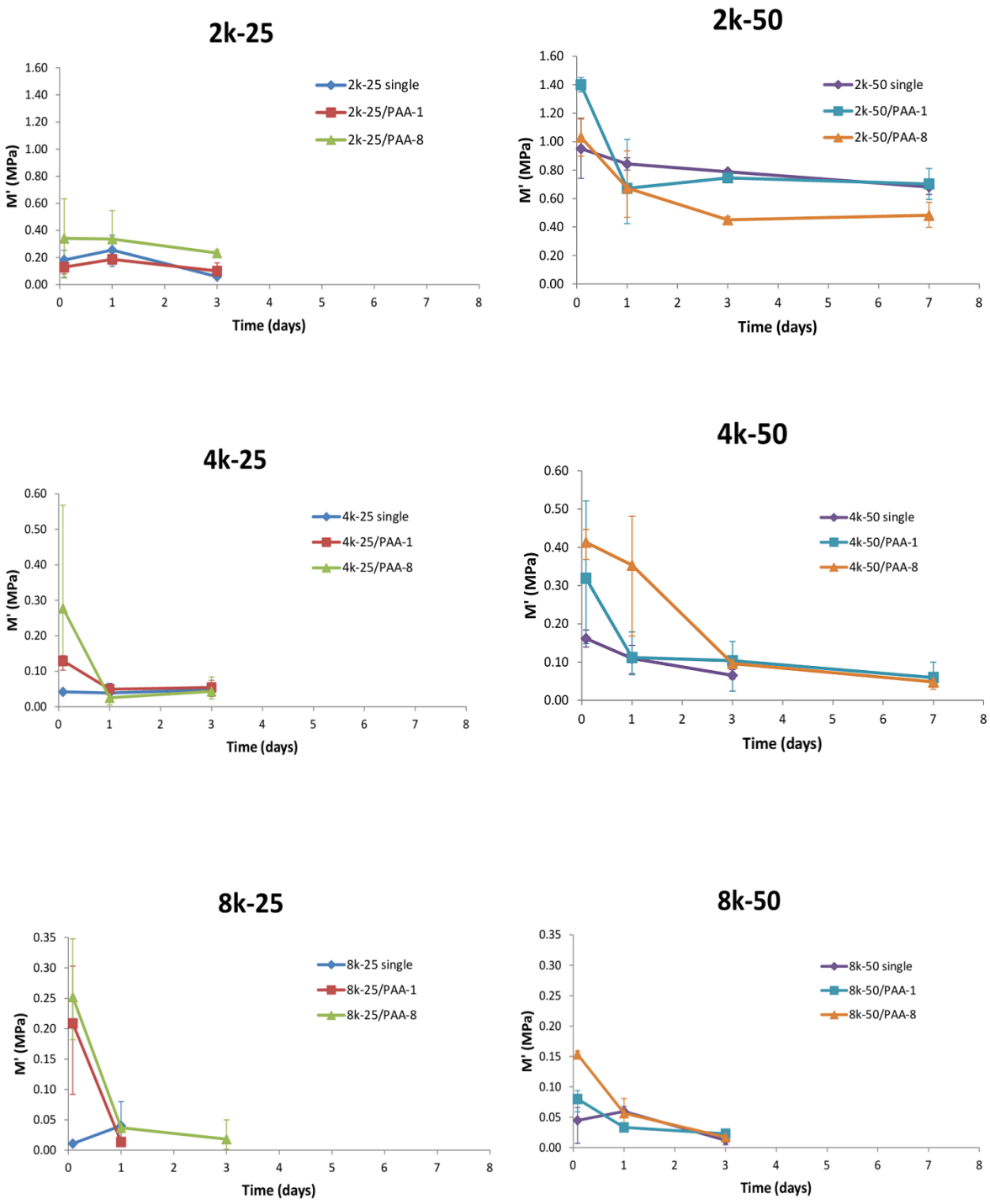

Figure 5.12. Compressive storage modulus of the PLA-PEG-PLA/PAA DN hydrogels. Results for the single network PLA-PEG-PLA hydrogels are also shown for comparison.

consisting of a 2k-50 PLA-PEG-PLA 1st network had the highest moduli (in the range of 0.4 – 1.4 MPa). The 2k-25 and 4k-50 DN hydrogels also had relatively high moduli, in the range of 0.2 - 0.4 MPa. The 8k DN hydrogels had the lowest moduli, which began as high as 0.25 MPa but quickly dropped off to 0.05 MPa or less by 24 hrs. This matched up with the high swelling (Figure 5.6) and fast degradation (Figure 5.9) of the 8k DN hydrogels, which in turn was due to the high swelling and degradation of the single-network 8k-25 hydrogel components.

In comparing the effects of the PAA 2nd network component on DN hydrogel modulus, there tended to be very little difference between DNs made from PAA-1 and PAA-8. For a given PLA-PEG-PLA 1st network, modulus profiles obtained for DNs made from PAA-1 and PAA-8 often showed a great deal of overlap. Therefore, the effect of the second network seemed to be much less than the effect of the PLA-PEG-PLA component. This is probably due to two factors. First, the swelling profiles of PAA-1 and PAA-8 DNs made with the same 1st network are also very similar, with values overlapping at most time points over a two week period (Figure 5.6). As described above, this was due to the high degree of cyclization that likely occurred for PAA-8 network components which limited their crosslink density. As a result, it makes sense that the modulus values of the PAA-1 and PAA-8 DNS are also very similar. Additionally, a second factor could be related to the sequential polymerization process used for formation of the DNs. A number of previous studies have found that variation of the characteristics of the 1st network in a seq-IPN tend to have a greater influence on the IPN's properties than variation of the 2nd network [116, 141]. The reason for this is believed to be the guarantee of a continuous, more homogenous network for the first

component. While this has typically been observed for IPNs in the dry state, it would likely carry over to the swelling of the IPNs as well.

Compared to the moduli of the single-network PAA hydrogels (Figure 5.11), significant improvements in modulus occurred for the DN hydrogels, particularly when 2k and 4k PLA-PEG-PLA components were used as the 1st networks. However, this is expected since the swelling of the DN hydrogels are generally lower than that of the PAA hydrogels.

Most significantly, the modulus profiles of all of the DNs also matched up very closely with modulus profiles of their corresponding single-network PLA-PEG-PLA hydrogels. This occurred despite the higher swelling of the DN hydrogels compared to that of corresponding single-network PLA-PEG-PLA hydrogels. For instance, while the 2k-25/PAA-1 hydrogels had an initial PBS content of 91% and the 2k-25 single-network hydrogels had an initial PBS content of 81%, the initial moduli of the two hydrogels were very similar (0.12 and 0.18 MPa, respectively). In another instance, while the 2k-25/PAA-8 hydrogels had a 24-hour PBS content of 93% and the 2k-25 single-network hydrogels had a 24-hour PBS content of 81%, the 2k-25/PAA-8 DN actually had a higher modulus (0.34 MPa compared to 0.26 MPa). Similar results were seen in the comparison of these two hydrogels at 3 days.

While an increase in modulus wasn't seen for most of the DN hydrogels compared to the corresponding single-network PLA-PEG-PLA hydrogels, the moduli of the DN hydrogels overlapped with those of the corresponding single networks in most cases. This was seen especially for the DNs made with PLA-PEG-PLA 1st networks of 50% macromer concentration (2k-50, 4k-50 and 8k-50). The modulus values of these

DNs also tended to take longer to decay to values below 0.05 MPa, as a result of the initial modulus tending to be higher.

For DNs in previous studies, such as the PEG/PAA DN hydrogels, the existence of a "pre-stress" condition between the 1st network and 2nd network of the DNs was implicated in the DN modulus enhancements. In the present study, the observed swelling patterns of the degradable PLA-PEG-PLA/PAA DN hydrogels (Figure 5.6) suggest that a similar pre-stress condition is likely to also exist in the degradable DNs. As described above, the PLA-PEG-PLA 1st network seems to limit the swelling of the PAA component resulting in lower swelling of the 2k/PAA DNs compared to the 4k/PAA and 8k/PAA hydrogels. This suggests that, at least for the 2k/PAA DNs, the swelling of the PAA components (which swell to a higher degree on their own) is restricted by the PLA-PEG-PLA component.

In order to get a better understanding of whether or not a "pre-stress" condition played a role in the observed modulus behavior of the degradable DN hydrogels in this study, the density of effective network chains, ν_e^*, in the DN and single-network hydrogels was estimated. An assessment similar to one previously used for characterization of a PEG/PAA IPN was used [141]. However, the swelling of the hydrogels and the sequential polymerization of the DNs was incorporated into this analysis. First, Equation 23 (restated here for convenience) was used to calculate the effective crosslink density ν_e^* of the single-network and DN hydrogels based on their experimentally determined storage modulus, E:

$$E = RT\,\nu_{2,r}^{2/3}\nu_2^{1/3}\,\nu_e^* \tag{37}$$

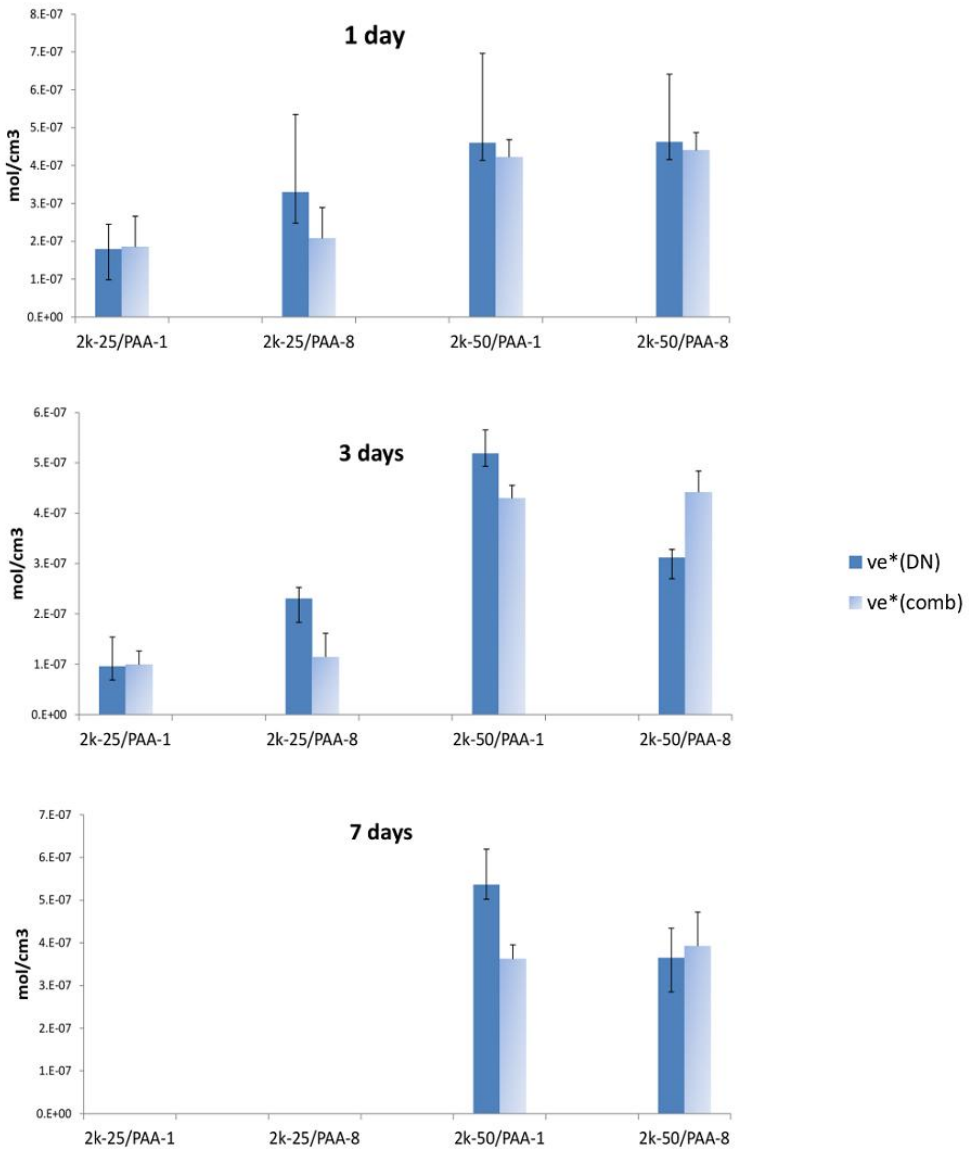

Figure 5.13. Experimental effective network chain density (ve*(DN)) versus theoretical effective network chain density (ve*(comb)) for the 2k DN hydrogels over 7 days

As was the case for calculations of $\bar{M}_c$, the approximation $\nu_{2,r} = 1$ was made, and $\nu^*_{e(PEG-PLA)}$, $\nu^*_{e(PAA)}$ and $\nu^*_{e(DN)}$ were calculated for the single and DN hydrogels. Then, using the relationships defined in Equation 25 for the modulus of a seq-IPN, the

theoretical effective crosslink density $\nu^*_{e(comb)}$ was calculated for the DN hydrogels based on $\nu^*_{e(PEG-PLA)}$ and $\nu^*_{e(PAA)}$ of the single networks (Equation 38):

$$\nu^*_{e(comb)} = \emptyset_1^{1/3}\, \nu^*_{e(PEG-PLA)} + \emptyset_2\, \nu^*_{e(PAA)} \quad (38)$$

where $\emptyset_1$ and $\emptyset_2$ are the volume fractions of the PLA-PEG-PLA network and PAA network inside the DN (in the dry state), respectively, where $\emptyset_1 + \emptyset_2 = 1$ [116] .

Equation 37 and Equation 38 are suitable for hydrogels and IPNs above their T_g. While this situation can't be guaranteed for the single-network PAA hydrogels or the DN PLA-PEG-PLA/PAA hydrogels (which have T_g's in the range of 83 – 93 °C and 24 – 68 °C, respectively, in the dry state), the absorbed water in hydrogels typically acts a plasticizer that lowers T_g significantly below the 37 °C experimental temperature used in this study [3]. Additionally, based on the values published in the literature for the T_g of crosslinked PEG (PEG $T_g \approx$ -60 to -70 °C in the dry state), at 37 °C the PLA-PEG-PLA network is expected to be significantly above its water-swollen T_g. Therefore use of these equations is assumed to be safe, particularly for characterization of the 2k DN hydrogels, where all of the 2k single-network and DN hydrogels (which have T_g's around or below 37 °C even in the dry state) have modulus values a full order or two greater than those of the PAA single-network hydrogels.

The results for the 2k DNs are shown in Figure 5.13. For most of the DN hydrogels, the values of $\nu^*_{e(DN)}$ are either equal to or greater than those predicted by combination of the network components, $\nu^*_{e(comb)}$. This suggests that interpenetration of the two networks in the DN hydrogels is enhanced to some degree above what is predicted for a seq-IPN hydrogel. Combined with the swelling results, these results

support the possibility that a pre-stress condition could be responsible for the sustained modulus properties of the high-swelling DN hydrogels in this study.

5.4.4 Conclusions

The thermal, swelling, degradation and storage modulus properties of the single-network PLA-PEG-PLA and PAA hydrogels mostly followed expected patterns based on modulation of $\bar{M}_c$. This confirmed the effects of variations in parameters such as PEG MW and macromer concentration of the 1st network and the crosslinker concentration of the 2nd network. However, for the PAA hydrogels, while increasing the crosslinker concentration was found to have a desired effect to some degree, high degrees of cyclization likely prevented better control in obtaining a lower $\bar{M}_c$ for the PAA-8 hydrogels. The results of this were seen for the DN hydrogels, where networks composed of PAA-1 and PAA-8 often had very similar macroscopic properties.

The thermal behavior of the PLA-PEG-PLA/PAA DN hydrogels, in combination with the earlier FTIR results, provided strong evidence that hydrogen bonding occurs between the PLA-PEG-PLA and PAA networks in the dry state. This suggests that the interaction of the degradable PLA-PEG-PLA networks with the degradable PAA networks is still dominated by PEG and PAA. For the swollen hydrogels at pH 7.4, hydrogen bonding between the two networks becomes much less significant because of the high degree of swelling (which spreads the chains far apart) and because of the high degree of dissociation of PAA. As a result, the macroscopic properties of the DN hydrogels appeared to be dependent on physical interpenetration at equilibrium swelling, as evidenced by the low swelling and the generally higher-than-expected density of

effective network chains of the 2k DN hydrogels. These results show that the DN strategy can successfully be applied to the degradable PLA-PEG-PLA/PAA hydrogels in this study, and that the "pre-stress" condition may be as significant for degradable DN hydrogels as for non-degradable in enhancing the modulus. The DN hydrogels achieved similar moduli to the PLA-PEG-PLA single-networks despite significantly higher swelling as measured through PBS content. At the same time, it is possible that maintenance of the DN storage modulus over time may be better compared to the single networks.

CHAPTER 6

CONCLUDING REMARKS AND FUTURE WORK

This study shows that application of the DN scheme to fully degradable, injectable hydrogel combinations based on PEG and PAA successfully leads to sustained stiffness of the hydrogels at very high degrees of swelling. Future studies on the biocompatibility of these DN hydrogels in tissue engineering applications, particularly for the degradable PAA component, would also be necessary for use in the body. At the same time, this system serves as a model where PLA-PEG-PLA hydrogels could be combined with degradable polyelectrolyte hydrogels for sustained stiffness properties of high-swelling biodegradable hydrogels.

For the PLA-PEG-PLA/PAA DN hydrogels, the modulus enhancements exhibited at very high degrees of swelling could be further investigated by a study on the pH dependence of the DN hydrogel modulus. Such work could help to elucidate more specifically the role played by a pre-stress condition in the modulus enhancement of these DN hydrogels. At the same time, extending the degradation time periods could be beneficial, as differences in the modulus of the DN and single-network hydrogels may be further distinguished at longer degradation times. Additionally, the stress-strain behavior and the ultimate fracture strength of these hydrogels are yet to be investigated.

These PLA-PEG-PLA/PAA DN hydrogels could potentially be investigated for the regeneration of cartilage with large fibril diameters, towards the high end of the 20 – 150 nm range [22]. For regeneration of these types of cartilage, the combination of high stiffness and high mesh sizes may be particularly favorable. Another possible application

could involve the controlled release of large biomolecules or drugs in harsh environments where the structural integrity of the hydrogels is also significant [142].

.

APPENDIX A

GPC CHROMATOGRAMS

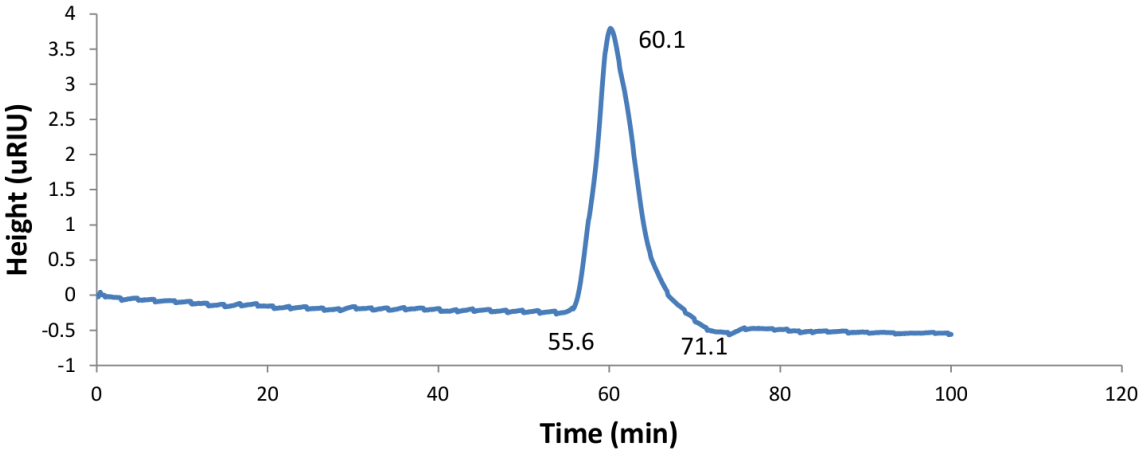

Figure A.1. GPC Curve – PAA Sample

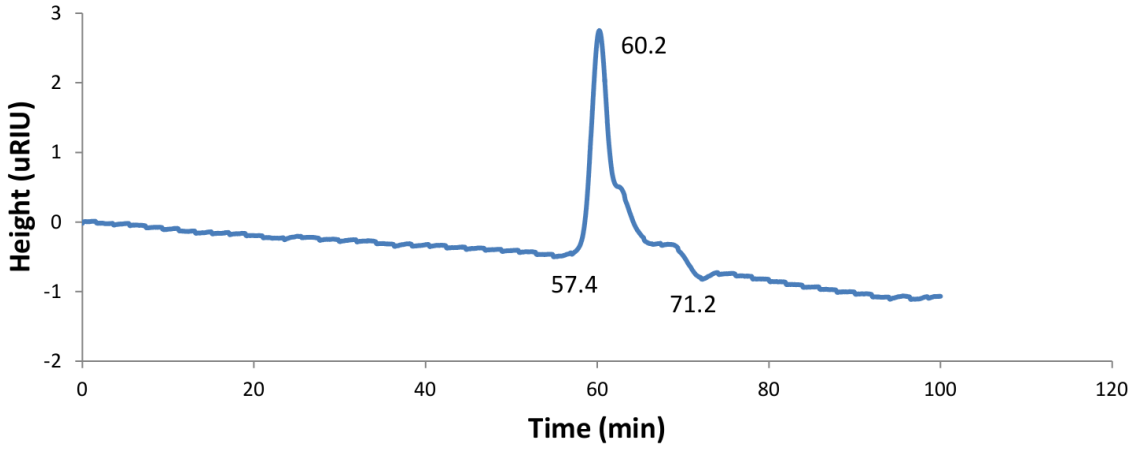

Figure A.2. GPC Curve – PAA Standard (50,000 g/mol)

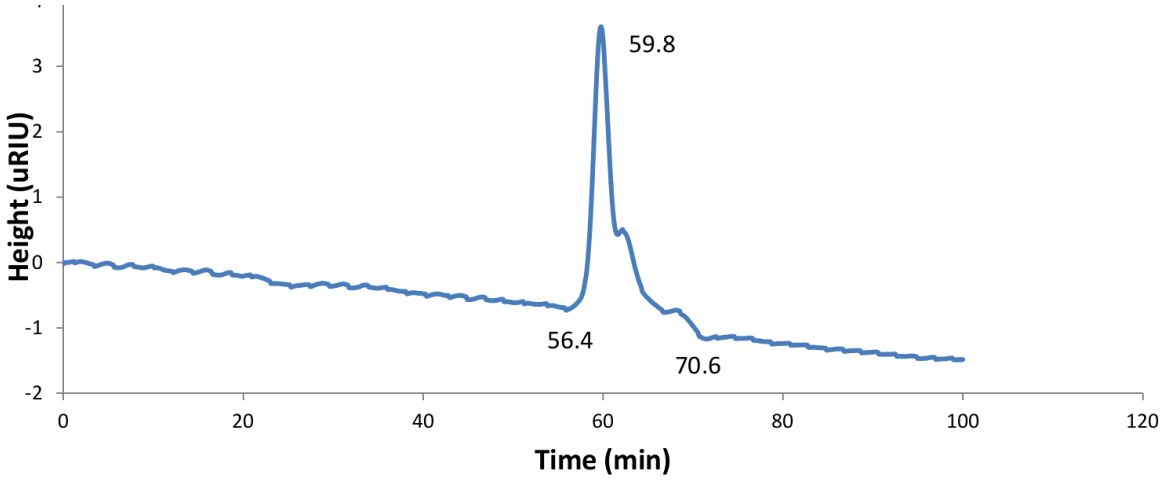

Figure A.3. GPC Curve – PAA Standard (100,000 g/mol)

REFERENCES

1. Park, K. *Superporous hydrogels for pharmaceutical & other applications*. Drug development and Delivery, 2002. **2**.

2. Wichterle, O. and D. Lim, *Hydrophilic gels for biological use.* Nature, 1960. **185**(4706): p. 117-118.

3. Slaughter, B.V., et al., *Hydrogels in Regenerative Medicine.* Advanced Materials, 2009. **21**(32-33): p. 3307-3329.

4. Barbucci, R., *Hydrogels Biological Properties and Applications* 2009, Milano: Springer-Verlag Milan.

5. Peppas, N.A., *Hydrogels in medicine and pharmacy*1986, Boca Raton, Fla.: CRC Press.

6. Drury, J.L. and D.J. Mooney, *Hydrogels for tissue engineering: scaffold design variables and applications.* Biomaterials, 2003. **24**(24): p. 4337-4351.

7. Barcili, B., *Hydrogels for tissue engineering and delivery of tissue-inducing substances.* Journal of Pharmaceutical Sciences, 2007. **96**(9): p. 2197-2223.

8. Nguyen, K.T. and J.L. West, *Photopolymerizable hydrogels for tissue engineering applications.* Biomaterials, 2002. **23**(22): p. 4307-4314.

9. Osada, Y., J.P. Gong, and T. Narita, *Intelligent gels.* Materials Research Society Symposium - Proceedings, 2000. **604**: p. 149-159.

10. Hoare, T.R. and D.S. Kohane, *Hydrogels in drug delivery: Progress and challenges.* Polymer, 2008. **49**(8): p. 1993-2007.

11. Mellott, M.B., K. Searcy, and M.V. Pishko, *Release of protein from highly cross-linked hydrogels of poly(ethylene glycol) diacrylate fabricated by UV polymerization.* Biomaterials, 2001. **22**(9): p. 929-941.

12. Zhang, Z., et al., *Thermo- and pH-responsive HPC-g-AA/AA hydrogels for controlled drug delivery applications.* Polymer, 2011. **52**(3): p. 676-682.

13. Lin, C.C. and A.T. Metters, *Hydrogels in controlled release formulations: Network design and mathematical modeling.* Advanced Drug Delivery Reviews, 2006. **58**(12-13): p. 1379-1408.

14. Park, K., *Superporous hydrogels for pharmaceutical & other applications.* Drug Development and Delivery, July/August 2002.

15. Nguyen, M.K. and D.S. Lee, *Injectable Biodegradable Hydrogels.* Macromolecular Bioscience, 2010. **10**(6): p. 563-579.

16. Li, Y.L., J. Rodrigues, and H. Tomas, *Injectable and biodegradable hydrogels: gelation, biodegradation and biomedical applications.* Chemical Society Reviews, 2012. **41**(6): p. 2193-2221.

17. Kamath, K.R. and K. Park, *Biodegradable Hydrogels in Drug Delivery.* Advanced Drug Delivery Reviews, 1993. **11**(1-2): p. 59-84.

18. Roberts, J.J., et al., *Comparative study of the viscoelastic mechanical behavior of agarose and poly(ethylene glycol) hydrogels.* Journal of Biomedical Materials Research Part B-Applied Biomaterials, 2011. **99B**(1): p. 158-169.

19. Chung, C. and J.A. Burdick, *Engineering cartilage tissue.* Advanced Drug Delivery Reviews, 2008. **60**(2): p. 243-262.

20. Bryant, S.J. and K.S. Anseth, *Hydrogel properties influence ECM production by chondrocytes photoencapsulated in poly(ethylene glycol) hydrogels.* Journal of Biomedical Materials Research, 2002. **59**(1): p. 63-72.

21. Cha, C., et al., *Tuning the dependency between stiffness and permeability of a cell encapsulating hydrogel with hydrophilic pendant chains.* Acta Biomaterialia, 2011. **7**(10): p. 3719-3728.

22. Buxton, A.N., et al., *Design and characterization of poly(ethylene glycol) photopolymerizable semi-interpenetrating networks for chondrogenesis of human mesenchymal stem cells.* Tissue Engineering, 2007. **13**(10): p. 2549-2560.

23. Liao, H., et al., *Influence of hydrogel mechanical properties and mesh size on vocal fold fibroblast extracellular matrix production and phenotype.* Acta Biomaterialia, 2008. **4**(5): p. 1161-1171.

24. Kuntz, R.M. and W.M. Saltzman, *Neutrophil motility in extracellular matrix gels: Mesh size and adhesion affect speed of migration.* Biophysical journal, 1997. **72**(3): p. 1472-1480.

25. Griffith, L.G., *Emerging design principles in biomaterials and scaffolds for tissue engineering*, in *Reparative Medicine: Growing Tissues and Organs*2002. p. 83-95.

26. Ghosh, K. and D.E. Ingber, *Micromechanical control of cell and tissue development: Implications for tissue engineering.* Advanced Drug Delivery Reviews, 2007. **59**(13): p. 1306-1318.

27. Bryant, S.J., et al., *Encapsulating Chondrocytes in degrading PEG hydrogels with high modulus: Engineering gel structural changes to facilitate cartilaginous tissue production.* Biotechnology and Bioengineering, 2004. **86**(7): p. 747-755.

28. Bryant, S.J. and K.S. Anseth, *Controlling the spatial distribution of ECM components in degradable PEG hydrogels for tissue engineering cartilage.* Journal of Biomedical Materials Research Part A, 2003. **64A**(1): p. 70-79.

29. Benoit, D.S.W., A.R. Durney, and K.S. Anseth, *Manipulations in hydrogel degradation behavior enhance osteoblast function and mineralized tissue formation.* Tissue Engineering, 2006. **12**(6): p. 1663-1673.

30. Tabata, Y., *The importance of drug delivery systems in tissue engineering.* Pharmaceutical Science & Technology Today, 2000. **3**(3): p. 80-89.

31. Lee, S.-H. and H. Shin, *Matrices and scaffolds for delivery of bioactive molecules in bone and cartilage tissue engineering.* Advanced Drug Delivery Reviews, 2007. **59**(4-5): p. 339-359.

32. Tabata, Y., *Significance of release technology in tissue engineering.* Drug Discovery Today, 2005. **10**(23-24): p. 1639-1646.

33. Brandl, F., F. Sommer, and A. Goepferich, *Rational design of hydrogels for tissue engineering: Impact of physical factors on cell behavior.* Biomaterials, 2007. **28**(2): p. 134-146.

34. Lo, C.-M., et al., *Cell Movement Is Guided by the Rigidity of the Substrate.* Biophys. J., 2000. **79**(1): p. 144-152.

35. Peyton, S.R., et al., *The use of poly(ethylene glycol) hydrogels to investigate the impact of ECM chemistry and mechanics on smooth muscle cells.* Biomaterials, 2006. **27**(28): p. 4881-4893.

36. Tew, G.N., et al., *New properties from PLA-PEO-PLA hydrogels.* Soft Matter, 2005. **1**(4): p. 253-258.

37. Engler, A.J., et al., *Matrix Elasticity Directs Stem Cell Lineage Specification.* Cell, 2006. **126**(4): p. 677-689.

38. Engler, A.J., et al., *Myotubes differentiate optimally on substrates with tissue-like stiffness: pathological implications for soft or stiff microenvironments.* J. Cell Biol., 2004. **166**(6): p. 877-887.

39. Li, L., et al., *Functional modulation of ES-derived hepatocyte lineage cells via substrate compliance alteration.* Annals of Biomedical Engineering, 2008. **36**(5): p. 865-876.

40. Ying J. Li, E.H.C.R.T.R.M.T.F.K.E.H., *Hydrogels as artificial matrices for human embryonic stem cell self-renewal.* Journal of Biomedical Materials Research Part A, 2006. **79A**(1): p. 1-5.

41. Bott, K., et al., *The effect of matrix characteristics on fibroblast proliferation in 3D gels.* Biomaterials, 2010. **31**(32): p. 8454-8464.

42. Lutolf, M.P., et al., *Synthetic matrix metalloproteinase-sensitive hydrogels for the conduction of tissue regeneration: Engineering cell-invasion characteristics.* Proceedings of the National Academy of Sciences of the United States of America, 2003. **100**(9): p. 5413-5418.

43. Stammen, J.A., et al., *Mechanical properties of a novel PVA hydrogel in shear and unconfined compression.* Biomaterials, 2001. **22**(8): p. 799-806.

44. Martens, P.J., S.J. Bryant, and K.S. Anseth, *Tailoring the degradation of hydrogels formed from multivinyl poly(ethylene glycol) and poly(vinyl alcohol) macromers for cartilage tissue engineering.* Biomacromolecules, 2003. **4**(2): p. 283-292.

45. Armstrong, C.G. and V.C. Mow, *Variations in the intrinsic mechanical proterties of human articular-cartilage with age, degeneration, and water-content.* Journal of Bone and Joint Surgery-American Volume, 1982. **64**(1): p. 88-94.

46. Myung, D., et al., *Biomimetic strain hardening in interpenetrating polymer network hydrogels.* Polymer, 2007. **48**(18): p. 5376-5387.

47. Broom, N.D. and A. Oloyede, *The importance of physicochemical swelling in cartilage illustrated with a model hydrogel system.* Biomaterials, 1998. **19**(13): p. 1179-1188.

48. Baroli, B., *Photopolymerization of biomaterials: issues and potentialities in drug delivery, tissue engineering, and cell encapsulation applications.* Journal of Chemical Technology and Biotechnology, 2006. **81**(4): p. 491-499.

49. Elisseeff, J., et al., *Transdermal photopolymerization for minimally invasive implantation.* Proceedings of the National Academy of Sciences of the United States of America, 1999. **96**(6): p. 3104-3107.

50. Lin, C.-C. and K. Anseth, *PEG Hydrogels for the Controlled Release of Biomolecules in Regenerative Medicine.* Pharmaceutical Research, 2009. **26**(3): p. 631-643.

51. Lavik, E. and R. Langer, *Tissue engineering: current state and perspectives.* Applied Microbiology and Biotechnology, 2004. **65**(1): p. 1-8.

52. Sawhney, A.S., C.P. Pathak, and J.A. Hubbell, *Bioerodible Hydrogels Based on Photopolymerized Poly(Ethylene Glycol)-Co-Poly(Alpha-Hydroxy Acid) Diacrylate Macromers.* Macromolecules, 1993. **26**(4): p. 581-587.

53. Metters, A.T., K.S. Anseth, and C.N. Bowman, *Fundamental studies of a novel, biodegradable PEG-b-PLA hydrogel.* Polymer, 2000. **41**(11): p. 3993-4004.

54. Metters, A.T., C.N. Bowman, and K.S. Anseth, *A Statistical kinetic model for the bulk degradation of PLA-b-PEG-b-PLA hydrogel networks.* Journal of Physical Chemistry B, 2000. **104**(30): p. 7043-7049.

55. Shah, N.M., M.D. Pool, and A.T. Metters, *Influence of network structure on the degradation of photo-cross-linked PLA-b-PEG-b-PLA hydrogels.* Biomacromolecules, 2006. **7**(11): p. 3171-3177.

56. Mahoney, M.J. and K.S. Anseth, *Three-dimensional growth and function of neural tissue in degradable polyethylene glycol hydrogels.* Biomaterials, 2006. **27**(10): p. 2265-2274.

57. Mason, M.N., et al., *Predicting controlled-release behavior of degradable PLA-b-PEG-b-PLA hydrogels.* Macromolecules, 2001. **34**(13): p. 4630-4635.

58. Lu, S. and K.S. Anseth, *Release Behavior of High Molecular Weight Solutes from Poly(ethylene glycol)-Based Degradable Networks.* Macromolecules, 2000. **33**(7): p. 2509-2515.

59. Sanabria-DeLong, N., A.J. Crosby, and G.N. Tew, *Photo-Cross-Linked PLA-PEO-PLA Hydrogels from Self-Assembled Physical Networks: Mechanical Properties and Influence of Assumed Constitutive Relationships.* Biomacromolecules, 2008. **9**(10): p. 2784-2791.

60. Rashkov, I., et al., *Synthesis, characterization, and hydrolytic degradation of PLA/PEO/PLA triblock copolymers with short poly(l-lactic acid) chains.* Macromolecules, 1996. **29**(1): p. 50.

61. Dorati, R., et al., *Investigation of the degradation behaviour of poly(ethylene glycol-co-D,L-lactide) copolymer.* Polymer Degradation and Stability, 2007. **92**(9): p. 1660-1668.

62. Kim, I.S., et al., *Albumin release from biodegradable hydrogels composed of dextran and poly(ethylene glycol) macromer.* Archives of Pharmacal Research, 2001. **24**(1): p. 69-73.

63. Witte, R.P., et al., *Analysis of poly(ethylene glycol)-diacrylate macromer polymerization within a multicomponent semi-interpenetrating polymer network system.* Journal of Biomedical Materials Research Part A, 2004. **71A**(3): p. 508-518.

64. Nair, L.S. and C.T. Laurencin, *Biodegradable polymers as biomaterials.* Progress in Polymer Science, 2007. **32**(8-9): p. 762-798.

65. He, B., E. Wan, and M.B. Chan-Park, *Synthesis and degradation of biodegradable photo-cross-linked poly(alpha,beta-malic acid)-based hydrogel.* Chemistry of Materials, 2006. **18**(17): p. 3946-3955.

66. Lin, H.R., M.H. Ling, and Y.J. Lin, *High Strength and Low Friction of a PAA-Alginate-Silica Hydrogel as Potential Material for Artificial Soft Tissues.* Journal of Biomaterials Science-Polymer Edition, 2009. **20**(5-6): p. 637-652.

67. Li, S.F., et al., *In vitro degradation and protein release of Semi-IPN hydrogels consisted of poly(acrylic acid-acrylamide-methacrylate) and amylose.* Journal of Applied Polymer Science, 2007. **105**(6): p. 3432-3438.

68. Li, S.F. and X.L. Liu, *Synthesis, characterization, and evaluation of enzymatically degradable poly(N-isopropylacrylamide-co-acrylic acid) hydrogels for colon-specific drug delivery.* Polymers for Advanced Technologies, 2008. **19**(11): p. 1536-1542.

69. Wang, F., et al., *Injectable, rapid gelling and highly flexible hydrogel composites as growth factor and cell carriers.* Acta Biomaterialia, 2010. **6**(6): p. 1978-1991.

70. Akala, E.O., P. Kopeckova, and J. Kopecek, *Novel pH-sensitive hydrogels with adjustable swelling kinetics.* Biomaterials, 1998. **19**(11-12): p. 1037-1047.

71. Liu, Z.L., H. Hu, and R.X. Zhuo, *Konjac glucomannan-graft-acrylic acid hydrogels containing azo crosslinker for colon-specific delivery.* Journal of Polymer Science Part a-Polymer Chemistry, 2004. **42**(17): p. 4370-4378.

72. Zhao, S., et al., *Synthesis and characterization of biodegradable thermo- and pH-sensitive hydrogels based on pluronic F127/poly(ε-caprolactone) macromer and acrylic acid.* Macromolecular Research, 2009. **17**(12): p. 1025-1031.

73. Zhao, S.P., et al., *Synthesis and Properties of Photopolymerized pH-Sensitive Hydrogels of Methacrylic Acid and Biodegradable PEG-b-PCL Macromer.* Iranian Polymer Journal, 2011. **20**(4): p. 329-340.

74. Zhang, H.F., et al., *Modulate the phase transition temperature of hydrogels with both thermosensitivity and biodegradability.* Carbohydrate Polymers, 2010. **79**(1): p. 131-136.

75. Adachi, H., S. Nishi, and T. Kotaka, *Structure and mechanical-properties of sequential interpenetrating polymer networks. 2. Complex-forming polyoxyethylene - poly(acrylic acid) systems.* Polymer Journal, 1982. **14**(12): p. 985-992.

76. Nishi, S. and T. Kotaka, *Complex-forming poly(oxyethylene) - poly(acrylic acid) interpenetrating polymer networks .1. Preparation, structure, and viscoelastic properties.* Macromolecules, 1985. **18**(8): p. 1519-1525.

77. Nishi, S. and T. Kotaka, *Complex-forming poly(oxyethylene) poly(acrylic acid) interpenetrating polymer networks .2. Function as a chemical valve.* Macromolecules, 1986. **19**(4): p. 978-984.

78. Nishi, S. and T. Kotaka, *Complex-forming polyoxyethylene - poly(acrylic acid) interpenetrating polymer networks .3. Swelling and mechanochemical behavior.* Polymer Journal, 1989. **21**(5): p. 393-402.

79. Jang, S.S., W.A. Goddard, and M.Y.S. Kalani, *Mechanical and transport properties of the poly(ethylene oxide)-poly(acrylic acid) double network hydrogel from molecular dynamic simulations.* Journal of Physical Chemistry B, 2007. **111**(7): p. 1729-1737.

80. Kim, I.S., S.H. Kim, and C.S. Cho, *Drug release from pH-sensitive interpenetrating polymer networks hydrogel based on poly (ethylene glycol) macromer and poly (acrylic acid) prepared by UV cured method.* Archives of Pharmacal Research, 1996. **19**(1): p. 18-22.

81. Yim, E.S., et al., *Biocompatibility of poly(ethylene glycol)/poly(acrylic acid) interpenetrating polymer network hydrogel particles in RAW 264.7 macrophage and MG-63 osteoblast cell lines.* Journal of Biomedical Materials Research Part A, 2009. **91A**(3): p. 894-902.

82. Myung, D., et al., *Glucose-permeable interpenetrating polymer network hydrogels for corneal implant applications: A pilot study.* Current Eye Research, 2008. **33**(1): p. 29-43.

83. Waters, D.J. and C.W. Frank, *Hindered diffusion of oligosaccharides in high strength poly(ethylene glycol)/poly(acrylic acid) interpenetrating network hydrogels: Hydrodynamic vs. obstruction models.* Polymer, 2009. **50**(26): p. 6331-6339.

84. Myung, D., et al., *Characterization of poly(ethylene glycol)-poly(acrylic acid) (PEG-PAA) double networks designed for corneal implant applications.* Investigative Ophthalmology & Visual Science, 2005. **46**.

85. Koh, W.G., et al., *Synthesis and surface modification of double network hydrogel from poly(ethylene glycol) and poly(acrylic acid).* Investigative Ophthalmology & Visual Science, 2005. **46**.

86. Farooqui, N., et al., *Histological evaluation of poly(ethylene glycol)-poly(acrylic acid) (PEG-PAA) double network hydrogel corneal implant.* Investigative Ophthalmology & Visual Science, 2005. **46**.

87. *Interpenetrating polymer networks*. Advances in chemistry series 239, ed. D. Klempner, L.H. Sperling, and L.A. Utracki1994, Washington, DC: American Chemical Society.

88. Karino, T., M. Shibayama, and K. Ito, *Slide-ring gel: Topological gel with freely movable cross-links.* Physica B-Condensed Matter, 2006. **385**: p. 692-696.

89. Haraguchi, K., *Nanocomposite hydrogels.* Current Opinion in Solid State & Materials Science, 2007. **11**(3-4): p. 47-54.

90. Gong, J.P., et al., *Double-network hydrogels with extremely high mechanical strength.* Advanced Materials, 2003. **15**(14): p. 1155.

91. Huang, M., et al., *Importance of entanglement between first and second components in high-strength double network gels.* Macromolecules, 2007. **40**(18): p. 6658-6664.

92. Tominaga, T., et al., *The molecular origin of enhanced toughness in double-network hydrogels: A neutron scattering study.* Polymer, 2007. **48**(26): p. 7449-7454.

93. *Principles of polymer systems*. 5th ed. ed, ed. F. Rodriguez2003, New York :: Taylor & Francis.

94. Young, R.J., *Introduction to polymers / R.J. Young and P.A. Lovell*. 2nd ed. ed, ed. P.A. Lovell, London; New York: Chapman & Hall, 1991.

95. Flory, P.J., *Principles of polymer chemistry*. The George Fisher Baker non-resident lectureship in chemistry at Cornell University1953, Ithaca: Cornell University Press. 4.

96. Flory, P.J. and J. Rehner, *Statistical mechanics of cross-linked polymer networks II Swelling.* Journal of Chemical Physics, 1943. **11**(11): p. 521-526.

97. Sperling, L.H., *Introduction to physical polymer science*. 2nd ed. ed1992, New York :: Wiley.

98. Hassan, C.M., F.J. Doyle, and N.A. Peppas, *Dynamic Behavior of Glucose-Responsive Poly(methacrylic acid-g-ethylene glycol) Hydrogels.* Macromolecules, 1997. **30**(20): p. 6166-6173.

99. Odian, G.G., *Principles of polymerization*. 4th ed2004, Hoboken, N.J.: Wiley-Interscience. xxiv, 812 p.

100. Yarimkaya, S. and H. Basan, *Synthesis and swelling behavior of acrylate-based hydrogels.* Journal of Macromolecular Science Part a-Pure and Applied Chemistry, 2007. **44**(7-9): p. 699-706.

101. Emileh, A., E. Vasheghani-Farahani, and M. Imani, *Swelling behavior, mechanical properties and network parameters of pH- and temperature-sensitive hydrogels of poly((2-dimethyl amino) ethyl methacrylate-co-butyl methacrylate).* European Polymer Journal, 2007. **43**(5): p. 1986-1995.

102. Peppas, N.A., H.J. Moynihan, and L.M. Lucht, *The structure of highly crosslinked poly(2-hydroxyethyl methacrylate) hydrogels.* Journal of Biomedical Materials Research, 1985. **19**(4): p. 397-411.

103. Kovac, J., *Modified Gaussian Model for Rubber Elasticity.* Macromolecules, 1978. **11**(2): p. 362-365.

104. Peppas, N.A. and E.W. Merrill, *Poly(vinyl-alcohol) hydrogels: Reinforcement of radiation-crosslinked networks by crystallization.* Journal of Polymer Science Part a-Polymer Chemistry, 1976. **14**(2): p. 441-457.

105. Mark, J.E. and P.J. Flory, *The Configuration of the Polyoxyethylene Chain.* Journal of the American Chemical Society, 1965. **87**(7): p. 1415-1423.

106. Lee, H., et al., *Molecular Dynamics Studies of Polyethylene Oxide and Polyethylene Glycol: Hydrodynamic Radius and Shape Anisotropy.* Biophysical journal, 2008. **95**(4): p. 1590-1599.

107. Peppas, N.A. and E.W. Merrill, *Crosslinked poly(vinyl alcohol) hydrogels as swollen elastic networks.* Journal of Applied Polymer Science, 1977. **21**(7): p. 1763-1770.

108. Anseth, K.S., C.N. Bowman, and L. BrannonPeppas, *Mechanical properties of hydrogels and their experimental determination.* Biomaterials, 1996. **17**(17): p. 1647-1657.

109. Bae, Y.H., T. Okano, and S.W. Kim, *Temperature dependence of swelling of crosslinked poly(N,N'-alkyl substituted acrylamides) in water.* Journal of Polymer Science Part B: Polymer Physics, 1990. **28**(6): p. 923-936.

110. Ruiz, J., A. Mantecón, and V. Cádiz, *Synthesis and properties of hydrogels from poly (vinyl alcohol) and ethylenediaminetetraacetic dianhydride.* Polymer, 2001. **42**(15): p. 6347-6354.

111. Şen, M. and M. Sarı, *Radiation synthesis and characterization of poly(N,N-dimethylaminoethyl methacrylate-co-N-vinyl 2-pyrrolidone) hydrogels.* European Polymer Journal, 2005. **41**(6): p. 1304-1314.

112. Li, B.Y., et al., *Forced compatibility and mutual entanglements in Poly(Vinyl Acetate)/ poly(Methyl Acrylate) IPNs* in *Advances in Interpenetrating Polymer Networks: Volume I*1989, Lancaster, Pa. : Technomic Pub. Co. p. 203-220.

113. Thiele, J.L. and R.E. Cohen, *Synthesis, characterization, and viscoelastic behavior of single-phase interpenetrating polystyrene networks.* Polymer Engineering and Science, 1979. **19**(4): p. 284-293.

114. Siegfried, D.L., D.A. Thomas, and L.H. Sperling, *A Reexamination of Polystyrene/Polystyrene Homo Interpenetrating Polymer Networks: Aspects of*

Relative Network Continuity and Internetwork Coupling. Macromolecules, 1979. **12**(4): p. 586-589.

115. Li, B., et al., *Mutual entanglements in poly(vinyl acetate)/poly(methyl acrylate) interpenetrating polymer networks.* Polymer, 1992. **33**(13): p. 2740-2743.

116. Sperling, L.H., *Interpenetrating polymer networks and related materials*1981, New York :: Plenum Press.

117. Cai, L. and S.F. Wang, *Poly(epsilon-caprolactone) acrylates synthesized using a facile method for fabricating networks to achieve controllable physicochemical properties and tunable cell responses.* Polymer, 2010. **51**(1): p. 164-177.

118. Cai, L. and S.F. Wang, *Elucidating Colorization in the Functionalization of Hydroxyl-Containing Polymers Using Unsaturated Anhydrides/Acyl Chlorides in the Presence of Triethylamine.* Biomacromolecules, 2010. **11**(1): p. 304-307.

119. Li, F., S.M. Li, and M. Vert, *Synthesis and rheological properties of polylactide/poly(ethylene glycol) multiblock copolymers.* Macromolecular Bioscience, 2005. **5**(11): p. 1125-1131.

120. Zhu, W. and J.D. Ding, *Synthesis and characterization of a redox-initiated, injectable, biodegradable hydrogel.* Journal of Applied Polymer Science, 2006. **99**(5): p. 2375-2383.

121. Bajpai, S.K. and S. Singh, *Analysis of swelling behavior of poly(methacrylamide-co-methacrylic acid) hydrogels and effect of synthesis conditions on water uptake.* Reactive & Functional Polymers, 2006. **66**(4): p. 431-440.

122. Muniz, E.C. and G. Geuskens, *Compressive elastic modulus of polyacrylamide hydrogels and semi-IPNs with poly(N-isopropylacrylamide).* Macromolecules, 2001. **34**(13): p. 4480-4484.

123. Mark, J.E., *Rubberlike elasticity : a molecular primer*. 2nd ed. ed, ed. B. Erman2007, Cambridge ;: Cambridge University Press.

124. Bajpai, A.K. and A. Mishra, *Ionizable interpenetrating polymer networks of carboxymethyl cellulose and polyacrylic acid: Evaluation of water uptake.* Journal of Applied Polymer Science, 2004. **93**(5): p. 2054-2065.

125. Merrill, E.W., K.A. Dennison, and C. Sung, *Partitioning and diffusion of solutes in hydrogels of poly(ethylene oxide).* Biomaterials, 1993. **14**(15): p. 1117-1126.

126. Gudeman, L.F. and N.A. Peppas, *pH-sensitive membranes from poly(vinyl alcohol)/poly(acrylic acid) interpenetrating networks.* Journal of Membrane Science, 1995. **107**(3): p. 239-248.

127. Hernandez, R., D. Lopez, and C. Mijangos, *Preparation and characterization of polyacrylic acid-poly(vinyl alcohol)-based interpenetrating hydrogels.* Journal of Applied Polymer Science, 2006. **102**(6): p. 5789-5794.

128. Chatterji, P.R., *Cross-link dimensions in (gelatin-poly(acrylamide) interpenetrating hydrogel networks.* Macromolecules, 1991. **24**(14): p. 4214-4215.

129. Chen, W.N., et al., *Synthesis and properties of poly(L-lactide)-poly (ethylene glycol) multiblock copolymers by coupling triblock copolymers.* Polymers for Advanced Technologies, 2003. **14**(3-5): p. 245-253.

130. Du, Y.J., et al., *ABA type copolymers of lactide with poly(ethylene glycol). Kinetic, mechanistic, and model studies.* Macromolecules, 1995. **28**(7): p. 2124-2132.

131. Imani, M., et al., *Monitoring of Polyethylene Glycol-diacrylate-based Hydrogel Formation by Real Time NMR Spectroscopy.* Iranian Polymer Journal, 2007. **16**(1): p. 13-20.

132. Elliott, J.E., J.W. Anseth, and C.N. Bowman, *Kinetic modeling of the effect of solvent concentration on primary cyclization during polymerization of multifunctional monomers.* Chemical Engineering Science, 2001. **56**(10): p. 3173-3184.

133. Padmavathi, N.C. and P.R. Chatterji, *Structural Characteristics and Swelling Behavior of Poly(ethylene glycol) Diacrylate Hydrogels.* Macromolecules, 1996. **29**(6): p. 1976-1979.

134. Lowman, A.M., et al., *Structural and dynamic response of neutral and intelligent networks in biomedical environments,* in *Advances in Chemical Engineering*, A. Peppas and M.V. Sefton, Editors. 2004, Academic Press. p. 75-130.

135. Liu, G.Q., et al., *Shape-memory behavior of poly (methyl methacrylate-co -N-vinyl-2-pyrrolidone)/poly (ethylene glycol) semi-interpenetrating polymer networks based on hydrogen bonding.* Journal of Polymer Research, 2011. **18**(6): p. 2109-2117.

136. Liu, G.Q., et al., *Morphology and Thermal Behaviour of Poly (methyl methacrylate-co-N-vinyl-2-pyrrolidone)/Poly (ethylene glycol) Semi-interpenetrating Polymer Networks Based on Hydrogen Bonding Interaction.* Acta Chimica Slovenica, 2009. **56**(4): p. 946-952.

137. Xiao, H., M. Jiang, and T. Yu, *Controllable specific interactions and miscibility in polymer blends: 5. Effect of crosslink density in interpenetrating polymer networks.* Polymer, 1994. **35**(25): p. 5529-5535.

138. Choi, H.K., et al., *A novel mucoadhesive polymer prepared by template polymerization of acrylic acid in the presence of poly (ethylene glycol).* Journal of Applied Polymer Science, 1999. **73**(13): p. 2749-2754.

139. Myung, D., et al., *Progress in the development of interpenetrating polymer network hydrogels.* Polymers for Advanced Technologies, 2008. **19**(6): p. 647-657.

140. Smith, K.L., A.E. Winslow, and D.E. Petersen, *Association Reactions for Poly(alkylene Oxides) and Polymeric Poly(carboxylic Acids).* Ind. Eng. Chem., 1959. **51**(11): p. 1361-1364.

141. Oyama, H.T., W.T. Tang, and C.W. Frank, *Complex formation between poly(acrylic acid) and pyrene-labeled polyethylene glycol in aqueous solution.* Macromolecules, 1987. **20**(3): p. 474-480.

142. Omidian, H., K. Park, and J.G. Rocca, *Recent developments in superporous hydrogels.* Journal of Pharmacy and Pharmacology, 2007. **59**(3): p. 317-327.